UNIVERSIDAD DE CANTABRIA

DEPARTAMENTO DE
INGENIERÍA DE COMUNICACIONES

TESIS DOCTORAL

DISEÑO DE BEAMFORMERS PARA ARQUITECTURAS RF-MIMO SIMPLIFICADAS

Autor: Fouad Gholam
Directores: Ignacio Santamaría Caballero
Javier Vía Rodriguez

2011

Diseño de Beamformers para Arquitecturas RF-MIMO Simplificadas

Tesis que se presenta para optar al título de
Doctor por la Universidad de Cantabria

Autor: Fouad Gholam
Directores: Ignacio Santamaría Caballero
Javier Vía Rodriguez

Programa Oficial de Posgrado en Tecnologías de la Información y Comunicaciones en Sistemas de Telecomunicación
Grupo de Tratamiento Avanzado de Señal
Departamento de Ingeniería de Comunicaciones
Escuela Técnica Superior de Ingenieros Industriales y de Telecomunicación
Universidad de Cantabria
2011

Tesis Doctoral: Diseño de Beamformers para Arquitecturas RF-MIMO Simplificadas

Autor: Fouad Gholam

Directores: Ignacio Santamaría Caballero

Javier Vía Rodriguez

El tribunal nombrado para juzgar la tesis doctoral citada, compuesto por los señores

Presidente:

Vocales:

Secretario:

Acuerda otorgarle la calificación de

Santander, a de de 2011

To my family.

Afiliación

Grupo de Tratamiento Avanzado de Señal
Departamento de Ingeniería de Comunicaciones
Universidad de Cantabria

Este trabajo ha sido financiado por la beca MAEC-AECI del Ministerio Español de Asuntos Exteriores y de Cooperación.

Acknowledgements

This Thesis work was carried out at the Laboratory of the Advanced Signal Processing Group (GTAS) of the Communications Engineering Department (DICOM), University of Cantabria.

First and foremost, I wish to express my gratitude to my supervisors Dr. Ignacio Santamaría Caballero and Dr. Javier Vía Rodriguez for their many valuable suggestions, guidance through the early years of chaos and confusion, encouragement and the many inspiring discussions.

Secondly, I am again very grateful to Ignacio Santamaría Caballero, who has accepted me as a member of the GTAS Lab.

Furthermore, I want to thank all the professors of GTAS group: Prof. Jesús Ibáñez Díaz, Prof. Jesús Pérez Arriaga and Prof. Luis Vielva Martínez, for their support and advices.

For all my colleagues in the laboratory: Víctor Elvira shared with me his knowledge of analog antenna combining, Jesús Gutiérrez, Steven Van Vaerenbergh, David Ramírez, Óscar González and Alfredo Nazábal (who listed me as co-author of his paper journal). They all helped me to correct the chapters of this work and friendly encouragement. Not forgetting to thank: Alvaro who has listed me as co-author of his international conference paper, Christian and Miguel.

I had the pleasure to thank the Ministerio Español de Asuntos Exteriores y de Cooperación (AECI) which helped me with the "MAEC-AECI" scholarship, which was awarded to me for the period 2008–2011, was crucial to the successful completion of this project.

Of course, I am grateful to my parents for their patience and *love*. Without them this work would never have come into existence (literally). Also, I thank Khadija, my wife, for your *loving* support, prayers and endless patience.

Finally, I wish to thank my Moroccan friends and colleagues of Santander: Mohamed (for his helping to register in the university, to find the flat and information about the stay in Santander and for his friendship); Tribak (for his friendship); Serroukh, Kaoutar, Asmae, Latifa, Hala and Naima. It was a pleasure to meet and to pass with you unforgettable moments.

Resumen

La aparición de sistemas de múlti-antena en las comunicaciones inalámbricas ha ganado mucha atención en la última década. En los sistemas de múlti-antena, a menudo llamados sistemas MIMO (múlti-antena tanto en el transmisor como en el receptor o multiple-input multiple-output) convencionales, todos los caminos de propagación tienen que ser adquiridos y procesados de forma independiente en banda base. En consecuencia, para sitemas MIMO convencionales, los costes del hardware, el tamaño y el consumo de energía son incrementados, y por lo tanto su aplicación en el despliegue comercial de los transceptores inalámbricos de múlti-antena es limitada. Una arquitectura de radio frecuencia RF-MRB (radio-frequency maximum-ratio beamforming desarrollada por el proyecto MIMAX financiado por la UE) de baja energía y de bajo coste se ha propuesto para reducir significativamente la complejidad del hardware mediante la realización de la ponderación adaptiva y la combinación de las señales de antena en el frontal de RF. A pesar de que estas arquitecturas de combinación analógica se limitan a procesar un único flujo de datos, todavía pueden extraer la diversidad espacial y la ganancia de array del canal MIMO.

Siguiendo esta línea de investigación, esta tesis propone tres arquitecturas de combinación analógica de antena con el fin de reducir aún más la complejidad del sistema sin tener un alto impacto en el rendimiento. En la primera arquitectura, la que hemos denominado como RF-RWB (conformación de haz con peso real o real-weight beamforming) se aplica en cada rama de antena un sign switch seguido por un amplificador de ganancia variable (variable gain amplifier o VGA), que esencialmente aplica una multiplicacin con pesos reales directamente en el dominio de RF. El segundo esquema, la que hemos denominado como RF-EPB (conformación de haz con fase igual o equal-phase beamforming), sólo usa un VGA por cada rama de RF, que implementa una multiplicación con pesos reales y no negativos. Por último, la tercera arquitectura, que hemos denominado RF-EGB (conformación de haz con ganancia igual o equal-gain beamforming), sólo cambia las fases de las señales RF mediante los combinadores de fase analógicos en lugar de los moduladores vectoriales completos.

Desde el punto de vista banda base, cada arquitectura plantea un problema diferente del diseño de Los conformadores de haz (beamformers), donde los beamformers de transmisión/recepción se fuerzan a tener pesos reales, pesos reales no negativos o pesos complejos con módulos constantes, respectivamente. Suponiendo un conocimiento perfecto del canal en ambos lados de transmision y recepción, consideramos el problema de diseño de estos beamformers RF restringidos, ambos en escenarios de desvanecimiento plano (flat-fading) y bajo transmisiones de multiplexación por división de frecuencia ortogonal (orthogonal frequency division multiplexing o OFDM). En el primer caso, el problema consiste en la selección de los beamformers de transmisión y recepción que optimizan el rendimiento del sistema. En el segundo caso, consideramos un criterio general del beamforming, que depende de un parámetro único α. Este parámetro establece un compromiso entre la energía del canal SISO (una sóla entrada y salida o single-input single-output) equivalente (después de la aplicación de los pesos) y su planitud espectral. La función de coste propuesta adoptar los criterios más razonables para el diseño analógico de los beamformers de transmisión-recepción. Por lo tanto, para valores particulares del parámetro α el criterio propuesto se reduce a la minimización de el error cuadrático medio (criterio MinMSE), la maximización de la capacidad del sistema (criterio MaxCAP), o la maximización de la relación señal a ruido (criterio MaxSNR). En general, el criterio propuesto se reduce a un problema de optimización no convexa. Sin embargo, los casos SIMO (una sóla entrada y múltiples salidas o single-input multiple-output) y MISO (múltiples entradas y una sóla salida o multiple-input single-output) por MaxSNR, tienen cada uno una solución de forma cerrada o pueden ser reformulados como problemas convexos. Explotando este hecho, se utiliza un procedimiento de optimización alternativo para encontrar una solución subóptima para el caso MIMO. Mientras que para los demás criterios, se propone un algoritmo sencillo y eficiente de búsqueda de gradiente (gradient search). Los algoritmos propuestos para todos los criterios proporcionan muy buenos resultados en el estándar WLAN (por ejemplo 802.11a) basado en OFDM, con un método de inicialización adecuado. Por último, llegamos a la conclusión de que las arquitecturas propuestas representan una alternativa de bajo coste atractiva a los sistemas MIMO convencionales y a otras arquitecturas de combinación analógica de antenas (más costosas).

Abstract

The emergence of multiple antenna systems in wireless communications has gained much attention during the last decade. In multiple antenna systems, often called conventional multiple-input multiple-output (MIMO), all antenna paths must be independently acquired and processed at baseband. Consequently, for conventional MIMO, the hardware costs, size and power consumption are increased, and thus its application in the commercial deployment of multiple-antenna wireless transceivers is limited. A low-power and low-cost radio-frequency (RF) maximum-ratio beamforming (RF-MRB) architecture (developed by MIMAX EU-funded project) has been proposed to significantly decrease the hardware complexity by performing the adaptive weighting and combining of the antenna signals in the RF front-end. Although these analog combining architectures are restricted to process a single stream of data, they can still extract the spatial diversity and array gain of the MIMO channel.

Following this line of research, this thesis proposes three analog antenna combining architectures to further reduce the system complexity without having a high impact on performance. The first architecture, which we refer to as RF real-weight beamforming (RF-RWB) applies at each antenna branch a sign switch followed by a variable gain amplifier (VGA), which essentially implements a multiplication by real weighs directly in the RF domain. The second scheme, which we refer to as RF equal-phase beamforming (RF-EPB), uses only a VGA per RF branch, which implements a multiplication by a nonnegative real weight. Finally, the third architecture, which we refer to as RF equal-gain beamforming (RF-EGB), only changes the phase of the RF signals by means of analog phase shifters instead of complete vector modulators.

From a baseband point of view, each architecture poses a different beamforming design problem in which the transmit/receive beamformers are constrained to have real weights, nonnegative real weights, or constant-modulus complex weights, respectively. Assuming perfect channel knowledge at both the transmit and receive sides, we consider the problem of designing these constrained RF beamformers, both in flat-fading scenarios and under orthogonal frequency division multiplexing (OFDM) transmissions. In the first case, the problem consists in selecting the transmit and receive beamformers that optimize the system performance. In the second case, we consider

a general beamforming criterion which depends on a single parameter α. This parameter establishes a tradeoff between the energy of the equivalent single-input single-output (SISO) channel (after transmit-receive beamforming) and its spectral flatness. The proposed cost function embraces most reasonable criteria for designing analog transmit-receive beamformers. Hence, for particular values of α the proposed criterion reduces to the minimization of the mean square error (MinMSE criterion), the maximization of the system capacity (MaxCAP criterion), or the maximization of the received signal-to-noise ratio (MaxSNR criterion). In general, the proposed criterion results in a non-convex optimization problem. However, the MaxSNR single-input multiple-output (SIMO) and multiple-input single-output (MISO) cases either have a closed-form solution or can be reformulated as convex problems. Exploiting this fact, an alternating optimization procedure is used to find a suboptimal solution for the MIMO case. For the other criteria, we propose a simple and efficient gradient search algorithm. The proposed algorithms for all criteria provide very good results in practical OFDM-based WLAN standard such as 802.11a, with a proper initialization method. Finally, we conclude that the proposed architectures represent an attractive low-cost alternative to conventional MIMO systems and other (more costly) analog antenna combining architectures.

Notation and Acronyms

Used Notation

$\lvert\cdot\rvert$	Absolute value or set cardinality
$\lVert\cdot\rVert$	Euclidean norm
x	Scalar (lowercase boldface)
$\mathbf{x}$	Column vector (lowercase)
$\mathbf{x}[i]$	Instance of vector $\mathbf{x}$ at time step i
x_i	i-th component of vector $\mathbf{x}$
$\angle(\mathbf{x})$	Vector formed by the phase angles of $\mathbf{x}$
$\mathbf{X}$	Matrix (uppercase boldface)
$[\mathbf{X}]_{i,j}$	Element in row i and column j of the matrix $\mathbf{X}$
x^*	Complex conjugate of x
$\mathbf{X}^T$	Transpose of matrix $\mathbf{X}$
$\hat{\mathbf{x}}$	Estimate of $\mathbf{x}$
$\mathbf{X}^H$	Hermitian of matrix $\mathbf{X}$
$\mathbf{X}^{-1}$	Inverse of matrix $\mathbf{X}$
$\mathbf{X}^{1/2}$	Matrix square root
$\mathrm{tr}(\mathbf{X})$	Trace of matrix $\mathbf{X}$
$\mathrm{rank}(\mathbf{X})$	Rank of matrix $\mathbf{X}$
$\mathrm{diag}(\mathbf{X})$	Diagonal of a matrix $\mathbf{X}$
$\mathrm{vec}(\mathbf{X})$	Stacking of columns of a $(p \times q)$ matrix $\mathbf{X}$ into a $(pq \times 1)$ vector
$\mathrm{unvec}(\mathbf{x})$	Inverse of the $\mathrm{vec}(\mathbf{X})$ operation, i.e., $\mathrm{unvec}(\mathrm{vec}(\mathbf{X})) = \mathbf{X}$
$\mathbf{X} \succeq \mathbf{0}$	Means that $\mathbf{X}$ is Hermitian and positive semidefinite
$\mathbf{X} \geq \mathbf{0}$	Means that the elements of $\mathbf{X}$ are nonnegative

$\mathbb{R}$	Set of real numbers
$\mathbb{C}$	Set of complex numbers
$\Re(\mathbf{X})$	Real part of the complex matrix
$\mathbf{I}$	Identity matrix of appropriate dimensions
$\mathbf{0}$	Zero-matrix of appropriate dimensions
$E[x]$	Mathematical expectation of random variable x
$\otimes$	Kronecker product
$*$	Convolution
$\log_a(\cdot)$	Logarithm with respect to base a
$\frac{\partial}{\partial \mathbf{x}}$	Partial derivative with respect to $\mathbf{x}$
$\nabla_{\mathbf{x}}$	Gradient operator with respect to $\mathbf{x}$
$\mathcal{O}(\cdot)$	Order of the computational complexity
$f(x)$	Evaluation of a function $f = f(\cdot)$ in a point x
L	Number of channel taps

Acronyms

ADC	Analogue-to-digital converter
AWGN	Additive white Gaussian noise
BER	Bit Error Rate
CP	Cyclic prefix
CSI	Channel state information
DAC	Digital-to-analogue converter
DFT	Discrete Fourier transform
EGB	Equal-gain beamforming
EPB	Equal-phase beamforming
EVD	Eigenvalue decomposition
FFT	Fast Fourier transform
IDFT	Inverse discrete Fourier transform
IEEE	Institute of electrical and electronics engineers
IFFT	Inverse fast Fourier transform

i.i.d.	Independently and identically distributed
ISI	Inter-symbol interference
MIMO	Multiple-input multiple-output
MISO	Multiple-input single-output
MMSE	Minimum mean square error
MRB	Maximum-ratio beamforming
MRC	Maximum ratio combining
MRT	Maximum ratio transmission
MSE	Mean Square Error
OFDM	Orthogonal frequency-division multiplexing
QAM	Quadrature amplitude modulation
QPSK	Quadrature phase-shift keying
RF	Radio frequency
RWB	Real-weight beamforming
Rx	Receiver
SIMO	Single-input multiple-output
SISO	Single-input single-output
SNR	Signal-to-noise ratio
SVD	Singular value decomposition
Tx	Transmitter
WLAN	Wireless local area network

Table of Contents

Chapter 1

Introduction

1.1 Motivation

Wireless communication started in 19th century when Michael Faraday and James Maxwell predicted the existence of electromagnetic waves [Maxwell, 1865]. The theory of these radio waves was demonstrated by Heinrich Hertz in 1888 [Story, 1904]. In the first wireless systems the transmission of radio waves was only carried out over line-of-sight distances. These early communications networks were replaced in the 1890s when Guglielmo Marconi developed the telegraph network. Today, several types of wireless communications are based on new transmission techniques and have advanced rapidly to enable transmissions over larger distances with better quality, less power, and smaller, lower cost devices. They must operate reliably in various environments: macro, micro, and pico cellular; urban, suburban, and rural interior and exterior. In addition, they should enable people to reach tremendous amounts of information anywhere, anytime, with any mobile user terminal.

To exploit the benefits (e.g., diversity or multiplexing gain) obtained when multiple antennas are used at both the transmitter and the receiver, conventional multiple-input multiple-output (MIMO) systems require all antenna paths to be independently acquired and jointly processed at baseband. This increases the cost of the transceiver, which is approximately proportional to the number of analog-to-digital converters (ADCs) [Sandhu and Ho, 2003, Eickhoff et al., 2009]. For this reason, the implementation of conventional MIMO transceivers becomes a major problem in low-cost wireless terminals, where the hardware complexity is strictly limited. In order to increase the energy efficiency of such systems without excessively increasing the size and hardware cost, several schemes have been proposed based on shifting part of the spatial signal processing from the baseband to the radio-frequency (RF) front-end [Sandhu and Ho, 2003, Eickhoff et al., 2009, Vía et al, 2010a]. With this goal in mind, a RF-MIMO architecture that performs spatial processing directly in the

analog domain is currently being developed within the EU-funded project MIMAX[1] (MIMO systems for maximum reliability and performance). Although these analog combining architectures are restricted to process a single stream of data, they can still extract the spatial diversity and array gain of the MIMO channel.

In particular, the RF-MIMO architecture proposed in [Eickhoff et al., 2008,Eickhoff et al., 2009] uses at each branch a phase splitter and two variable gain amplifiers (VGA), which essentially implement a multiplication by a complex weight directly in the RF domain. Subsequently, the weighted RF signals are added before acquisition. In the case of flat-fading channels and assuming perfect channel state information, this RF-MIMO scheme, which we refer here to as maximum-ratio beamforming (RF-MRB), can implement the optimal MIMO beamforming solution by properly choosing the gains of the in-phase and quadrature signals at each branch. The problem is more involved in the case of frequency selective channels and orthogonal frequency division multiplexing (OFDM) transmissions, because the same analog beamformer is applied to all the subcarriers and thus the problem is inherently coupled [Vía et al, 2010a]. The RF-MRB architecture and its beamforming design algorithms have been thoroughly studied in several publications [Eickhoff et al., 2008, Eickhoff et al., 2009, Vía et al., 2009b, González et al., 2010, Vía et al., 2010b, Elvira and Vía, 2009].

1.2 Original Contributions

The works on RF-MRB architecture suggest that the performance gap with respect to conventional architectures is justified by the reduction in hardware cost and power consumption. Following this line of research, the motivation of this thesis is to investigate other alternative analog antenna combining architectures that could further reduce the system complexity without having a high impact on performance.

Analogously to RF-MRB, we consider three alternative architectures for analog antenna combining scheme to exploit spatial diversity and array gain. The basic idea of these new architectures is to simplify the hardware complexity of the RF-MRB transceiver. Specifically, they can significantly reduce the circuit complexity, power consumption, system costs and size using phase shifters and VGAs at each RF branch. Taking into account the nature of their associated beamformers these new architectures are:

1. The RF real-weight beamforming (RF-RWB) architecture applies at each branch a sign switch (i.e., a controllable $0°/180°$ phase shifter) followed by a VGA, which jointly permit to change the amplitude and sign of each incoming RF

[1] MIMAX is the European Union funded research project that aims to investigate and develop a more powerful WLAN device, see Section 3.2 for more details.

signal before adding them up. Specifically, this architecture uses a set of beamformers with real coefficients to perform analog antenna combining scheme.

2. RF equal-phase beamforming (RF-EPB) architecture, which uses only a VGA per RF branch. This architecture uses a nonnegative real weight to scale the amplitude of each transmitted or received signal without shifting its phase.

3. RF equal-gain beamforming (RF-EGB) architecture, which changes only the phases of the RF signals by means of analog phase shifters. Specifically, the vector modulators used in RF-MRB are substituted by wideband analog phase shifters.

From a baseband point of view, these three RF-MIMO architectures pose different constrained beamforming problems in which the beamformer weights, instead of being complex numbers (like those of the RF-MRB or the conventional MIMO schemes) are constrained to be real (RF-RWB), nonnegative real (RF-EPB) or constant-modulus complex numbers (RF-EGB), respectively. The main emphasis of this dissertation is on the beamforming design problems and system complexity; the tradeoffs related to the system size and power consumption of the different topologies require a separate study and falls outside the scope of this work.

Assuming perfect channel knowledge at the transceiver, we consider the problem of designing the transmit and receive RF beamformers. We first consider the case of flat-fading MIMO channels and then we extend the study to frequency-selective channels using multicarrier transmissions. Under OFDM, a general beamforming criterion is proposed, which depends on a single parameter α. This parameter establishes a tradeoff between the energy of the equivalent SISO channel (after transmit-receive beamforming) and its spectral flatness. The proposed cost function embraces most reasonable criteria for designing analog transmit-receive beamformers. Hence, for particular values of α the proposed criterion reduces to the minimization of the mean square error (MSE), the maximization of the system capacity, or the maximization of the received signal-to-noise ratio (SNR). Taking into account the constraints introduced by the different architectures, the beamforming design problems for MIMO channels are highly non-convex, and we have to resort to a set of iterative algorithms based on the successive solution of the equivalent single-input multiple-output (SIMO) and multiple-input single-output (MISO) problems. These iterative methods are guaranteed to converge (although not necessarily to the global optimum), and with a proper initialization method they provide very satisfactory results, both in the case of flat-fading and frequency-selective channels.

1.3 Thesis Outline

The remaining chapters of this thesis are organized as follows:

- **Chapter 2** summarizes the benefits of multiple antenna systems for wireless communications: spatial multiplexing techniques, spatial diversity techniques, and beamforming techniques (array gain). Then, it gives an overview on the system models of wireless channels used through this thesis to design of conventional and alternative MIMO architectures. It focuses on beamforming design for the conventional MIMO architecture under OFDM transmission, and introduces some concepts related to the performance of wireless communications. Finally, the IEEE 802.11a standard is reviewed and a brief summary concludes this chapter.

- **Chapter 3** presents the maximum-ratio beamforming architecture (RF-MRB) developed in the MIMAX project. Some of their details, such as frame format and channel estimation will be reviewed, and their benefits (i.e., spacial diversity, multiplexing and array gains) will be pointed out. Additionally, the extension to the multicarrier transmission for RF-MRB architecture is discussed. More importantly, Chapter 3 introduces the alternative RF architectures. That is, the real-weights beamforming (RF-RWB), the equal-phase beamforming (RF-EPB), and the equal-gain beamforming (RF-EGB), which are based on real, nonnegative real, and constant-modulus complex weights, respectively. Finally, a brief summary concludes the chapter.

- **Chapter 4** addresses the problem of designing the RF beamformers in the case of flat-fading channels. The closed-form solutions in the SIMO case are obtained for the different architectures. An alternating optimization algorithm is proposed to obtain the transmit and receive beamformer vectors for the MIMO case. Finally, the proposed simplified RF-MIMO architectures are evaluated by means of some numerical examples and a brief summary concludes the chapter.

- **Chapter 5** addresses the analog beamforming design problem for frequency-selective channels. The proposed RF combining architectures are now extended to broadband transmissions employing orthogonal frequency division multiplexing (OFDM) modulation. A general beamforming criterion which depends on a single parameter α is presented. Based on this parameter, three design criteria are obtained: the maximization of the received SNR (MaxSNR, $\alpha = 0$), the maximization of the system capacity (MaxCAP, $\alpha = 1$), and the minimization of the MSE (MinMSE, $\alpha = 2$) of the optimal linear receiver. The associated optimization problem is then analyzed, and the proposed beamforming algorithms

are also introduced. Finally, some simulation results and a brief summary conclude the chapter.

- **Chapter 6** summarizes the main results of this thesis, provides a list of derived publications, and suggests some future research lines.

Chapter 2

Multiple Antenna Communications

2.1 Introduction

The use of multiple antennas at the transmitter and the receiver has revolutionized wireless communications over the past decade. In the 90s, Foschini and Gans in [Foschini and Gans, 1998] and Telatar in [Telatar, 1999] predicted large capacity gains by using multiple antennas at both link ends. Unlike single-input single-output (SISO) systems, in multiple-input multiple-output (MIMO) each pair of transmit and receive antennas provides a signal path from the transmitter to the receiver. Specifically, it has been shown that if the signals fading between pairs of transmit and receive antenna elements are independent and identically distributed (i.i.d.), the capacity of MIMO systems can increase linearly with the number of antennas [Foschini and Gans, 1998].

These idealized conditions are however, not fully met in practice, because the performance of a real MIMO system is affected by non-ideal propagation conditions [Gesbert et al., 2003] and by mutual coupling effects due to finite spacing of antenna elements [Wallace and Jensen, 2004, Waldschmidt et al., 2004]. Additionally, the use of this scheme increases the hardware cost, complexity and power consumption. These drawbacks might explain, at least partially, why MIMO technologies have not found yet widespread use in low-cost wireless terminals. One way to overcome these drawbacks is to develop new simplified RF-MIMO schemes (such as those proposed in this thesis) that perform spatial processing directly in the analog domain, while still retaining some of the benefits provided by conventional MIMO (e.g., diversity and array gains).

Three types of fundamental gains can be obtained when multiple antennas are used in wireless communications systems at both the transmitter and the receiver [Gesbert et al., 2003, Loyka and Levin, 2007, Loyka and Levin, 2010]:

- Multiplexing gain r, shows how fast the outage capacity $C_{out,p}$ for a probability of outage p scales with increasing SNR, i.e.,

$$r = \lim_{\text{SNR}\to\infty} \frac{C_{out,p}}{\log_2(\text{SNR})}.$$

In the case of packet-based transmissions, transmitting at a given fixed rate of $C_{out,p}$ bps, $p^o/_o$ of the frames would be lost, while the other $1 - p^o/_o$ will be decoded without error.

- Diversity gain G_d, is defined as the asymptotic negative slope of the bit error rate (BER) or frame error rate (FER) versus the SNR in log-log scale,.i.e.,

$$G_d = \lim_{\text{SNR}\to\infty} -\frac{\log_2(\text{BER})}{\log_2(\text{SNR})}.$$

- Array gain is defined as the increase in average output SNR at the input of the receiver.

However, these three desirable attributes usually compete with one another, for example, an increase in data rate will in general come at the expense of an increase in either the error rate or transmit power. Specifically, it was proved in [Zheng and Tse, 2003,Tse and Viswanath, 2005], that both maximum gains[1] cannot be simultaneously achieved. In fact, for any MIMO communication system there is a tradeoff between both quantities (i.e., diversity and multiplexing gains) [Loyka and Levin, 2010], which can be formally expressed as

$$G_d(r) = (n_T - r)(n_R - r), \quad 0 \le r \le \min(n_T, n_R). \tag{2.1}$$

As can be seen from Figure 2.1, any MIMO scheme that aims at improving the transmission reliability by exploiting all the diversity gain, must transmit along a single spatial mode at a fixed rate (multiplexing gain). For example, if a MIMO system requires to improve the transmission reliability at the diversity gain $G_d = 9$, the multiplexing gain is fixed only at $r = 1$. Conversely, a MIMO system that exploit all the multiplexing gain and sends information along all the spatial modes (probably with some kind of adaptive modulation scheme), then it will not achieve spatial diversity gain.

This chapter summarizes the benefits of multiple antenna systems for wireless communications in Section 2.2. In Section 2.3, we will give an overview of the system models used through this thesis. Section 2.4 will focus on beamforming design for conventional MIMO architecture under orthogonal frequency division multiplexing (OFDM). Finally, in Section 2.5, the IEEE 802.11a standard is reviewed, then a brief summary concludes this chapter.

[1]For $n_T \times n_R$ (n_T, n_R are the number of transmit, receive antennas) MIMO system the maximum achievable diversity gain is $G_{d,max} = n_T n_R$, whereas the maximum achievable multiplexing gain is $r_{\max} = \min(n_T, n_R)$.

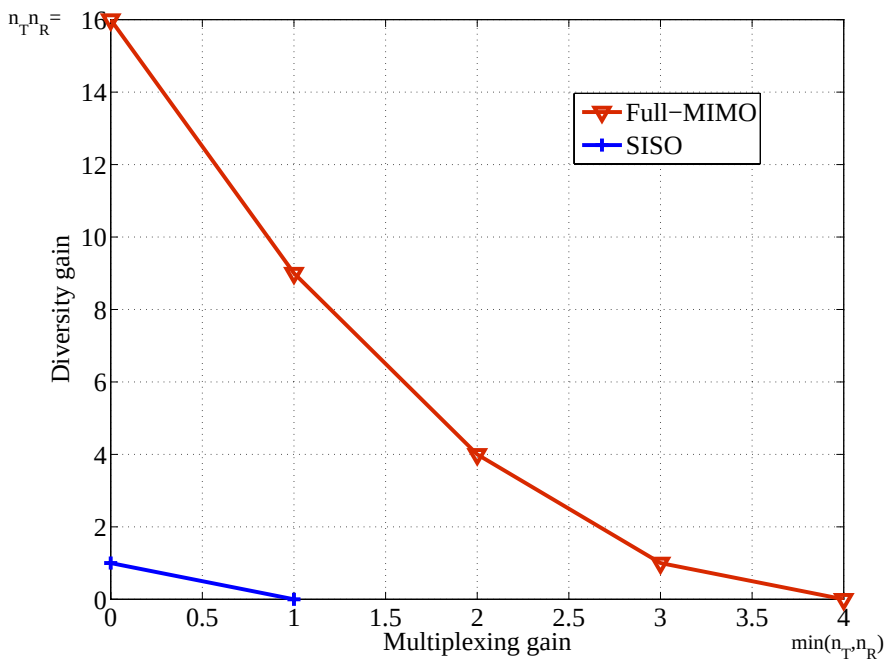

Figure 2.1: Achievable diversity-multiplexing curves for 4×4 system with Full-MIMO and SISO schemes.

2.2 Benefits of Multiple Antennas for Wireless Communications

The three types of multiple antenna techniques are discussed in detail in this section. In the first subsection, we will address spatial multiplexing techniques which permit to increase the transmitted data rate and hence the system capacity (multiplexing gain). Subsection 2.2.2 focuses on spatial diversity techniques, that increase the system reliability by decreasing the bit error rate (diversity gain). Finally, we introduce beamforming techniques used to improve the SNR by decreasing the required transmit power (array gain) of wireless systems.

2.2.1 Spatial Multiplexing

Spatial multiplexing techniques are used to achieve multiplexing gain benefit. In these techniques, a high rate signal is demultiplexed into multiple lower rate streams and each stream is transmitted from a different transmit antenna in the same frequency channel. At the receiver, these streams can be separated by means of MIMO decoding techniques. Spatial multiplexing is a very powerful technique for increasing channel capacity in comparison to single-antenna systems, and it can be used with or without

transmit channel knowledge [Mishra and Chauhan, 2011]. The maximum number of spatial streams depends on the number of antennas at the transmitter and at the receiver. In fact, the capacity of a MIMO system with n_T transmit and n_R receive antennas grows linearly with the minimum of n_T and n_R.

The basic structure of a spatial multiplexing system is illustrated in Figure 2.2, where the information bit sequences after the demultiplexing technique are modulated and transmitted simultaneously over the MIMO channel. At the receiver, the transmitted sequences are separated and further processed using a detection algorithm to extract the desired signal.

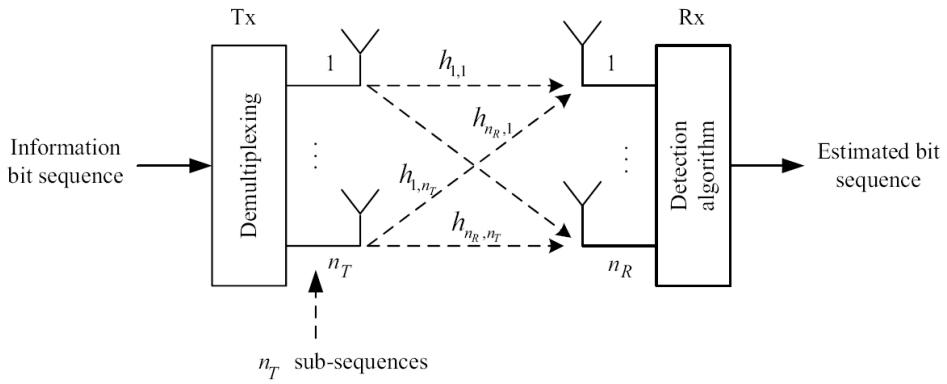

Figure 2.2: Basic principle of spatial multiplexing.

In practice, the presence of ISI due to multipath signal propagation in wireless channels can cause a significant degradation in the system performance. One approach to circumvent the ISI problem is to use a multicarrier transmission scheme and multiplex data symbols (e.g. OFDM modulation) onto quasi-flat parallel narrow subchannels. Thus, the transmission schemes developed for flat-fading channels can be applied within each subchannel.

2.2.2 Spatial Diversity

Spatial diversity can be considered as the maximum number of independent copies of the transmitted signal in a particular communication system. It may be obtained by transmitting the data signal over multiple independent fading paths and performing proper combining at the receiver [Buehrer et al., 2002]. This diversity technique is an attractive alternative that provides an increased average received SNR without sacrificing time or bandwidth, instead of time or frequency diversity that incurs in an expense of time or bandwidth, respectively. This is accomplished on the basis of a diversity gain.

Diversity reception techniques are applied in systems with a single transmit antenna and multiple receive antennas. With this setup, each receive antenna receives copies of the transmitted signal through different channels. As can be seen from Figure 2.3, this technique performs a linear combination of the individual received signals, in order to provide a diversity gain. There have been numerous methods proposed in the literature for combining the received signals. In the case of flat-fading channels, the optimum combining strategy in terms of maximizing the SNR at the combiner output is maximum ratio combining (MRC) [Brennan, 2003], which requires perfect channel knowledge at the receiver. In the literature, there are several suboptimal combining strategies to provide diversity gain, such as equal gain combining (EGC), where the receive signals are co-phased and added up, or selection diversity (SD), where the received signal providing the maximum SNR is selected, whereas all other received signals are discarded [Brennan, 2003, Vucetic and Yuan, 2003]. All three combining techniques achieve full diversity with regard to the number of the receive antennas [Balaban and Salz, 1992]. Note that, when using these combining schemes, the signals on the various antennas are multiplied by a complex coefficient w_i. Hence, diversity reception (or combining) can actually be seen as a form of beamforming where the received signal is weighted in amplitude and in phase by the complex weight vector $\mathbf{w} = [w_1, \ldots w_{n_R}]^T$, as shown in Figure 2.3. In the case of frequency-selective channels, optimal combining techniques were for example considered in [Eng and Milstein, 1996].

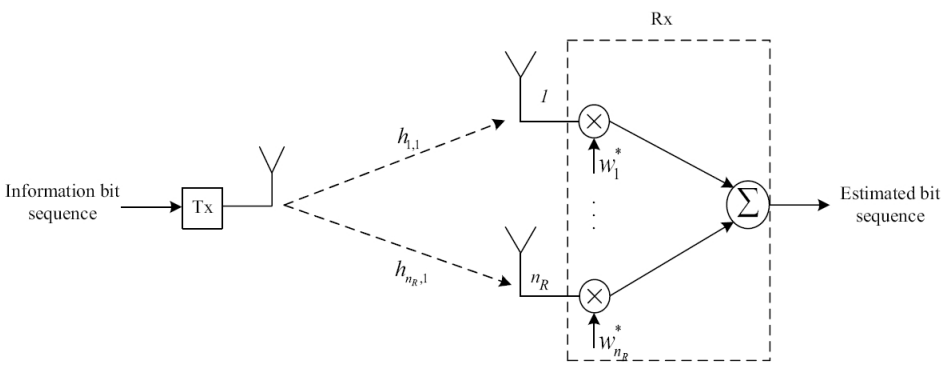

Figure 2.3: Basic principle of diversity combining system.

The second concept of spatial diversity (transmit diversity) is depicted in Figure 2.4. With transmit diversity, multiple antennas are only required at the transmitter, whereas multiple receive antennas are optional; these can be utilized to further improve performance. The main objective of transmit diversity is to provide a diversity or coding gain by sending redundant replicas of the transmitted information through

independent faded channels. Note that the same information is transmitted by multiple antennas (in contrast to spatial multiplexing, where independent bit sequences are transmitted), thus providing independent fading channels between transmitter and receiver. In addition, to achieve low correlation among these channels, the antennas must be sufficiently far from each other. Therefore, an adequate preprocessing of the signals is performed prior to transmission, typically with channel knowledge at the transmitter. In wireless mobile networks, to enhance the crucial downlink, and to reduce the cost and size of such terminals, transmit diversity is required and applied at the base station.

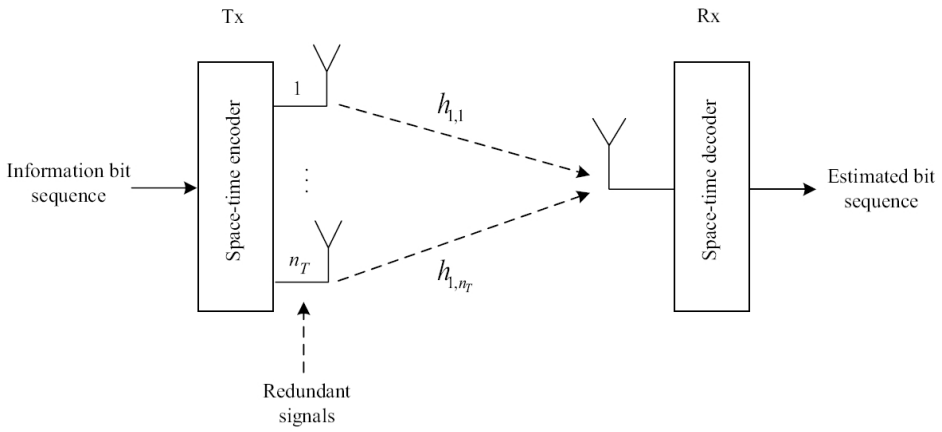

Figure 2.4: Basic principle of spatial transmit diversity.

2.2.3 Array Gain

The potential advantages of using multiple antennas do not end with increasing data rates (multiplexing gain) and improving error rates (diversity gain). They can also be utilized to improve the received signal-to-noise ratio (SNR) at the receiver in a single-user scenario. Furthermore, they can be used in multiuser scenarios to suppress co-channel interference (CCI), i.e., to improve the signal-to-interference-plus-noise ratio (SINR) at the receiver.

In this dissertation, beamforming techniques will be considered in order to achieve the array gain, and the beamforming techniques will be only addressed in a single user scenario. In this case, not only the phases of the received signals are handled, but the basic idea consists of applying the complex weights (gain factor and phase shift) or beamformers to the received signals as shown in Figure 2.5. Specifically, beamforming exploits the channel impulse response of each antenna element to find array weights that satisfy a desired criterion, typically maximizing the SNR. As long as the channel response is known at the transmitter, this technique steers the transmit

signal to the desired user by exploiting the eigenvalue decomposition of the channel response. This beamforming technique is more viable in realistic wireless broadband environments, which are expected to have significant local scattering.

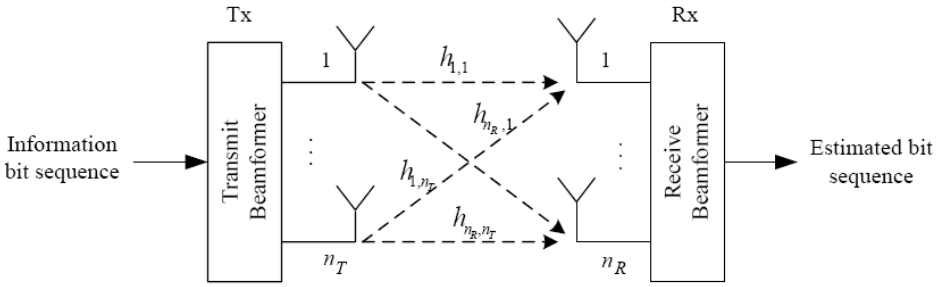

Figure 2.5: Basic principle of beamforming technique.

Analogously to spatial diversity, and as can be seen from Figure 2.5, beamforming techniques can be implemented at either the transmitter or the receiver to provide an array gain. Specifically, through this thesis, we use the term transmit beamforming to refer to a system in which the weights (or beamformers) are applied at the transmitter, and we use receive beamforming (or combining) to refer to those in which the weights are applied at the receiver [Lo, 1999]. The scenario is equivalent to the classical MRC (maximum ratio combining) technique [Jakes, 1974], where the signals from the received antenna elements are weighted such that the SNR of their sum is maximized.

2.3 System and Channel Model

In wireless communication channels, signals are free to travel in any direction, and they can be attenuated, reflected, and scattered by many obstacles in the direction of propagation. These phenomena affect the characteristics (amplitude, phase, polarization) of the signals and can be detrimental to a wireless communication systems if not well understood and accounted for. In this section, we present a brief overview of the basic properties for both flat-fading and frequency-selective channels used in this thesis for transceiver design in the case of MIMO systems.

2.3.1 Flat-Fading Channel

In practice, the signal reaches the receiver through multiple paths with attenuations and scattering phenomena. These paths usually have different lengths (delays), arrive from different directions (angles), and have different strengths. In the absence of multipath, the signal fades as the distance between the transmitter and the receiver grows. On the other hand, fading can be considered even if the transmitter and the

receiver are close to each other. In this case, fading occurs because of destructive interfering paths.

There are several key parameters that can be used to capture the basic characteristics of fading models. The most important key parameters according to [Tse and Viswanath, 2005] are:

- Delay spread T_d, measures the maximum delay between the shortest and the longest paths [Tse and Viswanath, 2005, Ergen, 2009]. The delay spread will be low in indoor environments which are scattering rich but short distance. On the other hand, the delay spread will be high in outdoor environments (long distances and scattering rich).

- Coherence bandwidth $(\Delta f)_c$, measures the correlation of the channel at two different frequencies [Ergen, 2009]. It is the inverse of the delay spread given as

$$(\Delta f)_c \approx \frac{1}{T_d}. \tag{2.2}$$

- Coherence distance r_c, is the minimum distance between two points in space where the channel statistics are independent, and it depends on the carrier wavelength λ_0. In other words, r_c is defined as the minimum distance between a constructive interference and a destructive interference.

- Angular spread θ_d, is defined as the maximum angle between paths with significant energy. The angular spread in indoor environments is usually high, while in outdoor environments, it will be high at the mobile stations (for example, cellular networks), and low for the base stations.

- Coherence time $(\Delta t)_c$, gives a measure of temporal duration in which we can consider that the channel is essentially invariant. In other words, the coherence time depends on the velocity of both the transmitter and the receiver.

- Doppler spread D_s: When a signal is sent from a transmitter to a receiver and the latter is moving at a certain speed, there is a change in signal frequency. This phenomenon is called Doppler shift [Vucetic and Yuan, 2003, Ergen, 2009]. The doppler spread D_s is defined as the maximum difference in Doppler shift between any pair of paths. In other words, D_s is also inversely proportional to the coherence time $(\Delta t)_c$:

$$D_s = \frac{1}{(\Delta t)_c}. \tag{2.3}$$

In addition, for flat-fading channels the coherence bandwidth is greater than the bandwidth of the transmitted signal B_s [Goldsmith, 2005, Tse and Viswanath, 2005]. In the time domain, the delay spread will be smaller than the symbol time T_s. Then, all the frequency components of the transmitted signal undergo the same attenuation and phase shift when propagating through the channel.

System Model

In order to describe the system model for flat-fading channels, we consider a communication link between a transmitter and a receiver with n_T and n_R antennas, respectively. This system is conventionally referred to as $n_T \times n_R$ MIMO system. Initially, the signal bandwidth is assumed to be less than the coherence channel bandwidth, therefore, all frequency components of the signal will experience the same magnitude of fading. Thus, the complex baseband model of the MIMO system at time index n can be described as

$$\mathbf{y}\,(n) = \mathbf{H}\mathbf{s}\,(n) + \mathbf{n}(n), \tag{2.4}$$

where $\mathbf{s} \in \mathbb{C}^{n_T \times 1}$ and $\mathbf{y} \in \mathbb{C}^{n_R \times 1}$ are the transmitted and the received symbol vectors, respectively, and $\mathbf{H} \in \mathbb{C}^{n_R \times n_T}$ is the channel matrix with entries $h_{i,j}$. Each $h_{i,j}$ corresponds to the channel magnitude and phase response between the j-th transmit and the i-th receive antenna. Furthermore, $\mathbf{n} \in \mathbb{C}^{n_R \times 1}$ is the noise vector with its entries being independent and identical distributed (i.i.d) complex Gaussian random variables with zero-mean and variance σ_n^2.

2.3.2 Frequency-Selective Channel

The impulse response of a frequency-selective fading channel has a delay spread that is greater than the time duration of the transmitted signal waveform, i.e., the spectrum of the transmitted signal has a bandwidth which is greater than the coherence bandwidth of the channel.

To describe the system model in the case of frequency-selective channels, we consider a channel that extends over L symbols, which can be described as a tapped delay line. In this case, for each of the L channel taps, the MIMO channel matrix can be written as $\mathbf{H}\,(l) \in \mathbb{C}^{n_R \times n_T}$, where $l = 0, \ldots, L-1$. Thus, the MIMO system model is given by

$$\mathbf{y}\,(n) = \sum_{l=0}^{L-1} \mathbf{H}\,(l)\,\mathbf{s}\,(l-n) + \mathbf{n}(n). \tag{2.5}$$

2.4 Beamforming for Conventional MIMO

2.4.1 Conventional MIMO Architecture

In this section, we present a conventional MIMO architecture, where the implementation of beamformers can be done in baseband, by first converting all signal information to the digital domain [Sandhu and Ho, 2003]. The general block diagram of this architecture is displayed in Figure 2.6, which shows the receiver side.

In this scheme, the received signal at each antenna branch must be downconverted and analog-to-digital converted (ADC) before combining. The downconversion to the baseband domain can be done based on I/Q demodulator, then two ADCs are required to sample both the in-phase and quadrature components of the baseband signal. In baseband, the complex weight vector **w** can be applied in the digital domain to combine the complex-baseband signals from each element. Therefore, performing the beamforming functions in the digital domain provides better performance than other beamforming schemes. It also makes the system highly flexible, as it is relatively easy to design the beamformers.

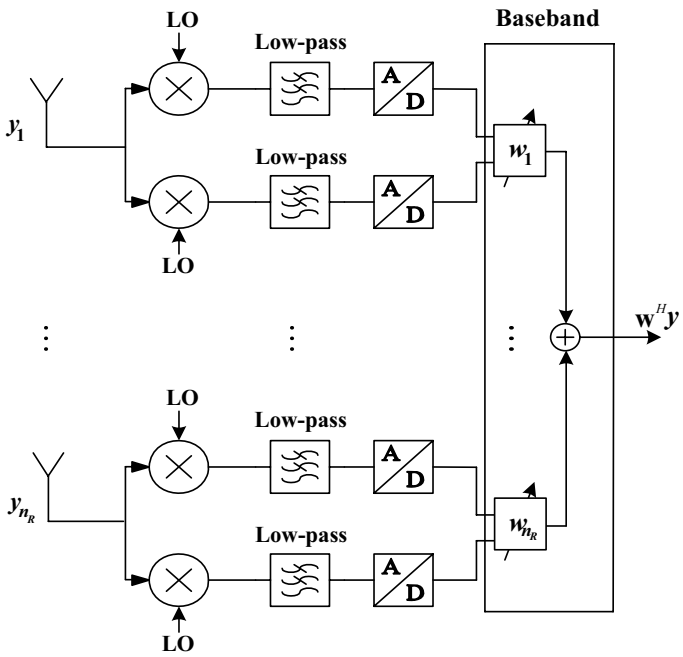

Figure 2.6: Conventional MIMO beamforming in the baseband domain.

Despite of the high flexibility provided by this scheme, its implementation into wireless communication transceivers is still limited by two important drawbacks: First, a digital beamformer requires a complete transceiver chain per antenna. This will result in a significant increase in cost and power consumption, which limits the scalability (in

the number of antennas) of this architecture. Second, the cost of conventional MIMO transceiver is approximately proportional to the number of used ADCs [Sandhu and Ho, 2003]. The power consumption of these ADCs is a major issue in the implementation of this architecture, as it can significantly reduce the battery life of small wireless equipments, which require a low power consumption.

On the other hand, the crucial points in the beamforming design scheme are the complexity, robustness and power dissipation. For that reason, other approaches will be proposed in order to reduce the hardware complexity and the implementation cost, which will be the main motivation of the next chapter.

2.4.2 System Model Under OFDM Transmissions

OFDM Basics

Multiple antenna systems can be used in combination with orthogonal frequency division multiplexing (OFDM) modulation to transmit data in parallel mode. In this scheme, the data is modulated on a set of parallel subcarriers separated by a minimum frequency bandwidth to maintain the orthogonality property. Specifically, each subcarrier uses a conventional modulation scheme (such as quadrature amplitude modulation (QAM) or phase-shift keying (PSK)) at a low symbol rate, maintaining total data rates similar to conventional single-carrier modulation schemes in the same bandwidth.

The most important advantage of OFDM over single-carrier schemes is its ability to cope with severe channel conditions (for example, narrowband interference and frequency-selective fading due to multipath) without complex equalization filters. Channel equalization is simplified because OFDM may be viewed as using many slowly-modulated narrowband signals rather than one rapidly-modulated wideband signal. The low symbol rate makes the use of a guard interval between symbols affordable, making it possible to handle time-spreading and eliminate intersymbol interference (ISI). For more details about this modulation technique see [Bingham, 1990, Bhai et al., 2004, Wang and Giannakis, 2000] and the references therein.

MIMO-OFDM System Model

In this subsection we focus on the general system model for conventional MIMO architecture under OFDM transmission in frequency-selective channels. Let us consider a MIMO system with n_T transmit (Tx) and n_R receive (Rx) antennas, and with unit-energy transmit and receive beamformers defined by the baseband weights in Figure 2.6. Assuming a transmission scheme based on OFDM with N_c data-carriers and using a cyclic prefix longer than the channel impulse response, the communication

system after Tx-Rx baseband beamforming may be decomposed into the following set of parallel and non-interfering single-input single-output (SISO) equivalent channels

$$y_k = \mathbf{w}_{R,k}^H \mathbf{H}_k \mathbf{w}_{T,k} s_k + \mathbf{w}_{R,k}^H \mathbf{n}_k, \qquad k = 1, \ldots, N_c, \tag{2.6}$$

where $y_k \in \mathbb{C}$ is the observation associated to the k-th data carrier, $s_k \in \mathbb{C}$ is the transmitted symbol, $\mathbf{n}_k \in \mathbb{C}^{n_R \times 1}$ represents the complex circular i.i.d. Gaussian noise with zero mean and variance σ^2, $\mathbf{w}_{T,k} \in \mathbb{C}^{n_T \times 1}$ and $\mathbf{w}_{R,k} \in \mathbb{C}^{n_R \times 1}$ are the transmit and receive beamformers in baseband (a pair of beamformers for each subcarrier k), and $\mathbf{H}_k \in \mathbb{C}^{n_R \times n_T}$ represents the MIMO channel for the k-th data-carrier.

2.4.3 Optimum Weights for the Conventional MIMO Architecture

This subsection is dedicated to the evaluation of conventional MIMO beamforming solutions applied to the frequency-selective channel models. In such channels, the conventional OFDM-MIMO receiver computes the DFT of each baseband signal and hence it can apply the optimal processing independently for each subcarrier. This scheme is sometimes called post-DFT and (in this dissertation) we will also refer to it as Full-MIMO processing.

Subsequently, the considered baseband Tx-Rx beamforming pair is designed for maximizing the received signal-to-noise ratio (SNR) at the k-th subcarrier. From the signal model presented in (2.6), under the assumption of flat-fading channel $\mathbf{H}_k$, and taking into account the power constraint at the transmitter, as well as the unit energy beamformers $\|\mathbf{w}_{T,k}\|^2 = \|\mathbf{w}_{R,k}\|^2 = 1$ for the k-th subcarrier, the SNR at the k-th subcarrier is expressed as

$$\mathrm{SNR}_k = \frac{E\left[\left|\mathbf{w}_{R,k}^H \mathbf{H}_k \mathbf{w}_{T,k} s_k\right|^2\right]}{E\left[\left|\mathbf{w}_{R,k}^H \mathbf{n}_k\right|^2\right]} = \frac{\left|\mathbf{w}_{R,k}^H \mathbf{H}_k \mathbf{w}_{T,k}\right|^2}{\sigma_n^2}. \tag{2.7}$$

In order to deduce the expression of the optimum Tx-Rx beamformer pair, the eigendecomposition of the channel matrix $\mathbf{H}_k$ is performed. More specifically, the optimal beamformers for the k-th subcarrier are given by the singular vectors associated to the largest singular value of $\mathbf{H}_k$. It should be noted that the optimization procedure for conventional MIMO-OFDM beamforming design requires full channel knowledge to obtain the optimal weights, $\mathbf{w}_{R,k}$, and $\mathbf{w}_{T,k}$, per subcarrier. This technique is also referred to as dominant eigenmode transmission (DET) [Andersen, 2000, Dahl et al., 2004], because the transmission occurs only along the dominant channel eigenmode.

Computational Complexity of Conventional MIMO-OFDM Systems

Under OFDM transmission, the conventional MIMO architecture in Figure 2.6 requires a separate DFT block for each antenna branch at the receiver (and a separate IDFT block at the transmitter). Thus, the signals in the individual receive antennas need to be processed by a separate N_c-point DFT. In practical communication systems, a fast Fourier transform (FFT) is used instead of DFT, although the computational complexity is still very important. Therefore, according to [Lee, 2009], the total computational complexity cost required to compute an N_c-point FFT or inverse FFT will be in the order of $\mathcal{O}\left(N_c \log_2 N_c\right)$ and thus, the overall computational complexity required for n_R received antennas amounts to $\mathcal{O}\left(n_R N_c \log_2 N_c + n_R N_c\right)$.

On the other hand, we take into account the computational complexity associated to compute the weight vector $\mathbf{w}_{R,k}$ per subcarrier k. Thus, in the case of conventional MIMO-OFDM systems, N_c eigenvalue decompositions (EVDs) blocks are needed to compute N_c beamvectors per subcarrier k. Therefore, from [Nesterov and Nemirovsky, 1994] a direct EVD method typically has a cost of $\mathcal{O}\left(n^3\right)$ operations for a square matrix of size n. In the considered case, the matrices $\mathbf{H}_k^H \mathbf{H}_k$ (for $k = 1, ..., N_c$) are of size $n_R \times n_R$ and thus, the total complexity of N_c EVDs will be of order $\mathcal{O}\left(N_c n_R^3\right)$.

2.5 Overview of IEEE 802.11a Standard

The first wireless local area network (WLAN) standard created by the Institute of Electrical and Electronics Engineers (IEEE) was the IEEE 802.11 standard. The IEEE 802.11 WLAN standard defines a set of specifications for medium access control (MAC) layer, MAC management protocols and services, and a physical layer (PHY).

The IEEE 802.11a WLAN is one of the 802.11 standard family which has been developed to extend the frequency band to 5 GHz. The PHY layer of IEEE 802.11a is based on OFDM modulation and provides eight different PHY modes with data rates ranging from 6 Mbps up to 54 Mbps [Yang et al., 2007, Ohrtman and Roeder]. This scheme provides higher data rates and bandwidths for wireless systems which have an increasing number of users. The basic OFDM parameters of IEEE 802.11a are summarized in Table 2.1 [IEEE 802.11a standard, 1999].

2.5.1 IEEE 802.11a OFDM PHY Layer and Frame Format

The 802.11 PHY layer is the interface between the MAC and the wireless medium where frames are transmitted and received. The frame exchange between MAC and PHY is generated in IEEE 802.11a PHY based on OFDM to mitigate the multipath effects without sacrificing transmission rate. Under OFDM transmissions, PHY layer splits the information signal across 52 separate subcarriers; four subcarriers are pilot

Parameter	Value
N_{FFT}: FFT/IFFT length	64
N_p: Number of pilot subcarriers	4
N_d: Number of data subcarriers	48
N_c: Number of total subcarriers	52 ($N_p + N_d$)
Δf: Subcarrier frequency spacing	312.5 kHz (=20 MHz/N_{FFT})
T_{FFT}: FFT/IFFT period	3.2 μs ($1/\Delta f$)
T_{GI}: Guard interval duration	0.8 μs ($T_{FFT}/4$)
T_{SYMBOL}: Total OFDM symbol duration	4.0 μs ($T_{GI} + T_{FFT}$)
BW: Occupied bandwidth	16.6 MHz ($\Delta f(N_c + 1)$)

Table 2.1: OFDM parameters of the IEEE 802.11a standard.

Mode	Modulation	Code rate	Data rate
1	BPSK	1/2	6 Mbps
2	BPSK	3/4	9 Mbps
3	QPSK	1/2	12 Mbps
4	QPSK	3/4	18 Mbps
5	16-QAM	1/2	24 Mbps
6	16-QAM	3/4	36 Mbps
7	64-QAM	2/3	48 Mbps
8	64-QAM	3/4	54 Mbps

Table 2.2: Eight PHY modes of the IEEE 802.11a PHY layer.

signals (for synchronization), and the remaining 48 subcarriers are considered to transmit the information bearing signal. The IEEE 802.11a PHY supports eight PHY modes (transmissions) with different modulation schemes and coding rates. Table 2.2 lists the data rate, modulation scheme, and coding rate.

The basic frame format of IEEE 802.11a based OFDM transmission is shown in Figure 2.7. At the beginning of the frame, a preamble composed of 10 repetitions of a short training sequence is used for signal detection, automatic gain control (AGC), timing acquisition and coarse frequency offset correction. This preamble is followed by two repetitions of a long training sequence, which is used for SISO channel estimation and fine frequency acquisition. The signal field is an OFDM symbol that contains information regarding length, modulation type and coding rate of the data field, which is composed of up to 4095 bytes. It is transmitted with the most robust combination of BPSK modulation and coding rate of $R = 1/2$.

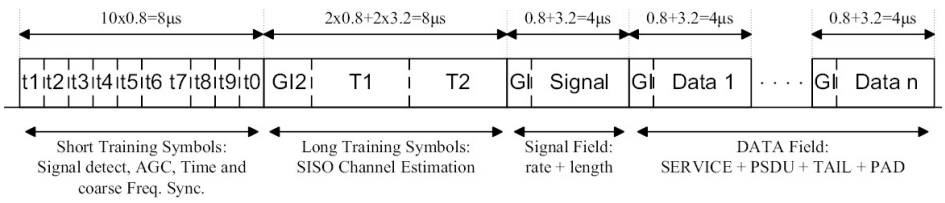

Figure 2.7: IEEE 802.11a frame format.

2.6 Summary

Wireless systems with multiple transmit and receive antennas, so-called multiple-input multiple-output (MIMO) systems, offer three types of fundamental gains over systems employing a single antenna at both ends of the link. In principle, they can be utilized to achieve diversity, multiplexing and array gains.

In the first part of this chapter, a detailed overview of the transmission and reception techniques for MIMO communication systems was discussed. Specifically, these techniques were categorized by spatial multiplexing techniques, spatial diversity techniques, and beamforming techniques. In the second part, the system models of flat-fading and frequency-selective channels for a general MIMO case were introduced. Finally, to overcome the frequency-selectivity of the transmitted wideband channels, a multicarrier orthogonal frequency division multiplexing modulation is presented for conventional MIMO architecture. In addition, the optimal weights design, the general system model, and the computational complexity associated to this architecture were briefly reviewed. Finally, the IEEE 802.11a standard was discussed along with its OFDM PHY layer and frame format.

Chapter 3

Simplified Architectures for Analog Antenna Combining

3.1 Introduction

In wireless communication environments, to achieve most of the benefits of multiple-input multiple-output (MIMO) channels (e.g., spatial diversity and array gain), several signal processing strategies were developed for the last generation of wireless systems. In addition, these systems permit to transmit high data rates over large bandwidth channels. In practice, the corresponding hardware size and power consumption are high, and the coverage range and reliability of these systems is rather limited, which might delay the market introduction of such concepts. Conventional MIMO scheme studied in Chapter 2 is one of such systems that requires all antenna paths to be independently acquired and processed at baseband.

A beamforming architecture proposed in [Eickhoff et al., 2008] called MIMAX scheme, that uses a vector modulator approach is considered an alternative for conventional MIMO. This scheme can implement the optimal maximum ratio transmission (MRT) and maximum ratio combining (MRC) at the transmitter and at the receiver, respectively. In this and subsequent chapters, we will refer to it as a maximum-ratio beamforming architecture (RF-MRB) instead of MIMAX. Just as a reminder, the basic idea of this scheme consists of applying complex weights (gain factor and phase shift) to the transmitted or the received signals at each branch. Until very recently, this RF combining scheme in the analog domain provided limited performance, especially because phase shifters tend to exhibit significant amplitude variations. However, some recent advances on SiGe-BICMOS-technology, jointly with some innovative concepts introduced for phase and amplitude control circuits [Ellinger, 2007] have made possible to develop a full 360° control range of phase shifter together with an amplitude control of more than 20 dB.

The crucial points in designing the beamforming scheme are the complexity, robustness and power dissipation. The purpose of our work is to provide a beamforming solution in order to further reduce the hardware complexity and power consumption for analog antenna combining. In this chapter, we introduce three new analog beamforming architectures (real-weights beamforming, equal-phase beamforming, and equal-gain beamforming) to achieve most of the benefits of MIMO system (e.g., spatial diversity and array gain). The proposed RF-MIMO architectures perform low complexity beamforming techniques providing satisfactory results, which will be illustrated in Chapters 4 and 5 by means of several numerical simulations.

This chapter is divided into four sections. In Section 3.2, the maximum-ratio beamforming architecture (RF-MRB) developed in the MIMAX project is presented, then some of their concepts such as frame format and channel estimation will be reviewed, and their benefits (i.e., spacial diversity, multiplexing and array gains) will be printed out. Also, the extension to the multicarrier transmission for RF-MRB architecture will be discussed. The RF real-weights beamforming (RF-RWB) architecture based on a set of beamformers with real coefficient will be presented in Subsection 3.3.1. In Subsection 3.3.2, the RF equal-phase beamforming (RF-EPB) architecture based on nonnegative real weights will be proposed. Then, the RF equal-gain beamforming (RF-EGB) architecture based on constant-modulus complex weights will be presented in Subsection 3.3.3. Finally, a brief summary concludes this chapter.

3.2 RF Maximum-Ratio Beamforming Architecture Developed in the MIMAX Project

The basic principle of the simplified schemes is to simplify the circuitry and the energy consumption of MIMO transceiver. In this section, we will review the RF-MRB architecture which implements antenna combining in radio frequency domain. The block diagram of this architecture is shown in Figure 3.1. In each receive path, a band pass filter is integrated in order to attenuate adjacent radio signals and extracting the desired signal. The low noise amplifier is used for mitigating the noises added to the received signals, and it can be switched between high and low gain operation modes. In this analog combining scheme, the vector modulator performs the complex weight multiplication of the received signals or, equivalently, changes the relative amplitude and phases with respect to the other antenna paths. In this way, after combining the weighted RF signals, a single stream of data must be acquired and processed using a downconverter circuit in baseband. Finally, the in-phase and quadrature baseband signals are low pass filtered and then digitized by an analog-to-digital-converter (ADC) for further signal processing in the digital baseband.

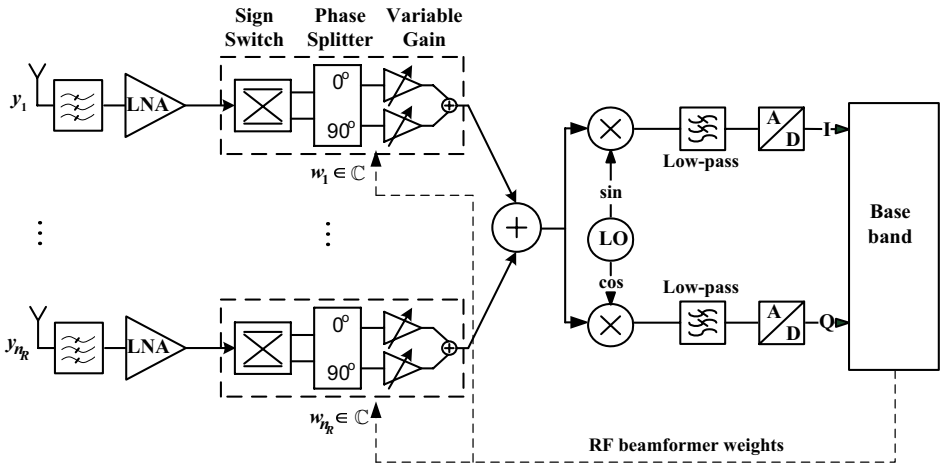

Figure 3.1: Maximum-ratio beamforming in the RF domain (RF-MRB).

As mentioned above, the complex weights (to adjust the amplitude and phase of RF signals) can be realized based on vector modulator block.[1] In practice, analog circuitries are coupled and correlated, which means that when changing the amplitude also the phase is changed. As a result, the phases and amplitudes of the complex weights cannot be adjusted independently from each other, and both are functions of the other variable. Consequently, to mitigate this issue, amplitude and phases controlling circuits must be added to spatial signal processing. Thus, the vector modulator approach (in the front-end of RF-MRB architecture) requires a sign switch controller along with a constant $\pi/2$ phase shift to produce in-phase and quadrature components.

The main advantages of the RF-MRB structure in Figure 3.1 are the lower cost, reduced power consumption and smaller size, in comparison to the conventional MIMO [Eickhoff et al., 2008]. Consequently, the price to pay for the simplicity of this analog combining architecture is that a single branch is processed after the RF analog combining stage, and consequently, the multiplexing gain is limited to one (see also Subsection 3.2.3). Therefore, a single stream of data is transmitted and received through an equivalent SISO channel, which is optimized with respect to the transmit and receive analog beamformers (RF weights). Nevertheless, in low SNR scenarios or for strongly correlated MIMO channels, the spatial degrees of freedom are limited, and the performance improvement of Full-MIMO due to spatial multiplexing is marginal compared to the RF-MRB architecture.

[1]Note that this can be also done by using a variable gain amplifiers in series to a phase shifters.

3.2.1 MIMAX Project

MIMAX is a research project within the 7th Framework Programme that aims to investigate and develop a more powerful WLAN device, which is compatible with the existing WLAN networks [Eickhoff et al., 2008]. The project concepts are based on wireless MIMO communication, which are similar to the approaches used in new WLAN standard 802.11n or WiMAX. Nevertheless, the main difference between MIMAX and the aforementioned standards is that, in MIMAX, the required signal processing is executed near the transmit and receive antennas, i.e., RF-MRB architecture is based on analog antenna combining.

3.2.2 MIMAX Concepts

Although the analog antenna combining could be applied to any wireless technology, market and technology analysis within the MIMAX project revealed the greatest potential offered by the wireless local area networks (WLAN). Especially, IEEE 802.11a provides promising market prospects for exploiting the benefits of spatial signal processing in the RF due to compact form factors, high revenues, and competitive system costs. For this reason, the MIMAX transceiver is based on 802.11a technology at 5 GHz with an analog antenna combining architecture as that shown in Figure 3.1.

Channel Estimation for MIMAX

In contrast to 802.11a standard, MIMAX channel estimator uses the $n_T \times n_R$ (n_T and n_R antennas at the Tx and Rx, respectively) training OFDM symbols included in training frame. Each training symbol is affected by a specific pair of Tx and Rx beamformers. Thus, the MIMO channel is projected into a SISO channel by means of these beamformers. Therefore, the $n_T \times n_R$ frequency-selective MIMO channel has to be recovered from the estimates of a number of MIMO channel projections (equivalent SISO channels) under different Tx-Rx beamformers. In consequence, these beamformers have to be carefully chosen.

In order to have a complexity-constrained and efficient channel estimation algorithm, several key aspects have to be taken into account:

- **Channel Estimation Procedure**: Assuming two terminals T1 and T2 equipped with n_T and n_R antennas, respectively. To acquire channel state information at the Tx and Rx (CSIT+CSIR), the channel estimation procedure comprises two phases.

  In the first phase, the equipment T1 sends to T2 a known OFDM pilot symbol $n_T n_R$ times. These symbols are transmitted and received using different combinations of orthogonal Tx-Rx beamformers (note that any set of weights

can be used for this scenario). Once T2 receives the OFDM symbols, it estimates the frequency-selective $n_T \times n_R$ MIMO channel and computes its optimal bemaforming vector using some practical performance criterion. Note that, due to the channel reciprocity, these are the optimal weights to be applied by T2 when either transmitting or receiving data.

In the second phase, and once the optimal beamformer has been fixed at T2, it transmits a known OFDM pilot symbol n_T times to T1. T1 receives these OFDM symbols through n_T orthogonal beamformer vectors, estimates the equivalent SIMO channel, and computes its optimal weights according to any of beamforming criteria. The beamformers[2] at both sides of the link remain fixed while the quality of the equivalent SISO channel is higher than a prescribed level, otherwise the procedure starts again. This re-estimation process is controlled by the MAC layer.

- **MIMAX Frame Format**: The channel estimation procedure requires the use of an specific frame, which is called MIMAX frame II. Its structure is depicted in Figure 3.2, and it contains a set of n training symbols for channel estimation (denoted by TW1 to TWn in Figure 3.2). These symbols are transmitted and received under different beamforming vectors. In the first phase of the channel estimation procedure, the MIMAX frame II comprises $n = n_T n_R$ training symbols, whereas in the second phase the frame has $n = n_T$ training symbols.

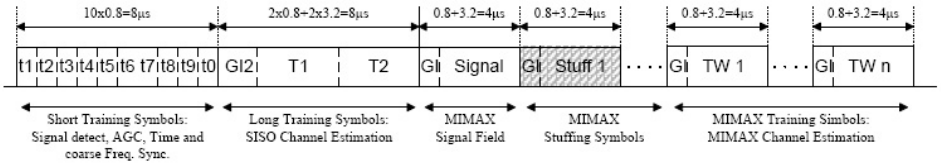

Figure 3.2: MIMAX frame II for channel estimation and RF weights selection.

- **Beamformers for Channel Estimation**: In practice, any set of orthogonal beamformers can be used for channel estimation. MIMAX uses the identity matrix as the training beamformer matrix at the transceiver, because a single pair of Tx/Rx antennas is active during the transmission/reception, and with this set of beamformers, the estimated channel is the MIMO channel without any rotation.

- **Most Adequate MIMO Channel Estimation Algorithm**: Regarding the MIMO channel estimation algorithms, the Least Squares (LS) estimator is used to estimate the $n_1 n_2$ equivalent SISO channels at the 52 active subcarriers. This

[2]The optimal RF vectors at each side must be transferred to the MAC processor.

algorithm is simple, and doses not require any information about the frequency-selectivity or statistics of the channel.

3.2.3 Benefits of MIMAX

In this subsection, we briefly review the main benefits of MIMAX, and some key differences between SISO, conventional MIMO and RF-MRB schemes in terms of diversity, multiplexing and array gains. For RF-MRB the multiplexing gain is limited to one, because of the lower hardware complexity. Table 3.1 summarizes the maximum achievable diversity, multiplexing and array gains of the three different concepts.

	Diversity gain	Multiplexing gain	array gain
MIMO	$n_T n_R$	$\min(n_T, n_R)$	n_R (CSIR)
			$n_T n_R$ (CSIT+CSIR)
RF-MRB	$n_T n_R$	1	n_R (CSIR)
			$n_T n_R$ (CSIT+CSIR)
SISO	1	1	1

Table 3.1: Maximum achievable diversity, multiplexing and array gains for Full-MIMO, RF-MRB and SISO systems.

Figure 3.3 shows the diversity-multiplexing tradeoff curves that are achievable by the different approaches considering a 4×4 system. Instead of Full-MIMO scheme (which can work at any point of the piecewise linear frontier depicted in red solid line), the RF-MRB concept can operate along the green line. As can be seen from the figure for the Full-MIMO and RF-MRB approaches to achieve the maximum diversity gain, one needs to communicate at a fixed rate.

3.2.4 General System Model for RF-MRB Architecture Under OFDM Transmission

Regarding the case of frequency-selective channels and orthogonal frequency division multiplexing (OFDM) transmission, the complexity of conventional MIMO beamforming scheme becomes very important, for that reason a pre-DFT combining scheme has been proposed to reduce the complexity [Matsuoka and Shoki, 2004]. Instead of employing baseband beamforming, the received signals in RF-MRB scheme are already combined in the RF domain prior to the DFT demodulation. Hence, only a single DFT block is required at the receiver. Subsequently, the same transmit ($\mathbf{w}_T \in \mathbb{C}^{n_T \times 1}$) and receive ($\mathbf{w}_R \in \mathbb{C}^{n_R \times 1}$) analog complex weights are applied to N_c subcarriers and kept fixed across all subcarriers for the entire OFDM symbol. In the following chapters, the selection of RF-MRB weights will be investigated based on

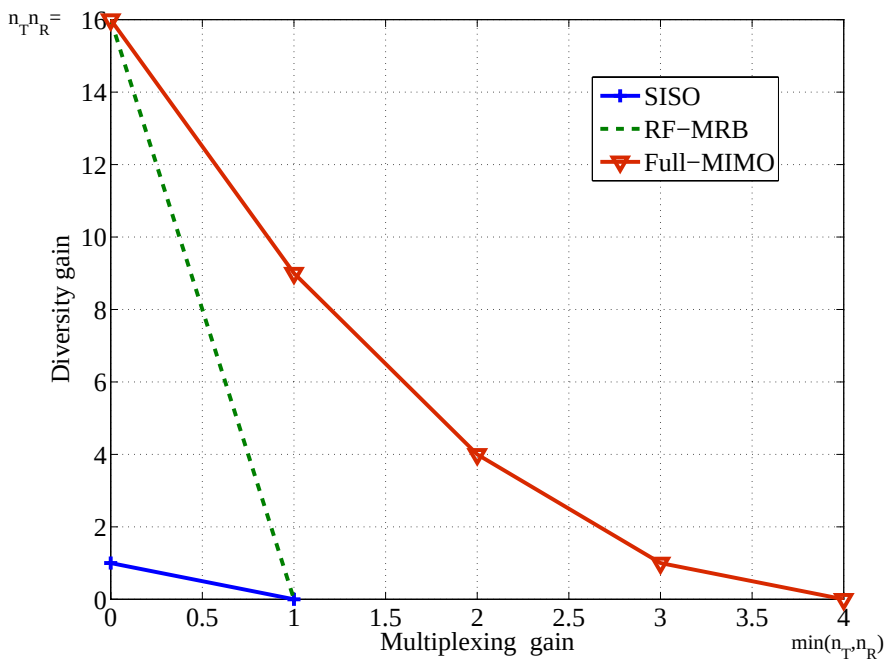

Figure 3.3: Achievable diversity-multiplexing curves for 4×4 system with Full-MIMO, RF-MRB, and SISO schemes.

maximizing the receive signal-to-noise ratio (SNR), maximizing the system capacity, and minimizing the mean square error (MSE) associated to the optimal linear receiver.

The expressions for the received signal on subcarrier k are similar to those in Section 2.4. In particular, after substituting $\mathbf{w}_{T,k} = \mathbf{w}_T$ and $\mathbf{w}_{R,k} = \mathbf{w}_R$, we get

$$y_k = \mathbf{w}_R^H \mathbf{H}_k \mathbf{w}_T s_k + \mathbf{w}_R^H \mathbf{n}_k, \qquad k = 1, ..., N_c. \tag{3.1}$$

In this thesis we assume that the analog circuitry is ideal and therefore each beamformer weight in (3.1) can take any value within the field of complex numbers. Therefore, for flat-fading MIMO channels this architecture can implement the optimal maximum-ratio beamforming at both sides of the link, which justifies the nomenclature RF-MRB. The key differences with the conventional MIMO architecture are twofold: On the one hand, the Tx and Rx beamformers are the same for all the subcarriers and, in consequence, the beamforming design problem under OFDM transmissions is coupled [Vía et al, 2010a]. On the other hand, the RF-MRB only requires one downconversion RF chain, and therefore it significatively reduces the complexity of the conventional MIMO transceiver. However, the RF-MRB architecture still requires a considerable amount of RF components, which motivates us to

present three alternative analog combining architectures with less hardware circuitry.

3.3 Alternative Analog Combining Architectures

In this section, the system models and the block diagrams of the alternative analog antenna combining architectures (RF-RWB, RF-EPB and RF-EGB) are presented.

3.3.1 RF Real-Weights Beamforming Architecture

The block diagram of the novel RF-RWB architecture is shown in Figure 3.4. In contrast to the RF-MRB architecture (performing spatial processing by changing the amplitude and phase of the transmitted-received RF signals using vector modulators), the real processing of this RF signals determines a set of beamformers with real coefficients, which are directly applied in the RF domain by analog signal processing circuits. These real weighted RF signals are then combined and afterwards only one signal path is required for down conversion, acquisition and baseband processing at the receiver.

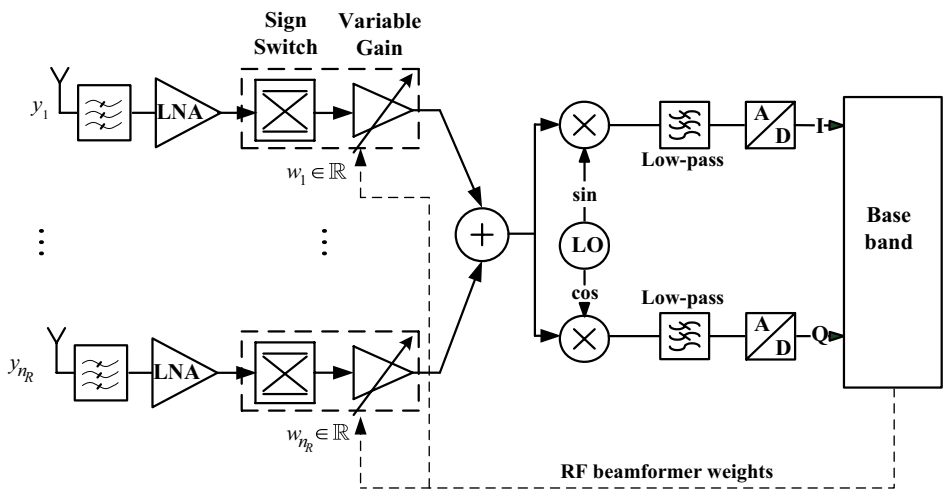

Figure 3.4: Real-weights beamforming in the RF domain (RF-RWB).

Multiplying the signals by real weights permits to exploit spatial diversity and array gain, which implies an improvement in the received signal-to-noise ratio (SNR). The performance and the reliability remains similar to those of the RF-MRB scheme (see Chapters 4 and 5). In practice, the real weights multiplication can be achieved by adjusting only the amplitudes of the signals. The use of an analog variable gain

amplifier (VGA) along with a sign switch, permits to change the amplitudes of the signals keeping constant the phases. In addition, RF-RWB is better in terms of additional hardware complexity cost because it uses only one VGA instead of two VGAs which are required for each antenna element. Also, it is seen in Figure 3.4, that the number of adders is reduced in the RF-RWB scheme, and the phase splitter is removed. This makes the RF transceiver hardware less complex, less expensive and the power dissipation will be greatly reduced compared to the RF-MRB approach of Figure 3.1.

The baseband model of the RF-RWB architecture is derived considering transmit and receive real weights. In contrast to RF-MRB architecture, the complex data symbol s_k is now modulated at the transmitter by a real weight beamformer before the transmission over the MIMO channel. At the receiver, after processing with the real weight combining vector, the combined baseband signal is deduced from that in expression (3.1) by considering

$$\mathbf{w}_T \in \mathbb{R}^{n_T \times 1}, \qquad \mathbf{w}_R \in \mathbb{R}^{n_R \times 1}, \tag{3.2}$$

while the rest of terms in expression (3.1) (MIMO channel, noise, etc) are still complex. Therefore, for optimum performance, the transceiver is assumed to have perfect knowledge of the channel state information and also, $\mathbf{w}_T$ and $\mathbf{w}_R$ should be chosen to maximize the received signal-to-noise ratio (SNR). Therefore, in the next chapters we will address the design of the transmit-receive real weight beamformers in both flat-fading and frequency-selective channels.

3.3.2 RF Equal-Phase Beamforming Architecture

In this section we propose an additional simplification, which allows us to remove the sign-switch block in RF-RWB described in the previous subsection. This scheme, which we refer to as RF equal-phase beamforming (RF-EPB), is still simpler to implement than the RF-RWB scheme due to the removal of the sign switch controller. This beamforming scheme is used to scale the amplitude of each transmitted or received signal without shifting its phase. Specifically, the RF-EPB architecture is proposed using only nonnegative real weights instead of complex weights. Consequently, EPB signal multiplication in the radio-frequency domain reduces the amount of system components and its complexity and, consequently, the power consumption, the system costs and size can be significantly reduced to the state-of-the-art achieving similar performance as RF-MRB system. The block diagram of RF-EPB is shown in Figure 3.5. As can be seen from this figure, the equal phase beamformers are implemented only with a variable gain amplifier (VGA) to control signal amplitudes range variation.

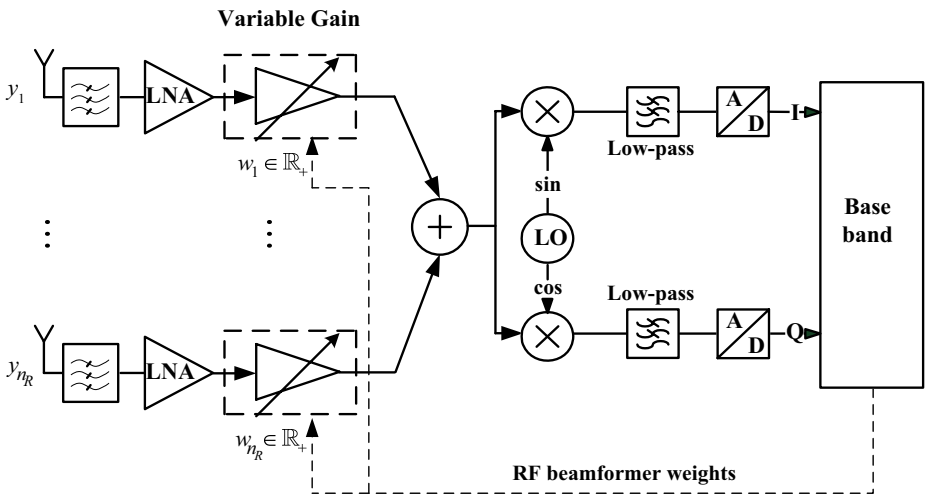

Figure 3.5: Equal-phase beamforming in the RF domain (RF-EPB).

At the receiver, and from a baseband point of view, the model in equation (3.1) remains valid with the additional constraint of having beamformers with nonnegative entries, i.e.,

$$\mathbf{w}_T \in \mathbb{R}_+^{n_T \times 1}, \qquad \mathbf{w}_R \in \mathbb{R}_+^{n_R \times 1}, \tag{3.3}$$

where $\mathbb{R}_+$ denotes the nonnegative orthant.

3.3.3 RF Equal-Gain Beamforming Architecture

In this subsection we present the third simplified architecture, which we refer to as equal-gain beamforming (RF-EGB). The block diagram of this architecture, is schematically shown in Figure 3.6. Essentially, the vector modulators in Figure 3.1 are now substituted by wideband analog phase shifters. This approach is well-known in the beamforming literature [Zheng et al., 2007], and [Love and Heath, 2003], since it avoids the wide power variations that can happen in maximum-ratio beamforming schemes. As long as the gains of the amplifiers of the various branches match, the rest of the parameters can be relaxed and inexpensive amplifiers can then be utilized. Unlike the RF-RWB and the RF-EPB schemes, which only make sense when applied in the RF domain, the RF-EGB can be applied either in baseband [Zheng et al., 2007], [Love and Heath, 2003] or in RF.

From a baseband point of view, the baseband model of expression (3.1) is again valid but now with the additional constraint of having Tx and Rx beamformers with constant-modulus complex elements, i.e.,

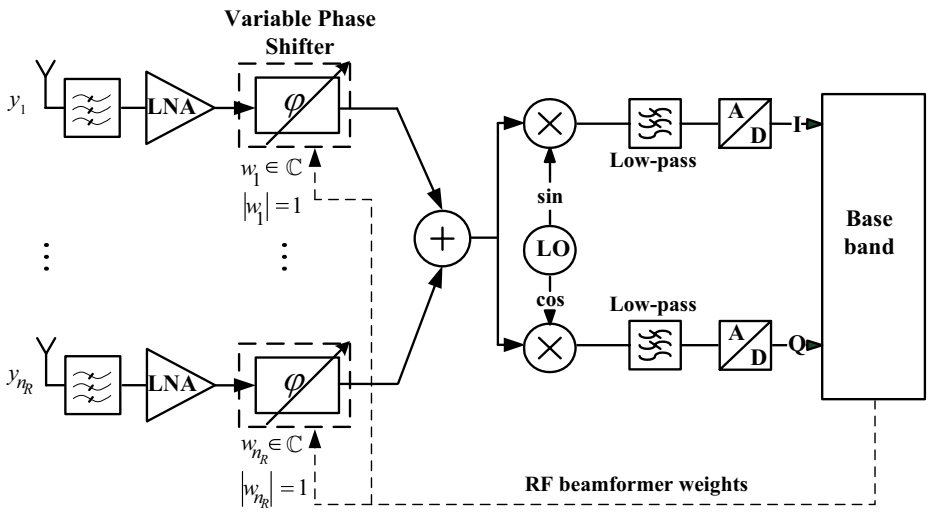

Figure 3.6: Equal-gain beamforming in the RF domain (RF-EGB).

$$\mathbf{w}_T \in \mathbb{C}^{n_T \times 1}, \quad \text{where} \quad |w_{T,i}| = \frac{1}{\sqrt{n_T}}, \quad i = 1, 2, \ldots, n_T, \tag{3.4}$$

and

$$\mathbf{w}_R \in \mathbb{C}^{n_R \times 1}, \quad \text{where} \quad |w_{R,i}| = \frac{1}{\sqrt{n_R}}, \quad i = 1, 2, \ldots, n_R. \tag{3.5}$$

3.4 Summary

Conventional MIMO architecture provides the best performance in terms of BER, achieving full diversity by implementing beamforming algorithms in baseband, but the hardware cost, size, and power consumption are increased. RF-MRB architecture performing spatial processing in the RF domain is a good alternative in order to reduce the hardware cost and system size, as well as to increase the energy-efficiency of the system, but still requires a considerable amount of components.

In this chapter, to further reduce the hardware complexity we have proposed three new simplified architectures for analog antenna combining. Firstly, we have presented a simplified scheme denoted as RF-RWB. This scheme applies the real-weight combining concept and only uses a variable gain amplifier (VGA) in series with a sign switch before the analog combiner, instead of full vector modulators used for RF-MRB scheme. Secondly, we have proposed another simplified architecture denoted as RF-EPB that applies the equal-phase combining concept. In contrast to

RF-RWB, RF-EPB only uses a variable gain amplifier (VGA) before the analog combiner. Thirdly, we have presented RF-EGB simplified architecture, which applies the equal-gain combining concept and only uses phase shifters before the analog combiner, instead of full vector modulators of RF-MRB architecture.

Chapter 4

Beamforming Design for Flat-Fading Channels

4.1 Introduction

The aim of this chapter is the design of the transmit and receive beamformers for the different analog antenna combining architectures proposed in Chapter 3. Specifically, we focus here on the case of flat-fading channels. Taking into account the constraints introduced by the different architectures, the beamforming design problems for MIMO channels are highly non-convex, and we have to resort to an iterative algorithm based on the successive solution of the equivalent single-input multiple-output (SIMO) and multiple-input single-output (MISO) problems. This alternating optimization algorithm is guaranteed to converge, and with a proper initialization method, it provides very satisfactory results.

The chapter is organized as follows, the beamforming optimization problem is formulated in Section 4.2. Subsections from 4.2.2 to 4.2.5, give the closed-form solutions associated to different architectures in the SIMO or MISO cases. Section 4.3 introduces the alternating optimization algorithm used to obtain the Tx and Rx beamforming vectors for the MIMO channel. Finally, the proposed simplified RF-MIMO architectures are evaluated in Section 4.4 by means of some numerical examples.

4.2 Problem Formulation

In this section we address the problem of designing the transmit ($\mathbf{w}_T$) and receive ($\mathbf{w}_R$) beamformers maximizing the SNR for the different analog antenna combining architectures. At this point, assuming flat-fading channels (i.e., narrowband wireless communication system), and taking into account the unit power constraint i.e., $E\left[|s|^2\right] = 1$ at the transmitter, as well as the unit energy beamformers ($\|\mathbf{w}_T\|^2 = \|\mathbf{w}_R\|^2 = 1$), the received signal-to-noise ratio SNR can be computed as

$$\mathrm{SNR} = \frac{E\left[\left|\mathbf{w}_R^H \mathbf{H} \mathbf{w}_T s\right|^2\right]}{E\left[\left|\mathbf{w}_R^H \mathbf{n}\right|^2\right]} = \frac{\left|\mathbf{w}_R^H \mathbf{H} \mathbf{w}_T\right|^2}{\sigma_n^2}, \tag{4.1}$$

where the SISO equivalent channel $h = \left|\mathbf{w}_R^H \mathbf{H} \mathbf{w}_T\right|^2$ is a function of the transmit and receive beamformer vectors, which will be designed in the following section.

Thus, the general optimization problem for the beamforming design associated to the proposed RF-MIMO schemes is given by the following quadratically constrained quadratic program (QCQP):

$$\begin{aligned} \underset{\mathbf{w}_T, \mathbf{w}_R}{\text{maximize}} \quad & \left|\mathbf{w}_R^H \mathbf{H} \mathbf{w}_T\right|^2 \\ \text{subject to} \quad & \|\mathbf{w}_T\| \leq 1, \quad \mathbf{w}_T \in \mathcal{S}^{n_T \times 1}, \\ & \|\mathbf{w}_R\| \leq 1, \quad \mathbf{w}_R \in \mathcal{S}^{n_R \times 1}, \end{aligned} \tag{4.2}$$

where we have replaced the equality constraints $\left(\|\mathbf{w}_T\|^2 = \|\mathbf{w}_R\|^2 = 1\right)$ with inequalities because the objective function is monotonically increasing in $\|\mathbf{w}_T\|$ and $\|\mathbf{w}_R\|$, and where $\mathcal{S}^{n \times 1}$ represents a subset of the complex field (i.e., $\mathcal{S}^{n \times 1} \subseteqq \mathbb{C}^{n \times 1}$) that reflects the constraints imposed by the particular RF-MIMO beamforming architecture.

Unfortunately, in the general MIMO case, the optimization problem in (4.2) is a complicated nonconvex problem and no closed-form solution is known. For that reason, following the procedure in [Zheng et al., 2007] we use an alternating optimization algorithm to optimize the transmit-receive beamformers in (4.2). This algorithm iterates between the equivalent SIMO (with the Tx beamformer fixed) and MISO (with the Rx beamformer fixed) problems (see Section 4.3 for more details). As we will show later, it provides satisfactory results, and has a low computational complexity. Equipped with this alternating optimization approach, in the following subsections we focus on how to solve the SIMO/MISO cases for the different architectures.

4.2.1 Optimum Receive Beamformer in SIMO case

The MIMO problem in (4.2) can be particularized for a SIMO case (the MISO case can be solved in a similar manner) by fixing the transmit beamformer $\mathbf{w}_T \in \mathcal{S}^{n_T \times 1}$. The problem can be now expressed as

$$\begin{aligned} \underset{\mathbf{w}_R}{\text{maximize}} \quad & \mathbf{w}_R^H \mathbf{R}_{\text{SIMO}} \mathbf{w}_R \\ \text{subject to} \quad & \|\mathbf{w}_R\| \leq 1, \quad \mathbf{w}_R \in \mathcal{S}^{n_R \times 1}, \end{aligned} \tag{4.3}$$

where $\mathbf{R}_{\text{SIMO}}$ is a $n_R \times n_R$ complex matrix given by

$$\mathbf{R}_{\text{SIMO}} = \mathbf{h}_{\text{SIMO}}\mathbf{h}_{\text{SIMO}}^{H}, \tag{4.4}$$

and $\mathbf{h}_{\text{SIMO}} = \mathbf{H}\mathbf{w}_T$ is the $n_R \times 1$ complex SIMO channel.

Note that the problem in (4.3) has a closed-form solution for all architectures. In the case of the RF-MRB scheme the solution is given in Subsection 4.2.2. For RF-RWB, the solution is given by the largest eigenvector of a $n_R \times n_R$ real matrix in Subsection 4.2.3. While for the RF-EPB architecture, the closed-form solution is achieved by reformulating the problem in (4.3) by means of the semidefinite relaxation (SDR) technique, as we will see in Subsection 4.2.4. Finally, for the RF-EGB architecture, an approximated closed-form solution can be obtained from the phases of SIMO channel [Gonzalo et al., 2010, Love and Heath, 2003].

4.2.2 RF-MRB Architecture

In this subsection, we address the design of the transmit and receive beamformers which implement the RF-MRB architecture in flat-fading channels. The optimal beamformer implements the well-known MRC criterion and can be obtained as

$$\mathbf{w}_R = \frac{\mathbf{h}_{\text{SIMO}}}{\|\mathbf{h}_{\text{SIMO}}\|}, \tag{4.5}$$

and $\mathcal{S}^{n_R \times 1} = \mathbb{C}^{n_R \times 1}$.

For this architecture, it is also known that the MIMO problem admits a closed-form solution for the Tx-Rx beamformers, which is given by the singular vectors associated to the largest singular value of the channel matrix $\mathbf{H}$ [Andersen, 2000] (in a conventional MIMO scheme, this technique is denoted as dominant eigenmode transmission). Therefore, in this case, there is no need to apply an alternating optimization approach to find the transmit-receive beamformers.

4.2.3 RF-RWB Architecture

The RF-RWB architecture cannot implement the MRC solution because is restricted to work with beamformers whose weights are real (i.e., $\mathcal{S}^{n_R \times 1} = \mathbb{R}^{n_R \times 1}$). However, for the SIMO case, it has been proved in [Gholam et al., 2009] that the optimal RWB can be easily obtained in closed-form (see Appendix A for more details) by taking the real part of matrix in (4.4), i.e.,

$$\mathbf{G}_{\text{SIMO}} = \Re\left(\mathbf{R}_{\text{SIMO}}\right), \tag{4.6}$$

and calculating its principal eigenvector, which obviously will have real entries.

4.2.4 RF-EPB Architecture

The RF-EPB architecture introduces the additional constraint of having beamformers with nonnegative entries, that is, $\mathcal{S}^{n_R \times 1} = \mathbb{R}_+^{n_R \times 1}$. In the SIMO case, the problem in (4.3) is not convex, which precludes its solution by means of standard convex optimization tools [Boyd and Vandenberghe, 2004]. In this subsection, we introduce a method, based on relaxing the nonconvex optimization problem into a semidefinite program (SDP), referred to as the SDP relaxation or semidefinite relaxation (SDR).

Defining now the rank-one beamforming matrix $\mathbf{W}_R = \mathbf{w}_R \mathbf{w}_R^T$, and

$$\mathbf{W}_R = \mathbf{w}_R \mathbf{w}_R^T \Longleftrightarrow \mathbf{W}_R \succeq 0, \quad \operatorname{rank}(\mathbf{W}_R) = 1. \tag{4.7}$$

Using this observation, we can linearize the optimization problem in (4.3) by representing it in terms of the matrix variable $\mathbf{W}_R$. Specifically, we note that $\mathbf{w}_R^T \mathbf{G}_{\text{SIMO}} \mathbf{w}_R = \operatorname{Tr}(\mathbf{G}_{\text{SIMO}} \mathbf{W}_R)$, so (4.3) can be rewritten as

$$\begin{aligned} \underset{\mathbf{W}_R}{\text{maximize}} \quad & \operatorname{Tr}(\mathbf{G}_{\text{SIMO}} \mathbf{W}_R) \\ \text{subject to} \quad & \operatorname{Tr}(\mathbf{W}_R) \leq 1, \\ & \mathbf{W}_R \geq 0, \\ & \mathbf{W}_R \succeq 0, \\ & \operatorname{rank}(\mathbf{W}_R) = 1. \end{aligned} \tag{4.8}$$

Since in (4.8) the only nonconvex constraint is $\operatorname{rank}(\mathbf{W}_R) = 1$, one can directly relax the last constraint, to obtain the following SDP:

$$\begin{aligned} \underset{\mathbf{W}_R}{\text{maximize}} \quad & \operatorname{Tr}(\mathbf{G}_{\text{SIMO}} \mathbf{W}_R) \\ \text{subject to} \quad & \operatorname{Tr}(\mathbf{W}_R) \leq 1, \\ & \mathbf{W}_R \geq 0, \\ & \mathbf{W}_R \succeq 0. \end{aligned} \tag{4.9}$$

In contrast to the original nonconvex problem (4.3), the SDP relaxed problem (4.9) is a convex optimization problem, with an optimal solution $\mathbf{W}_R$, which is not necessarily rank-one. Finally, we propose to obtain the receive beamformer $\mathbf{w}_R$ as the principal eigenvector of the matrix $\mathbf{W}_R$.

4.2.5 RF-EGB Architecture

In the case of equal-gain beamforming, the elements of the receive beamformer have a constant modulus of $1/\sqrt{n_R}$, and $\mathcal{S}^{n_R \times 1} = \mathbb{C}^{n_R \times 1}$.

Fortunately, in the SIMO case the optimal beamformer is obtained in closed-form as [Zheng et al., 2007, Love and Heath, 2003]

$$\mathbf{w}_R = \frac{e^{j\angle \mathbf{h}_{\text{SIMO}}}}{\sqrt{n_R}}, \tag{4.10}$$

where $e^{j\angle \mathbf{h}_{\text{SIMO}}}$ denotes the vector with unit-modulus entries and the same phases as the vector $\mathbf{h}_{\text{SIMO}}$. It is easy to prove that, for SIMO flat-fading channels, the optimal beamformer is directly given by the projection of the channel coefficients onto the complex unit circle.

4.3 Alternating Optimization Algorithm for Flat-Fading MIMO Channels

By exploiting the above optimal beamforming solutions for the SIMO and MISO cases, the suboptimal solution of (4.2) is now obtained for the MIMO case. Thus, the transmit-receive beamformers can be obtained by running the alternating optimization algorithm as follows: after initializing the weights $\mathbf{w}_T$ and $\mathbf{w}_R$ from (4.12), the first step updates of the Rx beamformer by solving the problem in (4.3) for the equivalent (after fixing the Tx beamformer) SIMO channel. Similarly, the next step updates of the Tx beamformer for the equivalent (after fixing the Rx beamformer) MISO channel. Then, the steps are repeated until convergence. The overall technique pseudo-code is summarized in Algorithm 1.

It must be noted that the proposed iterative algorithm converges because the cost function is bounded and it cannot increase with the progress of the algorithm. In the following subsection, we give the proper initialization to provide a satisfactory solution of the Algorithm 1.

4.3.1 Initialization Method

In order to guarantee the fast convergence of the proposed algorithm, we propose an adequate initialization point that can be obtained in closed-form. This initialization method obtains the approximated weights in closed-form to maximize the received signal-to-noise ratio (SNR). Here, we start by rewriting the problem in (4.2) as

Initialize the beamformers $\mathbf{w}_T$, $\mathbf{w}_R$ from the solution of the equivalent SIMO problem in (4.12).
repeat
  Update of the receive beamformer Rx
  Obtain the equivalent SIMO channel $\mathbf{h}_{\text{SIMO}} = \mathbf{H}\mathbf{w}_T$.
  Solve the optimization problem in (4.3) for the SIMO channel $\mathbf{h}_{\text{SIMO}}$.
  Use the solution as the new receive beamformer $\mathbf{w}_R$.
  Update of the transmit beamformer Tx
  Obtain the equivalent MISO channel $\mathbf{h}_{\text{MISO}} = \mathbf{H}^H\mathbf{w}_R$.
  Solve the optimization problem in (4.3) for the MISO channel $\mathbf{h}_{\text{MISO}}$.
  Use the solution as the new transmit beamformer $\mathbf{w}_T$.
until Convergence

Algorithm 1: Proposed alternating optimization algorithm for analog antenna combining beamforming in flat-fading channel.

$$\begin{aligned} \underset{\mathbf{w}_T,\mathbf{w}_R,\mathbf{w}}{\text{maximize}} \quad & |\mathbf{h}\mathbf{w}|^2 \\ \text{subject to} \quad & \|\mathbf{w}_T\| \leq 1, \quad \mathbf{w}_T \in \mathcal{S}^{n_T\times 1}, \\ & \|\mathbf{w}_R\| \leq 1, \quad \mathbf{w}_R \in \mathcal{S}^{n_R\times 1}, \\ & \mathbf{w} = \mathbf{w}_T \otimes \mathbf{w}_R^*, \end{aligned} \tag{4.11}$$

where $\mathbf{h} = \text{vec}\,(\mathbf{H})$ is the vectorized version of the MIMO channel. Now, let us rewrite the optimization problem in (4.11) as

$$\begin{aligned} \underset{\mathbf{w}_T,\mathbf{w}_R,\mathbf{w}}{\text{maximize}} \quad & \mathbf{w}^T\mathbf{R}\mathbf{w} \\ \text{subject to} \quad & \|\mathbf{w}\| \leq 1, \quad \mathbf{w} \in \mathcal{S}^{n_T n_R\times 1}, \\ & \mathbf{w} = \mathbf{w}_T \otimes \mathbf{w}_R^*, \end{aligned} \tag{4.12}$$

where $\mathbf{R} = \mathbf{h}\mathbf{h}^H$. Obviously, the above problem is nonconvex due to the Kronecker product constraint. However, if we relax the last constraint, the optimization problem becomes identical to that in (4.3) for SIMO channels, where now we have an $n_T n_R \times n_T n_R$ matrix $\mathbf{R}$ and the beamvector $\mathbf{w} \in \mathcal{S}^{n_T n_R\times 1}$ that combines the Tx and Rx beamformers. This family of problems has been (approximately) solved in the previous section, and the only issue here is how to extract the beamformers $\mathbf{w}_T$ and $\mathbf{w}_R$ from $\mathbf{w}$. In this chapter, we propose to use the best approximation in terms of the Euclidean norm. That is, the Tx-Rx beamformers are obtained from the singular vectors associated to the largest singular value of the $n_T \times n_R$ matrix $\mathbf{W} = \text{unvec}(\mathbf{w})$, where $\text{unvec}(\cdot)$ denotes the inverse operator of $\text{vec}(\cdot)$. Notice that the constraint

$\mathbf{w} \in \mathcal{S}^{n_T n_R \times 1}$ is explicitly taken into account in (4.12) and consequently the initialization is specific to each architecture.

4.3.2 Computational Complexity

In this subsection, the computational complexity of the proposed techniques in flat-fading channels is discussed. Specifically, the alternating optimization algorithm heavily relies on the eigenvalue decomposition (EVD) technique which is required to compute the Tx and Rx beamformers. For square matrices of size $n = \max(n_T, n_R)$, direct EVD methods typically have a cost of $\mathcal{O}(n^3)$ operations [Demmel, 1997]. On the other hand, the costs required to obtain the matrix $\mathbf{R}_{\text{SIMO}}$ and to solve a semidefinite programming problem (with $n \times n$ matrices and one linear constraint), are $\mathcal{O}(n^2)$ and $\mathcal{O}(n^7)$, respectively [Golub and Loan, 1983, Nesterov and Nemirovsky, 1994]. Thus, it is easy to see that the computational complexity (per iteration) is of order $\mathcal{O}(n^2 + n^3)$ for the RF-MRB and RF-RWB, and $\mathcal{O}(n^2 + n^7)$ for the RF-EPB and RF-EGB schemes.

Finally, for the computational complexity associated with the initialization approaches in flat-fading channels, the complexity is of order $\mathcal{O}\left(n_T^3 n_R^3\right)$.

4.4 Simulation Results

The proposed simplified RF-MIMO architectures are evaluated in this section by means of some numerical examples. In all the simulations, the transmitted signals belong to a QPSK constellation. The performance is evaluated in terms of the bit error rate (BER), and we have compared all the approaches in flat-fading channels.

In this case, we have compared the following schemes:

- RF-MRB architecture with complex beamformer weights (Figure 3.1).
- RF-RWB architecture with real beamformer weights (Figure 3.4) .
- RF-EPB architecture with nonnegative real beamformer weights (Figure 3.5) .
- RF-EGB architecture with complex constant-modulus weights (Figure 3.6).
- SISO system.

In this numerical simulations, the flat-fading channel is generated according to an i.i.d. Rayleigh channel model. In the first simulation example, we have considered a scenario with only one transmit antenna, therefore the alternating optimization procedure is not needed. The obtained results are shown in Figures 4.1 and 4.2 in the

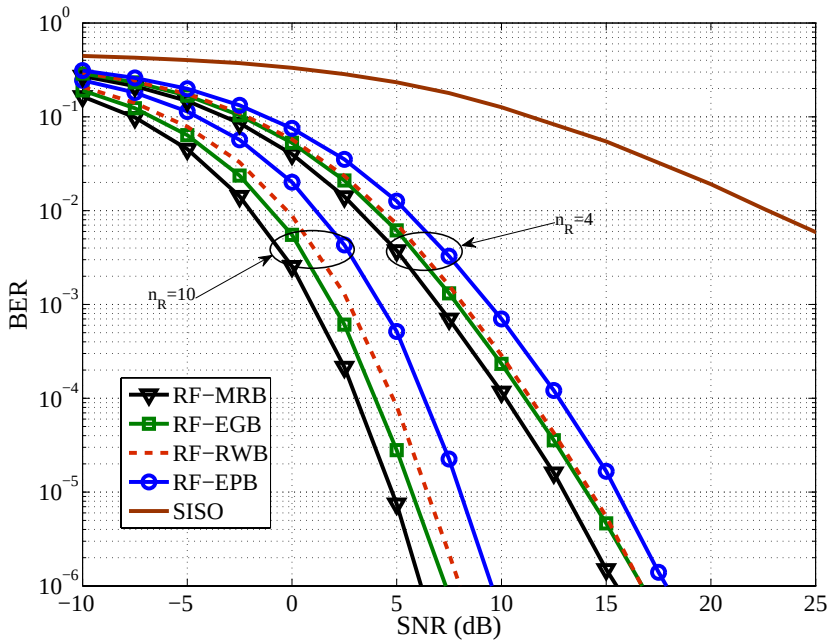

Figure 4.1: Performance of the different RF architectures in $1 \times n_R$ SIMO flat-fading channels.

case of $n_R = 4$ and $n_R = 10$ receive antennas. On the one hand, Figure 4.1 shows the bit error rate for the five compared schemes. On the other hand, Figure 4.2 shows the results in the case of correlated channels. In particular, we have employed the Jake·s model [Dent et al., 1993] with antenna spacing $d = \lambda/4$. In both cases, we can see that the proposed simplified analog antenna combining architectures are able to exploit all the diversity in the SIMO system, and their performance is close to that of the RF-MRB scheme, which for flat-fading channels represents the optimal solution. Furthermore, they clearly outperform the SISO system. The comparison among the proposed architectures shows that the best results are obtained by the RF-EGB transceiver, which are very close to those of the RF-RWB architecture. Obviously, the performance of the RF-RWB outperforms the RF-EPB (which has a reduced complexity), but in any case the gap with respect to a RF-MRB scheme never exceeds 3 dB.

Figure 4.3 shows the results for a 4×4 MIMO system. Again, the simplified RF-MIMO beamforming architectures achieve the same spatial diversity as the optimal MRB scheme and the RF-EGB is the best performing one.

Finally, Figure 4.4 illustrates the convergence behavior of Algorithm 1 by plotting how the equivalent channel energy evolves over the iterations. This figure shows that the Algorithm 1 quickly converges when it is given a good initial point.

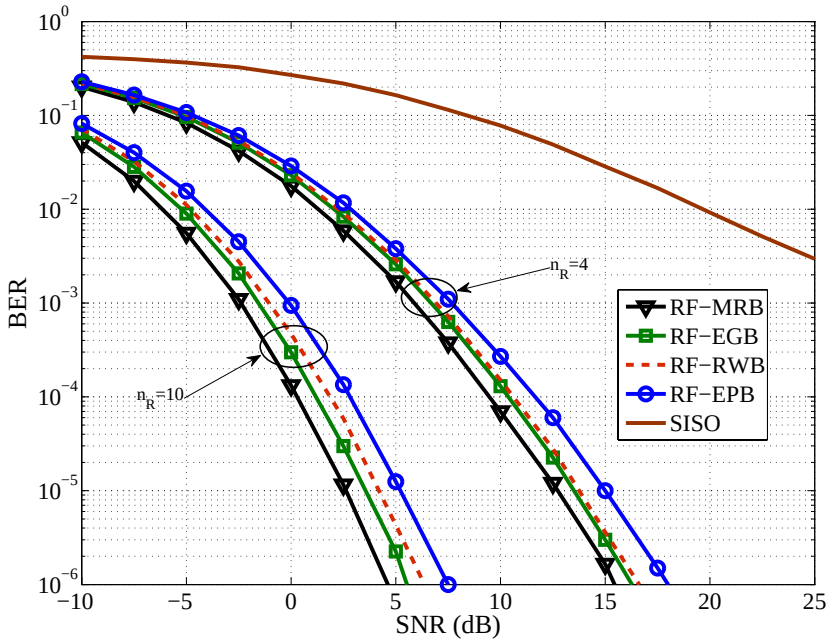

Figure 4.2: Performance of the different RF architectures in correlated $1 \times n_R$ SIMO flat-fading channels with antenna spacing $d = \lambda/4$.

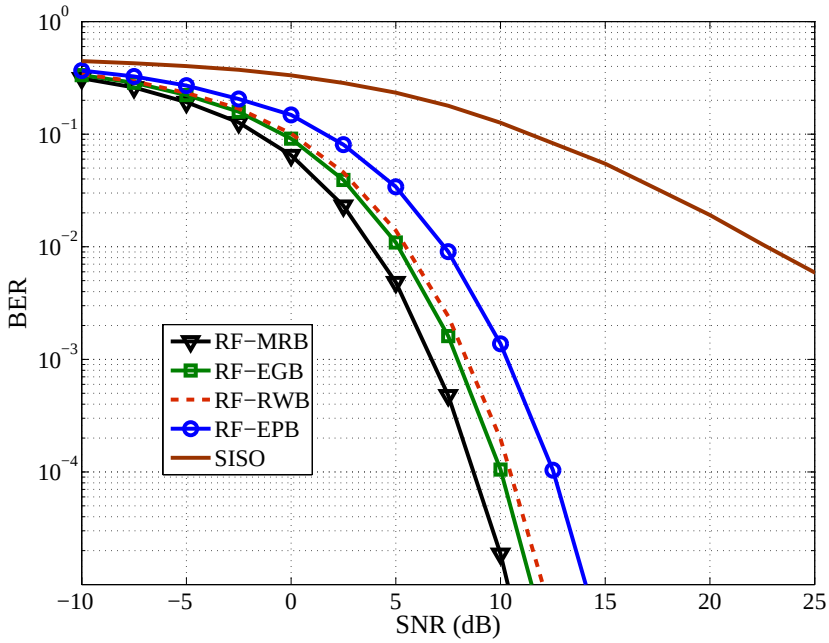

Figure 4.3: Performance of the different RF architectures in 4×4 MIMO channel.

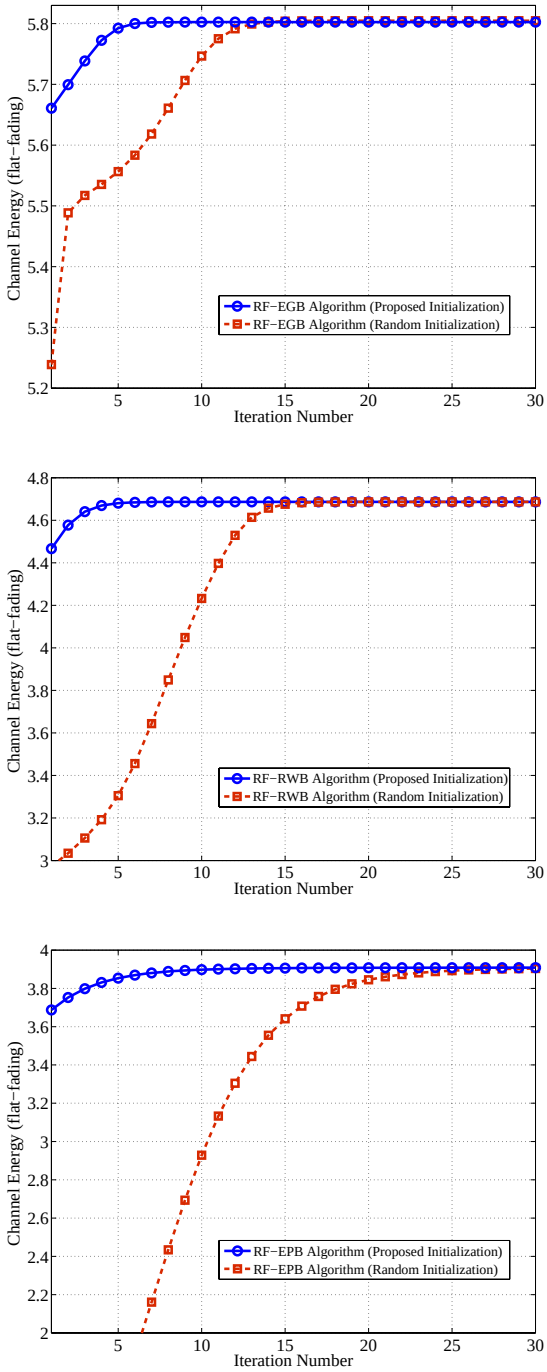

Figure 4.4: Convergence of the Algorithm 1 for flat-fading channels. Initialization in the approximated solution of (4.12) or in a pair of unit-norm random vectors $\mathbf{w}_T$, $\mathbf{w}_R$.

4.5 Summary

In this chapter we have proposed a beamformer design method for the three simplified analog antenna combining architectures (RF-RWB, RF-EPB and RF-EGB) in flat-fading channels and under the assumption of perfect channel knowledge at the transceiver. From a baseband point of view, the three architectures result in new beamforming design problems, in which the Tx-Rx beamformers are constrained to have real weights (RWB), nonnegative real weights (EPB) or constant-modulus complex weights (EGB). For SIMO or MISO cases, the RWB was obtained in closed-form as the largest eigenvector of a $n_R \times n_R$ real matrix. For the EGB, we have proposed a simple closed-form solution as vector formed by the phases of the SIMO channel. While for EPB, the beamforming design problem reduces to an nonconvex optimization problem, which has been solved using convex relaxation techniques. For the MIMO case, we have used an alternating optimization algorithm, which equipped with a proper initialization technique, converges very quickly to a satisfactory solution. The performance of the proposed architectures and algorithm has been illustrated by means of several simulation results, which allows us to conclude that the proposed architectures represent an attractive low-cost alternative to conventional MIMO systems and other (more costly) analog antenna combining architectures. Finally, the best results are provided by the RF-EGB architecture, which reveals the importance of the phase of the RF signals in comparison to their amplitude in beamforming problems.

Chapter 5

Beamforming Design for OFDM-Based Systems

5.1 Introduction

In the previous chapter, we have addressed the design of transmit and receive beamformers associated to the analog combining architectures in flat-fading channels. In this chapter, our proposed RF combining architectures (RF-RWB, RF-EPB and RF-EGB) are extended to frequency-selective channels employing orthogonal frequency division multiplexing (OFDM) transmissions.

Under OFDM transmissions, conventional MIMO schemes have access to the signals at each one of the transmitting/receiving antennas and, consequently, can obtain a different pair of beamformers for each subcarrier (see Section 2.4.3 for more details). However, with the novel analog RF combining architectures presented in Chapter 3, a per-carrier beamforming design is not possible since all the orthogonal MIMO channels $\mathbf{H}_k$ are affected by the same pair of beamformers. Notice that with the proposed RF combining architectures, a single FFT must be computed after the analog beamforming (at the receiver side), and from the baseband point of view, the coupling among subcarriers imposes some tradeoffs and represents the main challenge for the design of the beamformers. In fact, those problems are closely related to the design of pre-FFT schemes, which have been proposed to reduce the computational cost of conventional OFDM-MIMO transceivers [Rahman et al., 2004].

In this chapter we propose a general beamforming criterion which depends on a single parameter α. This parameter establishes a tradeoff between the energy and the spectral flatness of the equivalent SISO channel (after Tx-Rx beamforming). Furthermore, it allows us to obtain several interesting beamforming criteria, such as the maximization of the received SNR (MaxSNR, $\alpha = 0$) [Sandhu and Ho, 2003], the maximization of the system capacity (MaxCAP, $\alpha = 1$) [Vía et al., 2009b], and minimization of the mean square error (MSE) associated to the optimal linear receiver

(MinMSE, $\alpha = 2$) [Vía et al., 2009a]. Interestingly, in the case of low SNR, the proposed MaxCAP and MinMSE beamforming criteria are equivalent to maximizing the received SNR (MaxSNR criterion), while they significantly differ for moderate or high SNRs. In particular, as α increases, the proposed criteria sacrifices part of the received SNR in order to improve the channel response of the worst subcarriers, which translates into significant advantages in terms of capacity and MSE.

In the general MIMO case, and for all RF schemes, the proposed beamforming criterion results in a non-convex optimization problem. However, the SIMO and MISO cases for the MaxSNR criterion have a closed-form solution or can be reformulated as convex problems. Exploiting this fact, an alternating optimization procedure is used to find a suboptimal solution for maximizing the received SNR in the MIMO case. While for MaxCAP and MinMSE criteria, we propose a suboptimal gradient search algorithm. These iterative algorithms, in combination with effective initialization techniques, can provide very accurate results in most of the practical scenarios. Finally, the performance of the different RF-MIMO architectures is compared by means of Monte Carlo simulations, which allows us to conclude that the architecture based solely on phase shifters (RF equal-gain beamforming) provides the best results, and shows the advantage of the proposed technique over the MaxSNR approach for both coded and uncoded transmissions.

This chapter is organized as follows: The main assumptions, the equivalent channel and the optimal receiver processing are presented in Section 5.2. The constrained beamformer design problem that results from each RF-MIMO architecture is introduced in Section 5.3 along with an alternating optimization algorithm for MaxSNR ($\alpha = 0$) criterion. In Section 5.4, we present the general beamforming criterion and discuss its main properties. The associated beamforming design for $\alpha \neq 0$ is presented in Section 5.5, where we also introduce the proposed beamforming algorithm. Sections 5.6 and 5.7 summarize the proposed initialization approach and the computational complexity. In Section 5.8, the good performance of the proposed method for all RF schemes is illustrated by means of several simulation examples. Finally, the main conclusions are summarized in Section 5.9.

5.2 Preliminaries

5.2.1 Main Assumption

For all RF-MIMO architectures, the main assumptions in this chapter are the following:

- For all RF schemes, assuming that the analog circuitries are ideal and therefore each associated beamformer weight can take any value within a subset $S^{n\times 1}$ of

the complex field number. In particular, we do not consider RF impairments such as I/Q imbalance, imperfections in the RF circuitry, or quantization errors in the RF weights.

- The MIMO channel and noise variance are perfectly known at the transceiver. We do not consider channel estimation errors due to the noise, the limited number of pilots, or the channel estimation process. On the other hand, note that the channel estimation process can be reduced to the sequential estimation of several SISO frequency selective channels.

5.2.2 Equivalent Channel After Tx-Rx beamforming

According to the system model in (3.1) (see Chapter 3), the SISO equivalent channel after transmit-receive beamforming is given by

$$h_k = \mathbf{w}_R^H \mathbf{H}_k \mathbf{w}_T, \quad k = 1, \ldots, N_c. \tag{5.1}$$

Notice that for MaxSNR beamforming, the transmit and receive beamformers are obtained by maximizing the overall energy of (5.1).

5.2.3 LMMSE Receiver

Although the results in this chapter are not restricted to a particular receiver, it will be useful to review the linear minimum mean square error (LMMSE) receiver. In particular, under perfect knowledge of the equivalent channel, and assuming unit transmit power per data carrier ($E\left[|s_k|^2\right] = 1$), the MMSE estimate of s_k is

$$\hat{s}_k = \frac{h_k^* y_k}{|h_k|^2 + \sigma^2}, \tag{5.2}$$

which yields a per-carrier MSE

$$\mathrm{MSE}_k = E\left[|\hat{s}_k - s_k|^2\right] = \frac{1}{1 + \gamma\,|h_k|^2}, \quad k = 1, ..., N_c, \tag{5.3}$$

where $\gamma = 1/\sigma^2$ is defined as the (expected) signal to noise ratio (SNR) at the transmitter side.

5.3 MaxSNR Beamforming Method

In this section, we consider the MaxSNR criterion to design the Tx-Rx beamformers for the proposed RF-MIMO simplified architectures under OFDM transmissions. Specifically, we propose to maximize the overall energy of the equivalent channel in

(5.1). Therefore, the general optimization problem associated to the analog antenna combining schemes can be written as

$$\begin{aligned} \underset{\mathbf{w}_T,\mathbf{w}_R}{\text{maximize}} \quad & \sum_{k=1}^{N_c} \left|\mathbf{w}_R^H \mathbf{H}_k \mathbf{w}_T\right|^2 \\ \text{subject to} \quad & \|\mathbf{w}_T\| \leq 1, \quad \mathbf{w}_T \in \mathcal{S}^{n_T \times 1}, \\ & \|\mathbf{w}_R\| \leq 1, \quad \mathbf{w}_R \in \mathcal{S}^{n_R \times 1}, \end{aligned} \tag{5.4}$$

Analogously to the flat-fading case, we propose to solve this non-convex optimization problem by means of an alternating optimization algorithm, and therefore in the following we concentrate on how to solve the SIMO case (the MISO case is mathematically identical). For SIMO-OFDM channels, our optimization problem is again (4.3) where $\mathbf{R}_{\text{SIMO}}$ is now averaged over all subcarriers

$$\mathbf{R}_{\text{SIMO}} = \sum_{k=1}^{N_c} \mathbf{h}_{\text{SIMO}_k} \mathbf{h}_{\text{SIMO}_k}^H, \tag{5.5}$$

and $\mathbf{h}_{\text{SIMO}_k} \in \mathbb{C}^{n_R \times 1}$ is the SIMO channel vector for the k-th data carrier.

As we will see, except for the RF-EGB architecture, the solutions for OFDM transmissions follow directly from the solutions already proposed for flat-fading channels in Chapter 4. For completeness, we present a brief description for each architecture.

5.3.1 RF-MRB Architecture

In this subsection, we consider how to find the complex weight beamformer which implements RF-MRB architecture. In the literature, the beamforming design problem for RF-MRB architecture under OFDM transmission has been analyzed in [Vía et al, 2010a, Rahman et al., 2004, Lei and Chin, 2004]. Specifically, for SIMO channel the optimal receive beamformer can be obtained in closed-form as the principal eigenvector of the matrix $\mathbf{R}_{\text{SIMO}}$ in (5.5).

5.3.2 RF-RWB Architecture

The optimal real weight beamformer, which implements RF-RWB combining architecture at the receiver can be obtained in closed-form as the principal eigenvector corresponding to the largest eigenvalue of

$$\mathbf{G}_{\text{SIMO}} = \Re\left(\mathbf{R}_{\text{SIMO}}\right). \tag{5.6}$$

5.3.3 RF-EPB Architecture

Following the lines as in the case of flat-fading channels, the optimal equal-phase receive beamformer can be obtained from the solution of the optimization problem in (4.9), where now the correlation matrices $\mathbf{R}_{\text{SIMO}}$ and $\mathbf{G}_{\text{SIMO}}$ are given, respectively, by (5.5) and (5.6). Thus, once the optimal beamforming matrix $\mathbf{W}_R$ has been obtained by solving a convex problem, the receive beamformer $\mathbf{w}_R$ is extracted as the principal eigenvector corresponding to the dominant eigenvalue of $\mathbf{W}_R$.

5.3.4 RF-EGB Architecture

For this architecture, the closed-form solution for flat-fading channels in (4.10) cannot be easily extended to OFDM systems. We follow a different approach here to obtain the equal-gain beamformer for OFDM-SIMO case and rewrite the optimization problem in (4.3) as

$$\begin{aligned} \underset{\mathbf{W}_R}{\text{maximize}} \quad & \operatorname{Tr}\left(\mathbf{R}_{\text{SIMO}}\mathbf{W}_R\right) \\ \text{subject to} \quad & \operatorname{diag}\left(\mathbf{W}_R\right) = \frac{1}{n_R}\mathbf{I}, \\ & \mathbf{W}_R \succeq 0, \\ & \operatorname{rank}\left(\mathbf{W}_R\right) = 1, \end{aligned} \tag{5.7}$$

where now the beamforming matrix is defined as $\mathbf{W}_R = \mathbf{w}_R\mathbf{w}_R^H$, and $\mathbf{R}_{\text{SIMO}}$ is given in (5.5).

Note that, in (5.7) excluding the rank-one constraint, the diagonal elements equality, the semidefinite inequality and the objective function, are linear in $\mathbf{W}_R$. The problem in (5.7) is nonconvex because of the rank-one constraint.

According to the semidefinite relaxation method (SDR), as previously discussed, the problem in (5.7) can be relaxed to a convex optimization by omitting the rank-one constraint obtaining the following problem

$$\begin{aligned} \underset{\mathbf{W}_R}{\text{maximize}} \quad & \operatorname{Tr}\left(\mathbf{R}_{\text{SIMO}}\mathbf{W}_R\right) \\ \text{subject to} \quad & \operatorname{diag}\left(\mathbf{W}_R\right) = \frac{1}{n_R}\mathbf{I}, \\ & \mathbf{W}_R \succeq 0. \end{aligned} \tag{5.8}$$

Finally, the receive beamformer $\mathbf{w}_R$ can be approximated using the phases of the principal eigenvector of the (in general not rank-one) beamforming matrix $\mathbf{W}_R$.

5.3.5 Alternating Optimization Algorithm

Following the lines in the previous chapter, we propose an iterative algorithm, which alternates the optimization of the transmit and receive beamformers for frequency-selective channels. The overall technique is summarized in Algorithm 2 and, in order to guarantee the fast convergence of the algorithm, an initialization point based on approximated MaxSNR (closed-form) solution is addressed in Section 5.6.

After initializing the Tx and Rx weights, the algorithm at each iteration, updates the Rx (Tx) beamformer by obtaining the equivalent SIMO (MISO) channels after fixing the Tx (Rx) weight, and then solve the optimization in (4.3) for the SIMO (MISO) case.

Initialize the beamformers $\mathbf{w}_T$, $\mathbf{w}_R$ from the solution of the equivalent SIMO problem in (5.20).
repeat
  Update of the receive beamformer
  Obtain the equivalent SIMO channel $\mathbf{h}_{\text{SIMO}_k} = \mathbf{H}_k \mathbf{w}_T$.
  Solve the optimization problem in (4.3) for the SIMO channel $\mathbf{h}_{\text{SIMO}_k}$.
  Use the solution as the new receive beamformer $\mathbf{w}_R$.
  Update of the transmit beamformer
  Obtain the equivalent MISO channel $\mathbf{h}_{\text{MISO}_k} = \mathbf{H}_k^H \mathbf{w}_R$.
  Solve the optimization problem in (4.3) for the MISO channel $\mathbf{h}_{\text{MISO}_k}$.
  Use the solution as the new transmit beamformer $\mathbf{w}_T$.
until Convergence

Algorithm 2: Proposed alternating optimization algorithm for RF-MIMO beamforming in frequency-selective channels.

5.4 General Analog Beamforming Criterion

In this section, a general criterion for the design of the Tx-Rx beamformers is introduced under perfect knowledge of the MIMO channel $\mathbf{H}_k$, as well as the noise variance, at the transceiver. Specifically, we propose to minimize the following cost function

$$f_\alpha\left(\mathbf{w}_T, \mathbf{w}_R\right) = \frac{1}{\alpha - 1} \log\left(\frac{1}{N_c} \sum_{k=1}^{N_c} \text{MSE}_k^{\alpha-1}\right), \tag{5.9}$$

where α is a real parameter which controls the overall system performance. Thus, our optimization problem may be written as

$$\begin{aligned} \underset{\mathbf{w}_T,\mathbf{w}_R}{\text{minimize}} \quad & f_\alpha\left(\mathbf{w}_T,\mathbf{w}_R\right) \\ \text{subject to} \quad & \|\mathbf{w}_T\| \leq 1, \quad \mathbf{w}_T \in \mathcal{S}^{n_T\times 1}, \\ & \|\mathbf{w}_R\| \leq 1, \quad \mathbf{w}_R \in \mathcal{S}^{n_R\times 1}. \end{aligned} \tag{5.10}$$

It is interesting to mention that (5.9) structurally resembles the definition of Renyi's entropy of order α for discrete random variable [Renyi, 1976]. Before addressing the optimization problem, let us analyze some interesting choices of α, which shed some light into the properties of the cost function (5.9).

5.4.1 Particular Cases of α

MaxSNR ($\alpha = 0$)

If the parameter α is set to zero, the cost function of the optimization problem in (5.10) can be rewritten as

$$f_\alpha\left(\mathbf{w}_T,\mathbf{w}_R\right) = \frac{1}{N_c}\sum_{k=1}^{N_c}|h_k|^2,$$

i.e., the proposed criterion reduces to the maximization of the received SNR or MaxSNR criterion proposed in the previous section.

MaxCAP ($\alpha = 1$)

When α approaches 1, the cost function of proposed criterion reduces to

$$f_\alpha\left(\mathbf{w}_T,\mathbf{w}_R\right) = \frac{1}{N_c}\sum_{k=1}^{N_c}\log\left(1+\gamma\,|h_k|^2\right),$$

which represents the capacity of the equivalent SISO channel after beamforming.

MinMSE ($\alpha = 2$)

In this case, the cost function of (5.10) is equivalent to

$$f_\alpha\left(\mathbf{w}_T,\mathbf{w}_R\right) = \frac{1}{N_c}\sum_{k=1}^{N_c}\mathrm{MSE}_k,$$

i.e., the proposed criterion amounts to minimizing the overall MSE of the optimal linear receiver. Moreover, it can be proved that, in the important case of quadrature amplitude modulation (QAM) constellations, and under optimal linear precoding of the information symbols, the minimization of the MSE is equivalent to the minimization of the bit error rate (BER) [Palomar and Jiang, 2006].

Other Cases of α

Although this chapter mainly considers three values of α (i.e., $\alpha = 0,\ 1,$ and 2), it should be noted that any other choice would be in principle possible. In particular, two other interesting cases are the following:

- MaxMin ($\alpha = \infty$): In this case, the summation in (5.9) is dominated by the worst data-carrier, i.e., by that with the smallest $|h_k|^2$. Therefore, for $\alpha \to \infty$, the proposed criterion reduces to the optimization of the worst data-carrier. Interestingly, for SIMO and MISO cases, the proposed criterion is mathematically identical to that of MaxMin fair multicast beamforming problem, which has been proven to be NP-hard [Sidiropoulos et al, 2006, Phan et al, 2009].

- MaxMax ($\alpha = -\infty$): For $\alpha \leq 1$ the proposed criterion can be rewritten as

$$\begin{aligned} \underset{\mathbf{w}_T, \mathbf{w}_R}{\text{maximize}} \quad & \sum_{k=1}^{N_c} \left(1 + \gamma\, |h_k|^2\right)^{1-\alpha} \\ \text{subject to} \quad & \|\mathbf{w}_T\| \leq 1, \quad \mathbf{w}_T \in \mathcal{S}^{n_T \times 1}, \\ & \|\mathbf{w}_R\| \leq 1, \quad \mathbf{w}_R \in \mathcal{S}^{n_R \times 1}, \end{aligned} \tag{5.11}$$

  then, it is easy to see that, when $\alpha \to -\infty$, the summation is dominated by the largest $|h_k|$. Therefore, the proposed criterion reduces to the optimization of the best data-carrier.

5.5 Beamforming Design for $\alpha \neq 0$

In general, for all the proposed RF architectures, the optimization problem in (5.10) is very difficult to solve (and has no closed-form solution for $\alpha \neq 0$), due to the coupling among the equivalent SISO channels. Therefore, we derive a pair of coupled eigenvalue problems which must be fulfilled by the Tx and Rx beamformers for RF-MRB architecture. Then, building upon these coupled problems, and taking into account the constraint on beamformers for each architecture, we propose a simple gradient descent method, equipped with a good initialization technique, to find the solution of the nonconvex problem in (5.10).

5.5.1 Coupled Eigenvalue Problems for RF-MRB Scheme

Specifically, by applying the Lagrange multipliers method it is easy to see that the solution of (5.10) for RF-MRB scheme must fulfill the following pair of coupled eigenvalue problems

$$\mathbf{R}_{\mathrm{SIMO}_\alpha}\mathbf{w}_R = \lambda \mathbf{w}_R, \qquad \mathbf{R}_{\mathrm{MISO}_\alpha}\mathbf{w}_T = \lambda \mathbf{w}_T, \tag{5.12}$$

where $\lambda = \sum_{k=1}^{N_c} \mathrm{MSE}_k^\alpha \left|h_k\right|^2$,

$$\mathbf{R}_{\mathrm{SIMO}_\alpha} = \sum_{k=1}^{N_c} \mathrm{MSE}_k^\alpha \mathbf{h}_{\mathrm{SIMO}_k}\mathbf{h}_{\mathrm{SIMO}_k}^H, \tag{5.13}$$

$$\mathbf{R}_{\mathrm{MISO}_\alpha} = \sum_{k=1}^{N_c} \mathrm{MSE}_k^\alpha \mathbf{h}_{\mathrm{MISO}_k}^H\mathbf{h}_{\mathrm{MISO}_k}, \tag{5.14}$$

can be seen as weighted covariance matrices and

$$\mathbf{h}_{\mathrm{SIMO}_k} = \mathbf{H}_k\mathbf{w}_T, \qquad \mathbf{h}_{\mathrm{MISO}_k} = \mathbf{w}_R^H\mathbf{H}_k, \tag{5.15}$$

are the SIMO (MISO) channels after fixing the transmit (receive) beamformer. For more details, see the analysis of the cost function minima in Appendix B.

5.5.2 Optimization Algorithm

Unfortunately, the pair of eigenvalue problems in (5.12) are coupled through the matrices $\mathbf{R}_{\mathrm{SIMO}_\alpha}$ and $\mathbf{R}_{\mathrm{MISO}_\alpha}$, which depend on both $\mathbf{w}_R$ and $\mathbf{w}_T$, and this precludes obtaining a closed-form solution for general case with $\alpha \neq 0$. In fact, unlike the MaxSNR criterion, closed-form general beamforming ($\alpha \neq 0$) solutions do not exist even for the simpler cases of SIMO and MISO channels. Therefore, the alternating optimization approach presented to the MaxSNR criterion can not be applied in this case. To avoid these problems, here we propose a gradient search algorithm based on the following updating rules

$$\mathbf{w}_R\left(t+1\right) = \mathbf{w}_R\left(t\right) + \mu\mathbf{R}_{\mathrm{SIMO}_\alpha}\mathbf{w}_R\left(t\right), \tag{5.16}$$

$$\mathbf{w}_T\left(t+1\right) = \mathbf{w}_T\left(t\right) + \mu\mathbf{R}_{\mathrm{MISO}_\alpha}\mathbf{w}_T\left(t\right), \tag{5.17}$$

where μ is a given step-size (or regularization parameter) and t denotes the iteration index.

From the above expressions, the solutions for RF architectures are obtained by taking in consideration the constraint on beamformers for each architecture. Specifically, the overall technique summarized in Algorithm 3, is considered as follows:

- includes a normalization step to force the unit energy constraint on the beamformers for every architecture (i.e., RF-MRB, RF-RWB, RF-EPB, and RF-EGB).

- obtains the real weight beamformers for RF-RWB architecture, by considering now the correlation matrices

$$\begin{aligned} \mathbf{G}_{\mathrm{SIMO}_\alpha} &= \Re\left(\mathbf{R}_{\mathrm{SIMO}_\alpha}\right), \\ \mathbf{G}_{\mathrm{MISO}_\alpha} &= \Re\left(\mathbf{R}_{\mathrm{MISO}_\alpha}\right), \end{aligned} \tag{5.18}$$

  for SIMO and MISO cases, respectively.

- forces the beamformers to be nonnegative real entries (i.e., $\mathbf{w}_T \geq \mathbf{0}$ and $\mathbf{w}_R \geq \mathbf{0}$) for RF-EPB architecture, where the correlation matrices are again (5.18).

- forces the elements of Tx and Rx beamformers to have a constant modulus of $1/\sqrt{n_R}$ and $1/\sqrt{n_T}$ for RF-EGB architecture. Specifically, the $\mathbf{w}_R$ and $\mathbf{w}_T$ beamformers can be approximated using the phases of the updated principal eigenvectors of $\mathbf{R}_{\mathrm{SIMO}_\alpha}$ and $\mathbf{R}_{\mathrm{MISO}_\alpha}$ in the updating rules (5.16) and (5.17), respectively. That is, we consider the expressions of Rx and Tx beamformers with $\mathbf{w}_R = \frac{1}{\sqrt{n_R}} e^{j\angle \mathbf{w}_R}$ and $\mathbf{w}_T = \frac{1}{\sqrt{n_T}} e^{j\angle \mathbf{w}_T}$, respectively.

Select μ; Initialize the beamformers $\mathbf{w}_T$, $\mathbf{w}_R$ from the solution of the equivalent SIMO problem in (5.20).
repeat
  Update of the receive beamformer
  Obtain the equivalent SIMO channel $\mathbf{h}_{\mathrm{SIMO}_k} = \mathbf{H}_k \mathbf{w}_T$.
  Update h_k and MSE_k for $k = 1, \ldots, N_c$.
  Update the beamformer $\mathbf{w}_R$ with (5.16).
  Select nonnegative weight $\mathbf{w}_R \geq \mathbf{0}$ for RF-EPB.
  Force $\mathbf{w}_R$ to have a constant modulus: $\mathbf{w}_R = \frac{1}{\sqrt{n_R}} e^{j\angle \mathbf{w}_R}$ for RF-EGB.
  Normalize the solution: $\mathbf{w}_R = \mathbf{w}_R / \|\mathbf{w}_R\|$.
  Update of the transmit beamformer
  Obtain the equivalent MISO channel $\mathbf{h}_{\mathrm{MISO}_k} = \mathbf{H}_k^H \mathbf{w}_R$.
  Update h_k and MSE_k for $k = 1, \ldots, N_c$.
  Update the beamformer $\mathbf{w}_T$ with (5.17).
  Select nonnegative weight $\mathbf{w}_T \geq \mathbf{0}$ for RF-EPB.
  Force $\mathbf{w}_T$ to have a constant modulus: $\mathbf{w}_T = \frac{1}{\sqrt{n_T}} e^{j\angle \mathbf{w}_T}$ for RF-EGB.
  Normalize the solution: $\mathbf{w}_T = \mathbf{w}_T / \|\mathbf{w}_T\|$.
until Convergence

Algorithm 3: Proposed beamforming algorithm based on gradient search.

Analogously to the Algorithm 2 for solving the MaxSNR criterion in MIMO case, the gradient method proposed in this section could suffer from local minima. Nevertheless, local minima can be avoided in practice by means of a proper initialization

technique. In particular, we propose to initialize the algorithm using the approximation of the MaxSNR beamformers described in Section 5.6. Simulation examples show that this initialization provides satisfactory results in most cases.

Finally, although it is beyond the scope of this chapter, we must note that the convergence speed of the proposed algorithm could be further improved by adaptively changing the learning rate μ, and that the algorithm can be easily modified to obtain a graduated nonconvexity technique [Blake and Zisserman, 1987].

5.5.3 Interpretation of the General Criterion Solution

Interestingly, in the low SNR regime (when $\gamma \left|h_k\right|^2 \ll 1$) and taking into account the first order Taylor series approximation of $f_\alpha\left(\mathbf{w}_T, \mathbf{w}_R\right)$ with respect to γ, it may be approximated by

$$f_\alpha\left(\mathbf{w}_T, \mathbf{w}_R\right) \simeq -\gamma \sum_{k=1}^{N_c} \left|h_k\right|^2, \tag{5.19}$$

and the MSE_k^α in the definition of the cost function (5.9) are now given as $\mathrm{MSE}_k^\alpha \simeq 1$ for $k = 1, ..., N_c$. In this case, the problem in (5.10) reduces to the maximization of the energy of the equivalent channel (or the MaxSNR criterion).

On the other hand, for high or moderate SNRs (when $\gamma \left|h_k\right|^2 \gg 1$), the mean square error $\mathrm{MSE}_k \simeq 1/\gamma \left|h_k\right|^2$ rapidly decreases with the energy of the k-th subchannel $\left|h_k\right|^2$. Consequently, in this regime different values (MSE_k^α) are used in the definition of the cost function (5.9).

5.6 Initialization Method Based on a Closed-Form Approximated MaxSNR Solution

In order to guarantee the fast convergence of the proposed algorithms, a sufficiently accurate initialization technique is proposed in this section. Let us start by briefly describing the initialization method, which obtains an approximated MaxSNR solution in closed-form. In particular, for $\alpha = 0$ (or $\gamma \simeq 0$) the optimization problem in (5.10) can be rewritten as

$$\begin{aligned} \underset{\mathbf{w}_T,\mathbf{w}_R,\mathbf{w}}{\text{maximize}} \quad & \sum_{k=1}^{N_c} \left|\mathbf{h}_k^H \mathbf{w}\right|^2 \\ \text{subject to} \quad & \|\mathbf{w}_T\| \leq 1, \quad \mathbf{w}_T \in \mathcal{S}^{n_T \times 1}, \\ & \|\mathbf{w}_R\| \leq 1, \quad \mathbf{w}_R \in \mathcal{S}^{n_R \times 1}, \\ & \mathbf{w} = \mathbf{w}_R \otimes \mathbf{w}_T^*, \end{aligned} \tag{5.20}$$

where $\mathbf{h}_k = \text{vec}(\mathbf{H}_k)$ is the vectorized version of the MIMO channel for the k-th data carrier. Thanks to the structure of the sets $\mathcal{S}$, the above problem is equivalent to

$$\begin{aligned} \underset{\mathbf{w}_T,\mathbf{w}_R,\mathbf{w}}{\text{maximize}} \quad & \sum_{k=1}^{N_c} \left|\mathbf{h}_k^H \mathbf{w}\right|^2 \\ \text{subject to} \quad & \|\mathbf{w}\| \leq 1, \quad \mathbf{w} \in \mathcal{S}^{n_T n_R \times 1}, \\ & \mathbf{w} = \mathbf{w}_R \otimes \mathbf{w}_T^*. \end{aligned} \tag{5.21}$$

Of course, (5.20) and (5.21) are non-convex problems due to the non-convex Kronecker structure constraint. However, if we relax this constraint the optimization problem becomes identical to that in (5.10) ($\alpha = 0$ or $\gamma \simeq 0$) for SIMO channels, where now we have a virtual SIMO channel $\mathbf{h}_k$ and a virtual beamformer $\mathbf{w}$ that combines the Tx and Rx beamformers. This family of problems has been (approximately) solved in the previous section, and the only issue here is how to extract the beamformers $\mathbf{w}_T$ and $\mathbf{w}_R$ from $\mathbf{w}$. Analogously to Chapter 4, we propose here to use the best approximation in terms of the Euclidean norm. That is, the Tx-Rx beamformers are obtained from the singular vectors associated to the largest singular value of the $n_R \times n_T$ matrix $\mathbf{W} = \text{unvec}(\mathbf{w})$. Notice that the constraint $\mathbf{w} \in \mathcal{S}^{n_T n_R \times 1}$ is explicitly taken into account in (5.21) and consequently the initialization is specific to each architecture.

5.7 Computational Complexity

In this section, we study the computational complexity of the considered optimization algorithms and its initialization approach for frequency-selective channels. We have already pointed out in previous chapters of this dissertation that a major advantage of analog combining architectures is that only a single DFT is required per terminal. Therefore, an $(n_T + n_R)/2$ fold saving of DFT processors is achieved with respect to conventional MIMO (or Full-MIMO), which needs a dedicated DFT per antenna element. Note that in terms of DFT complexity, analog combining schemes is equivalent to an OFDM-based single antenna system.

Algorithm 2

According to the algorithm proposed for analog beamforming schemes in flat-fading channels, the computational complexity depends on the eigenvalue decomposition used to find the Tx-Rx weights associated to those architectures. It should be mentioned that, the alternating optimization algorithm under OFDM transmission has a total complexity (per iteration) of $\mathcal{O}(N_c n^2)$ ($n = \max(n_T, n_R)$) to factor N_c matrices of the form $\mathbf{R}_{\text{SIMO}}$ obtained in SIMO case, and according to the complexity order of $\mathcal{O}(n^3)$ required for direct EVD methods to decompose a square matrix of size n [Nesterov and Nemirovsky, 1994]. The Table 5.1 gives us the computational complexity costs of the proposed techniques (for both flat-fading and frequency-selective channels) associated for the various analog combining schemes considered in this thesis.

Algorithm	Flat-fading	Frequency-selective
RF-MRB	$\mathcal{O}\left(n^2 + n^3\right)$	$\mathcal{O}\left(N_c n^2 + n^3\right)$
RF-RWB	$\mathcal{O}\left(n^2 + n^3\right)$	$\mathcal{O}\left(N_c n^2 + n^3\right)$
RF-EPB	$\mathcal{O}\left(n^2 + n^7\right)$	$\mathcal{O}\left(N_c n^2 + n^7\right)$
RF-EGB	$\mathcal{O}\left(n^2 + n^7\right)$	$\mathcal{O}\left(N_c n^2 + n^7\right)$

Table 5.1: Comparison of computational complexity (per iteration) of the proposed alternating optimization algorithms for different RF schemes.

Algorithm 3

For the gradient search technique, it is easy to find that one iteration of the proposed Algorithm 3 comes at a cost of order $\mathcal{O}\left(N_c\left(n_T + n_R\right)^2\right)$.

Initialization Approach

The computational complexity associated to the initialization approaches in frequency-selective channels, is of order $\mathcal{O}\left(N_c n_T^2 n_R^2 + n_T^3 n_R^3\right)$.

5.8 Simulation Results

In this section, we present several numerical examples to demonstrate the performance of the proposed simplified RF-MIMO architectures by considering the MaxSNR, MaxCAP and MinMSE criteria. In this chapter, we have chosen the European standard 802.11a for WLAN, which is based on the multicarrier modulation OFDM (64 carriers are used in the simulation) [IEEE 802.11a standard, 1999]. Also, we consider multiple antennas at both the transmitter and the receiver ($n_R = n_T = 4$). An i.i.d. Rayleigh

MIMO channel with the frequency selectivity is modeled using an exponential power delay profile. In particular, the power associated to the l-th tap is

$$E\left[\|H[l]\|^2\right] = (1-\rho)\rho^l n_T n_R, \qquad l = 0, \ldots, L_c - 1, \tag{5.22}$$

where L_c is the length of the channel impulse response ($L_c = 16$ in the simulations), and the exponential parameter ρ has been selected as $\rho = 0.4$ for low frequency-selectivity and $\rho = 0.7$ for high frequency-selectivity. In all experiments we have used QPSK constellations, which can be either coded or uncoded.

In this simulation, the proposed RF-MIMO schemes have been compared with a SISO system and a Full-MIMO scheme (conventional baseband MIMO-OFDM with maximum ratio transmission (MRT) and maximum ratio combining (MRC) per subcarrier, denoted as Full-MIMO), which can be seen as an upper bound for the performance of any of the analog antenna combining systems.

The performance is given in terms of BER (bit error rate) by means of Monte Carlo simulations. Specifically, in this section, each simulation consists in the generation of channel realization, the obtention of the transmit and receive beamformers, and the evaluation of the system performance which is based on the analysis of the equivalent SISO channel.

In all experiments, we have performed a minimum of 10000 Monte Carlo simulations, and for the MaxCAP and MinMSE approaches, the step-size has been fixed to $\mu = 0.1$, and the convergence criterion is based on the difference between the beamformers in two consecutive iterations. Specifically, the algorithm finishes when the Euclidian distance is lower than 10^{-3}. With these values, the proposed algorithm has never exceed 50 iterations.

5.8.1 MaxSNR ($\alpha = 0$) Method

• Uncoded Transmission

Figures 5.1 and 5.2 show the BER for frequency-selective channels with uncoded transmissions and exponential parameter $\rho = 0.4$ and $\rho = 0.7$, respectively. As can be seen, the gap between the analog antenna combining architectures and the Full-MIMO transceiver increases with the frequency selectivity of the channel, which is due to the fact that the Full-MIMO scheme is able to apply a different pair of beamformers for each subcarrier. However, we can also observe that the performance of the proposed simplified architectures is close to that of the RF-MRB scheme, and in all cases they outperform the conventional SISO system. Additionally, the ordering among the alternative architectures remains as in the flat-fading case, that is, RF-MRB, RF-EGC, RF-RWB and RF-EPB, from better to worse performance.

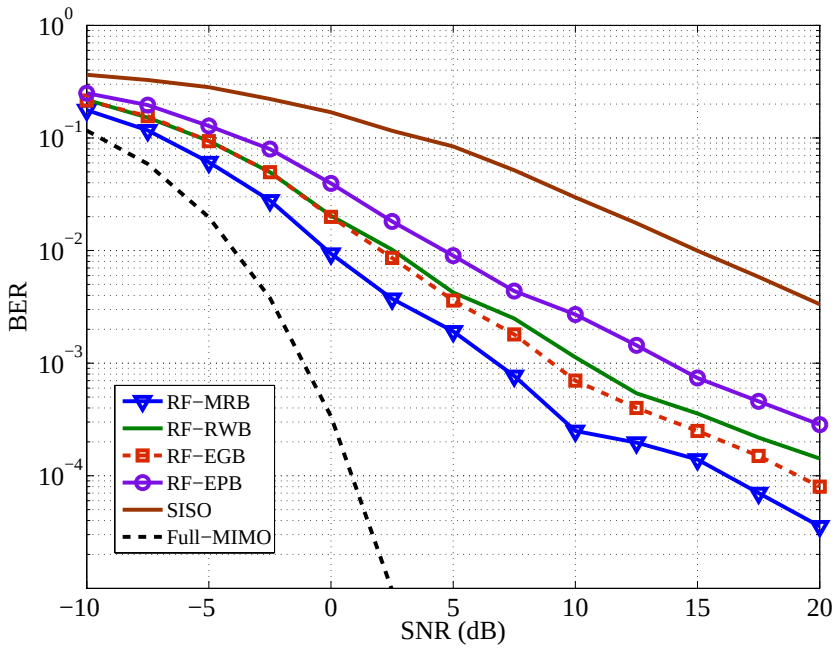

Figure 5.1: Bit error rate vs. SNR for the compared algorithms. Uncoded QPSK symbols for $\rho = 0.4$.

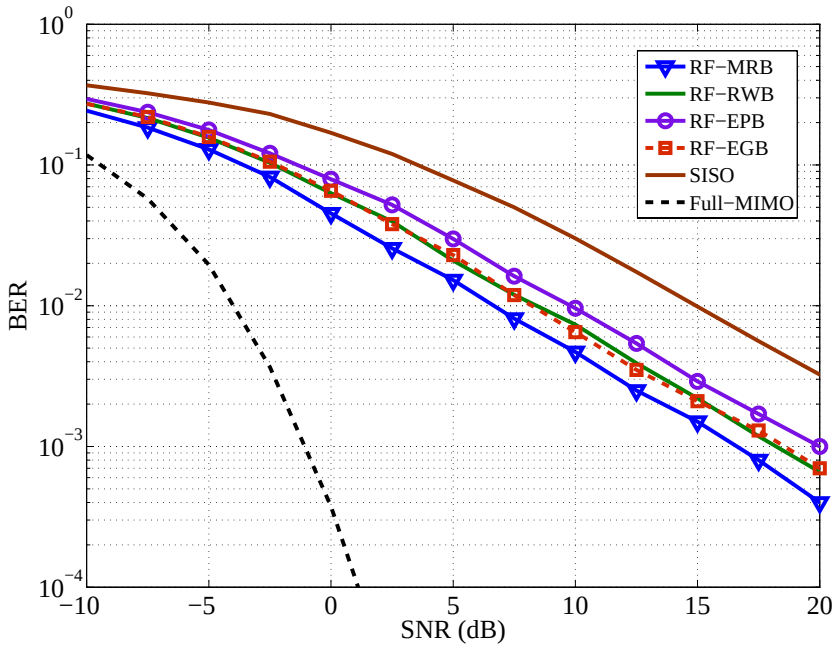

Figure 5.2: Bit error rate vs. SNR for the compared algorithms. Uncoded QPSK symbols for $\rho = 0.7$.

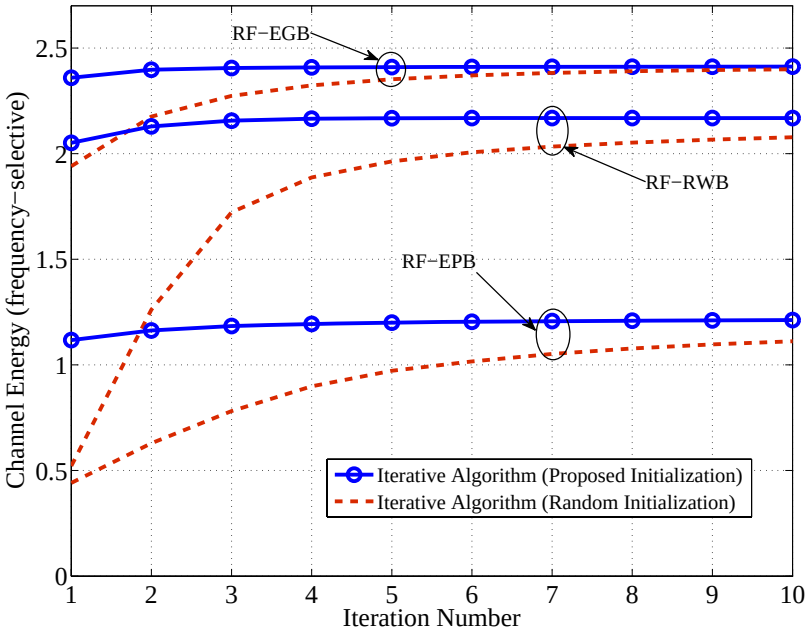

Figure 5.3: Convergence of the Algorithm 2 for frequency-selective channels. Initialization in the approximated solution of (5.21) or in a pair of unit-norm random vectors $\mathbf{w}_T$, $\mathbf{w}_R$.

Figure 5.3 illustrates the convergence of the proposed alternating optimization algorithm for SNR = 10 dB. As we can see, the proposed iterative algorithm converges very fast to the desired solution even in the case of a random initialization. As can be expect, the convergence is much faster with the proposed initialization.

- **Coded Transmission**

Figures 5.4 and 5.5 show similar results for the case of coded transmissions using the 802.11a standard [IEEE 802.11a standard, 1999], which uses $N_c = 48$ out of the 64 subcarriers for data transmission. In this case, we have selected a transmission rate of 12 Mbps, which uses QPSK signalling and a code rate 1/2. The data bits are encoded with a convolutional code and block interleaved as specified in the 802.11a standard. The receiver is based on the soft Viterbi decoder. In this case, the proposed analog antenna combining architectures offer an intermediate solution between the conventional SISO system and the complex Full-MIMO architecture. Furthermore, the convolutional encoder makes the slope of the BER curves very similar.

Finally, we must note that the ordering among the alternative architectures is the same in the three figures, that is, RF-MRB, RF-EGC, RF-RWB and RF-EPB,

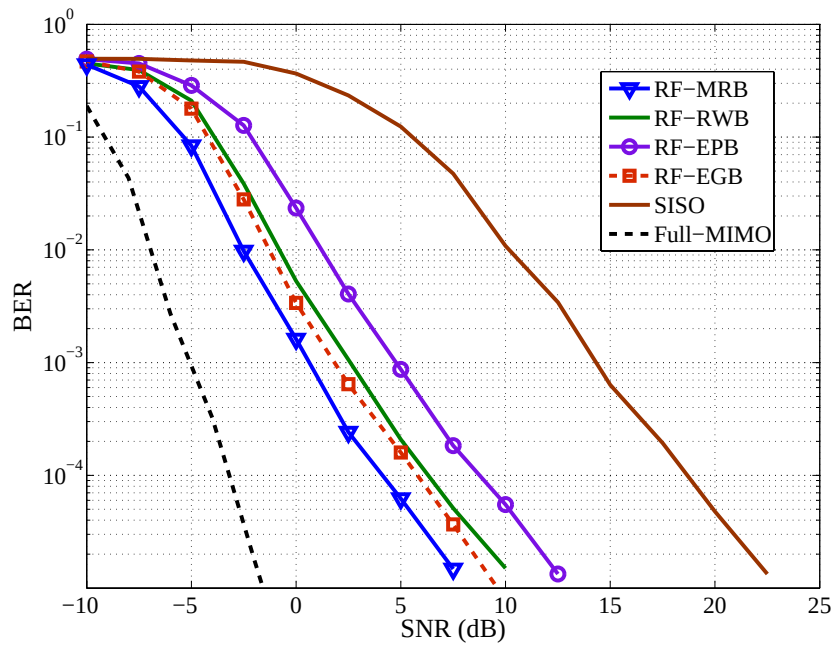

Figure 5.4: BER for 802.11a based system with transmission rate of 12Mbps, QPSK signaling and convolutional encoder of rate 1/2 for $\rho = 0.4$.

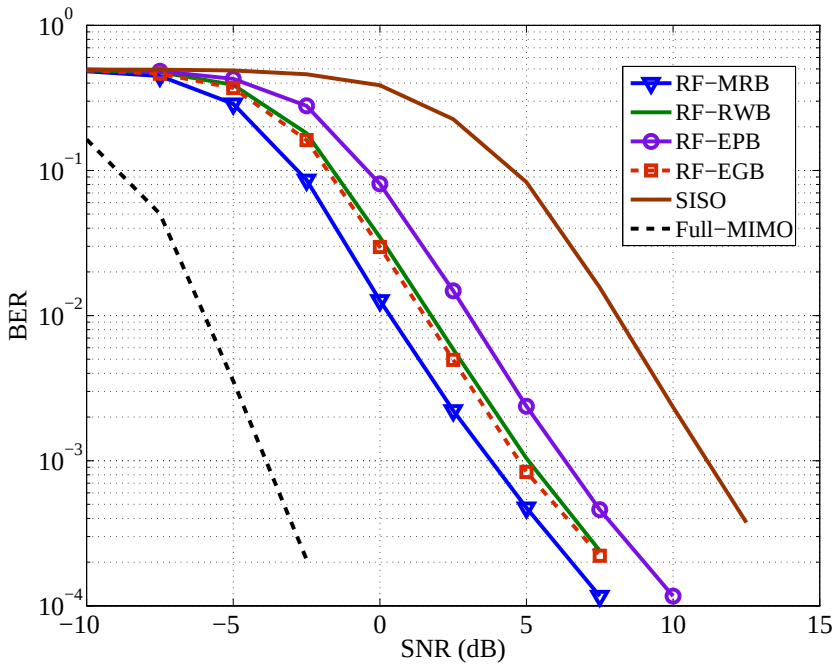

Figure 5.5: BER for 802.11a based system with transmission rate of 12Mbps, QPSK signaling and convolutional encoder of rate 1/2 for $\rho = 0.7$.

from better to worse performance. This is easily explained as a direct consequence of the feasibility regions (and complexity) of the proposed schemes. Thus, the feasible beamformers of the RF-EPB are only a subset ($\mathbb{R}_+$) of those for RF-RWB ($\mathbb{R}$), which at the same time are contained in the feasible region associated to the RF-MRB ($\mathbb{C}$). The explanation for the results of the RF-EGC architecture is a bit more complicated, but roughly speaking we say that it outperforms the RF-RWB architecture because, at least for Rayleigh channels, the phases of the beamformers are more informative than the amplitudes.

5.8.2 MaxCAP ($\alpha = 1$) and MinMSE ($\alpha = 2$) Methods

• Uncoded Transmission

For all simplified analog antenna combining architectures, the advantage of using the MaxCAP and MinMSE criteria over the MaxSNR approach becomes clearer when the system performance is evaluated in terms of BER. Figures from 5.6 to 5.9 show the BER for uncoded QPSK transmission with $N_c = 64$ data carriers, and in this case, the exponential parameter ρ has been selected as $\rho = 0.7$, which represents a high frequency-selective MIMO channel. As can be seen, the analog combining schemes incur in a degradation of the diversity order (slope of the BER-SNR curve) with respect to the Full-MIMO system. This degradation is due to the use of a common beamformer for all subcarriers and it increases with the frequency selectivity of the channel.[2] However, the diversity order of the MinMSE criterion is better than that of the MaxCAP, which is also better than that of the MaxSNR beamforming (which is in this example similar to that of a SISO system). In particular, the gap (for all RF schemes) between the MinMSE, MaxCAP and MaxSNR approaches is very significant in this case. This is due to the fact that, for uncoded transmissions, the overall system performance is dominated by the worst data carriers, which are improved by the MinMSE criterion. Therefore, since the MinMSE criterion assigns the highest weights (MSE_k^2) to these critical carriers, it provides better results than those of the MaxCAP and MaxSNR approaches. Therefore, the best criteria are (in order) MinMSE, MaxCAP, and MaxSNR. By comparing Figures from 5.6 to 5.9, it can be observed that the performance gap between the MinMSE approach for all schemes and the Full-MIMO system increases according to the alternative architectures (in order) RF-MRB, RF-EGB, RF-RWB and RF-EPB.

[2]Obviously, for a flat-fading channel, the performance of MaxSNR, MaxCAP and MinMSE criteria is identical to that of the Full-MIMO system.

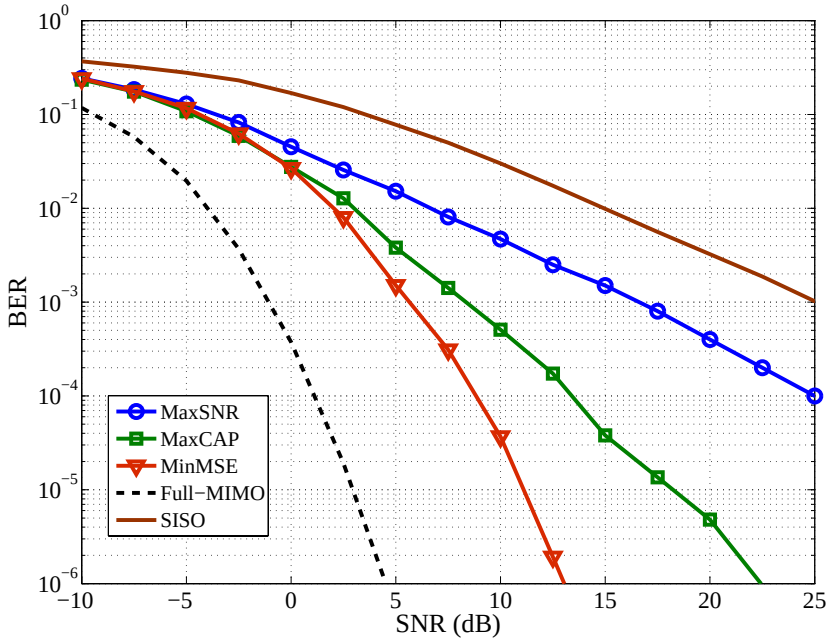

Figure 5.6: BER performance of RF-MRB algorithm. Uncoded QPSK symbols.

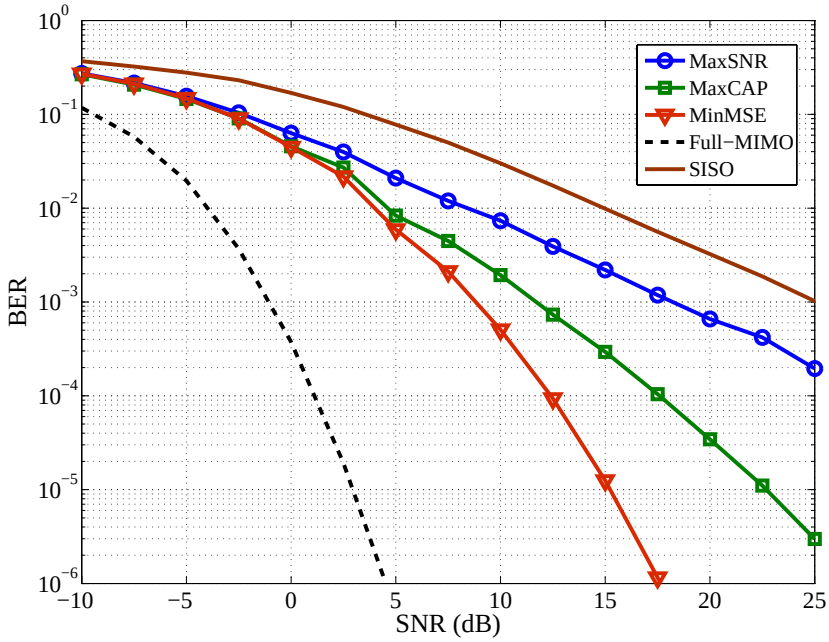

Figure 5.7: BER performance of RF-RWB algorithm. Uncoded QPSK symbols.

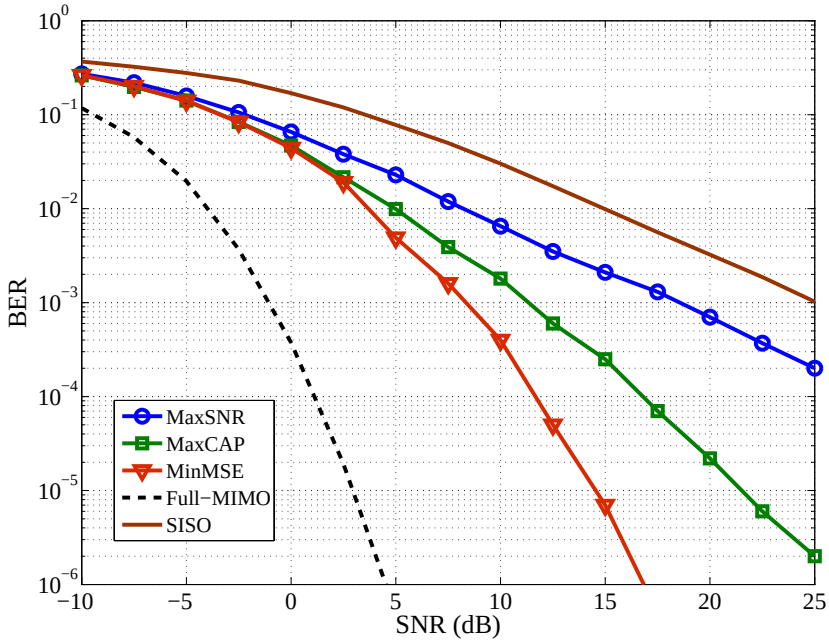

Figure 5.8: BER performance of RF-EGB algorithm. Uncoded QPSK symbols.

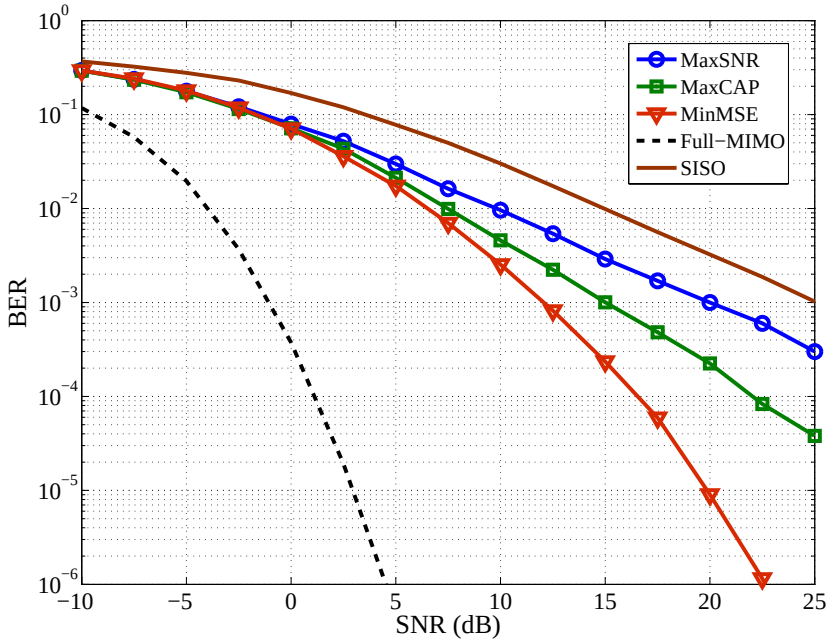

Figure 5.9: BER performance of RF-EPB algorithm. Uncoded QPSK symbols.

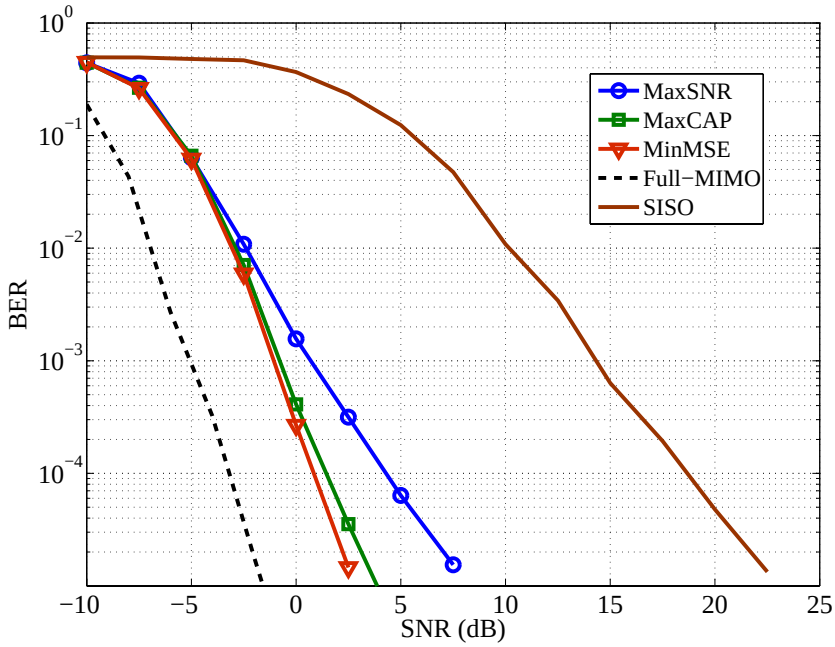

Figure 5.10: BER of RF-MRB scheme for 802.11a based system with transmission rate of 12Mbps, QPSK signaling and convolutional encoder of rate 1/2.

- **Coded Transmission**

In this subsection, for all analog antenna combining architectures, we have again chosen the scenario using coded transmissions under the 802.11a standard for a 12Mbps rate (QPSK modulation and a code rate of 1/2), and the exponential parameter ρ has been selected as $\rho = 0.4$, which represents a low frequency-selective MIMO channel. The data bits are encoded with a convolutional code and block interleaved as specified in the 802.11a standard. Finally, the receiver is based on soft decision Viterbi decoder.

In this case, as can be seen in Figures from 5.10 to 5.13 for all schemes, the best results are again provided by the MinMSE beamformers. Although by using a channel encoder followed by an interleaver all the bits are transmitted through all the subcarriers, we see that (for all RF schemes) the improvement of the worst subcarriers performed by MinMSE and MaxCAP criteria is still very effective in reducing the BER. Therefore, by comparing Figures from 5.10 to 5.13, it can be also observed that the performance gap between the MinMSE approach for all schemes and the Full-MIMO system increases according to the alternative architectures (in order) RF-MRB, RF-EGB, RF-RWB and RF-EPB.

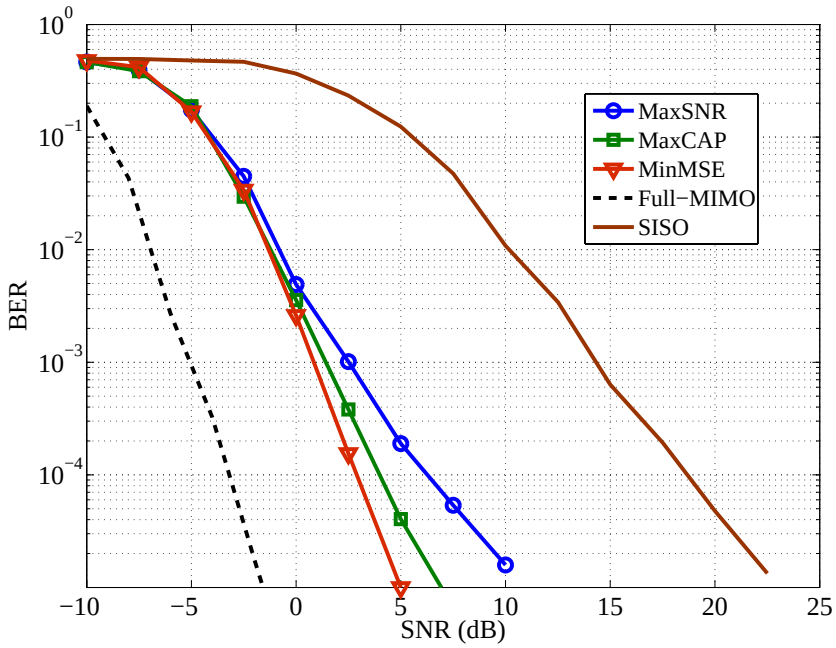

Figure 5.11: BER of RF-RWB scheme for 802.11a based system with transmission rate of 12Mbps, QPSK signaling and convolutional encoder of rate 1/2.

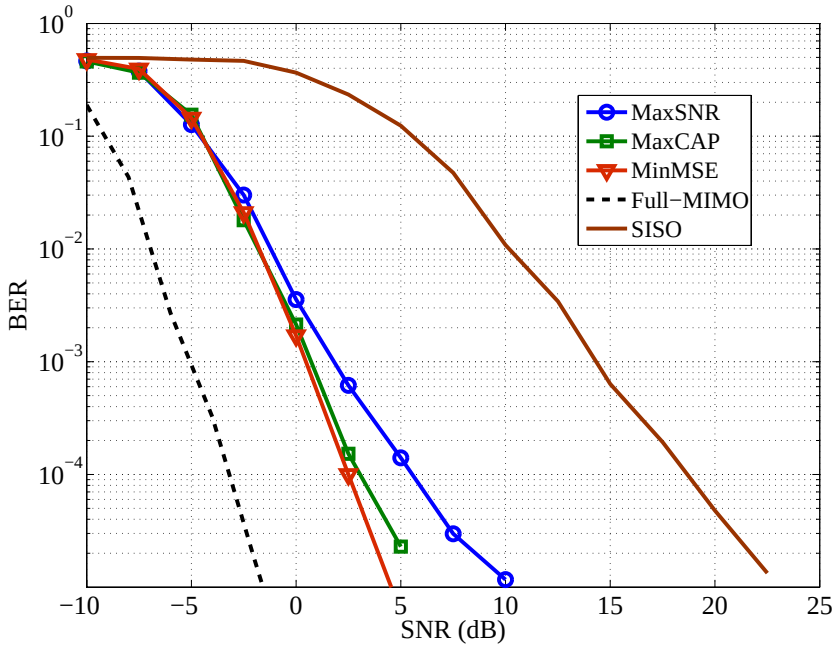

Figure 5.12: BER of RF-EGB scheme for 802.11a based system with transmission rate of 12Mbps, QPSK signaling and convolutional encoder of rate 1/2.

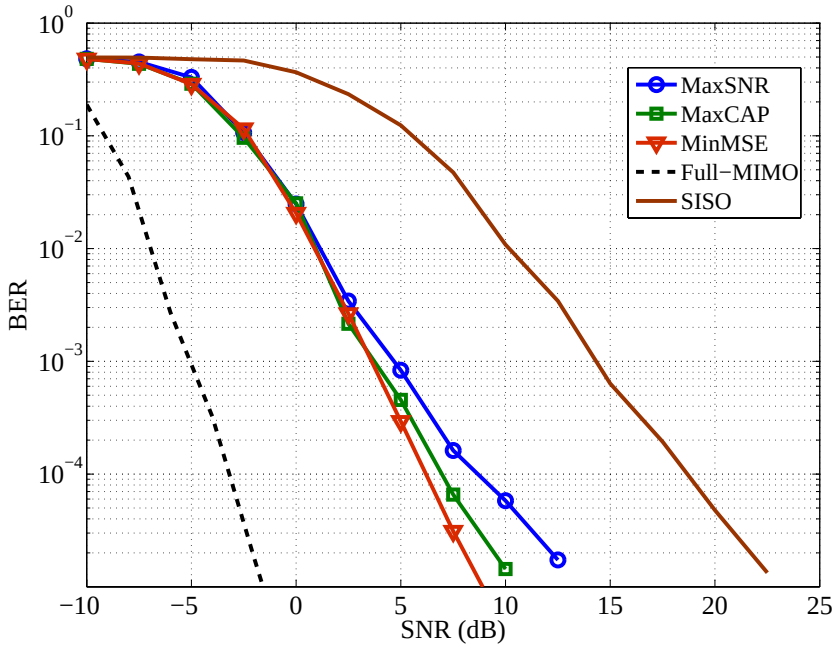

Figure 5.13: BER of RF-EPB scheme for 802.11a based system with transmission rate of 12Mbps, QPSK signaling and convolutional encoder of rate 1/2.

Finally, Figure 5.14 shows the convergence of the proposed gradient search algorithm (Algorithm 3) for SNR = 10 dB. For all RF schemes, the convergence is considered for MaxCAP criterion. As can be seen, with the proposed initialization, it always converges very fast to the desired solution.

5.8.3 Analysis of the Equivalent Channel

In this section, we analyze the equivalent channel after beamforming in frequency-selective channels. First, we will obtain the frequency response of the equivalent channel for the proposed RF architectures (i.e RF-RWB, RF-EPB, and RF-EGB). Specifically, the responses of these schemes will be compared to a Full-MIMO system which applies a different pair of beamformers for each subcarrier. Secondly, the effect of beamforming on the equivalent channel can be observed by considering the probability density function (PDF) of the equivalent channel amplitude for the conventional MIMO and or the proposed RF schemes.

- **Frequency Response of the Equivalent Channel**

Figures 5.15, 5.16, and 5.17 show the frequency responses of the equivalent channel for RF-RWB, RF-EPB, and RF-EGB schemes, respectively, compared to Full-MIMO

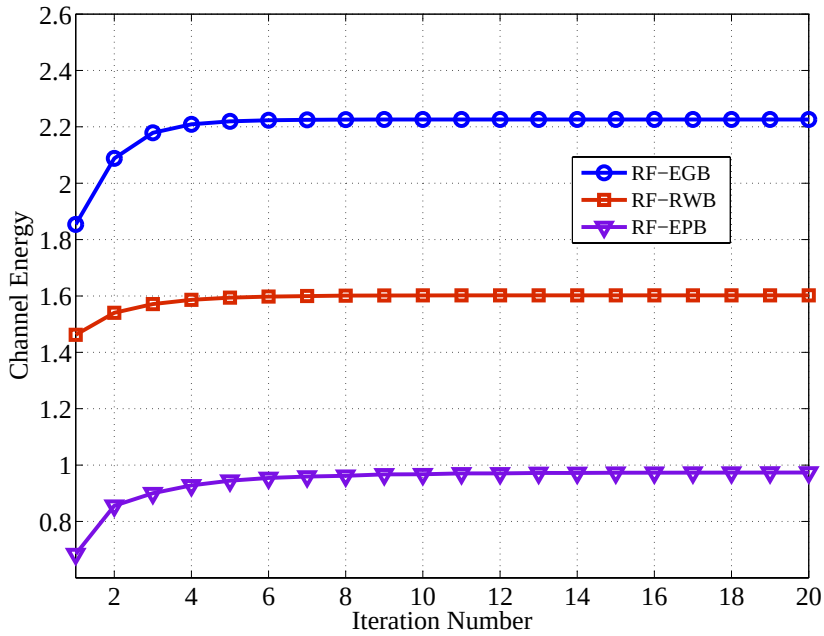

Figure 5.14: Convergence of the proposed gradient search algorithm for MaxCAP criterion.

and SISO systems. The analysis corresponds to one random channel realization and an SNR = 10 dB. As expected, the best response is that of the Full-MIMO system. However, for all proposed RF schemes, we can see that, unlike the MaxSNR approach, the MaxCAP and MinMSE criteria avoid deep nulls in the frequency response of the equivalent channel. In particular, MinMSE permits a slight degradation of the channel energy in order to improve the response of the worst data carriers. Also, the MaxCAP criterion (for all schemes) provides an intermediate solution between the MaxSNR and MinMSE criteria. Furthermore, for all schemes, the performance of the MaxSNR, MaxCAP and MinMSE approaches is between that of the SISO and Full-MIMO systems.

- **PDF of the Equivalent Channel**

Figures from 5.18 to 5.20 show the probability density function (obtained from 10000 random channel realizations) of squared amplitude of the equivalent channel for SNR of $\gamma = 10$ dB. The probability density functions for the proposed architectures, RF-RWB (Figure 5.18), RF-EPB (Figure 5.19) and RF-EGB (Figure 5.20) are compared to that of Full-MIMO and SISO systems. As can be seen, the MaxCAP and MinMSE approaches avoid values close to zero at the expense of slight degradation of the overall SNR.

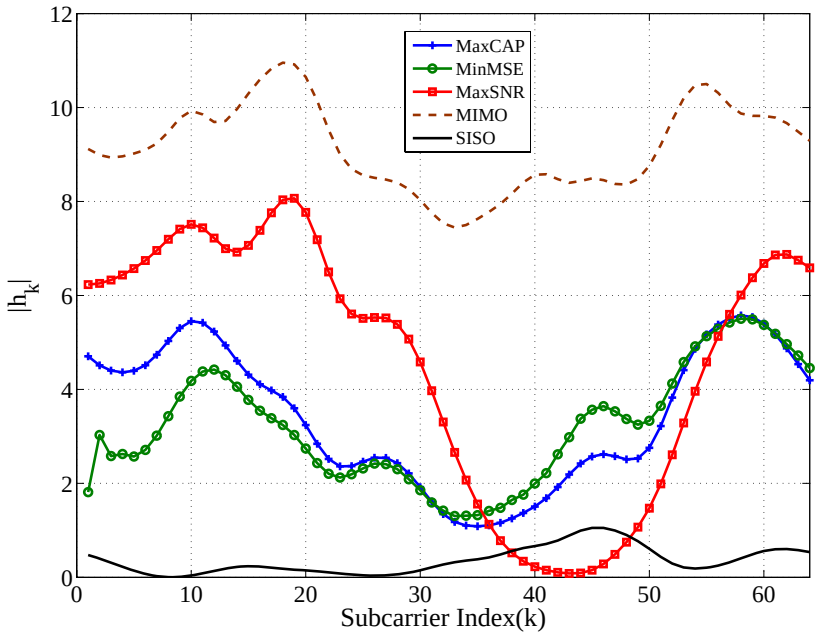

Figure 5.15: Channel response $|h_k|$ after real-weight beamforming for a channel realization.

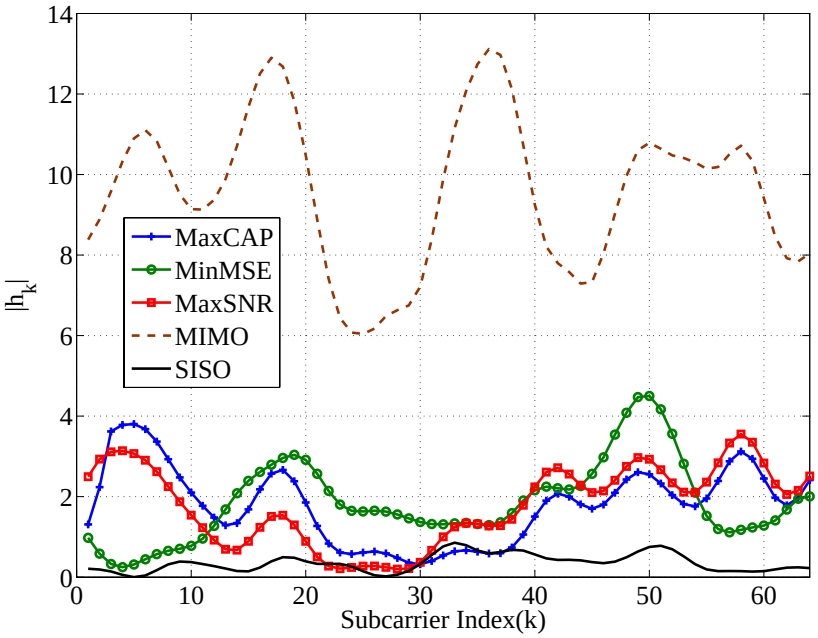

Figure 5.16: Channel response $|h_k|$ after equal-phase beamforming for a channel realization.

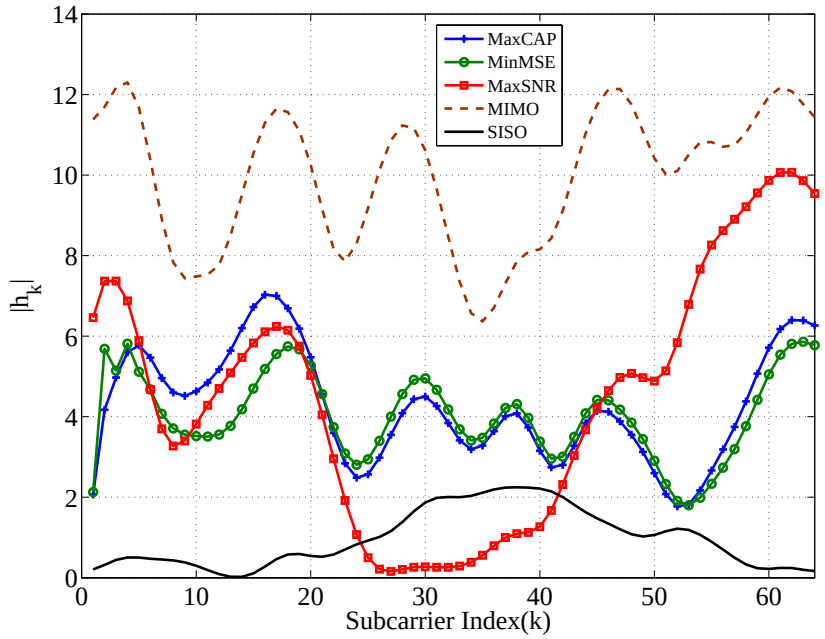

Figure 5.17: Channel response $|h_k|$ after equal-gain beamforming for a channel realization.

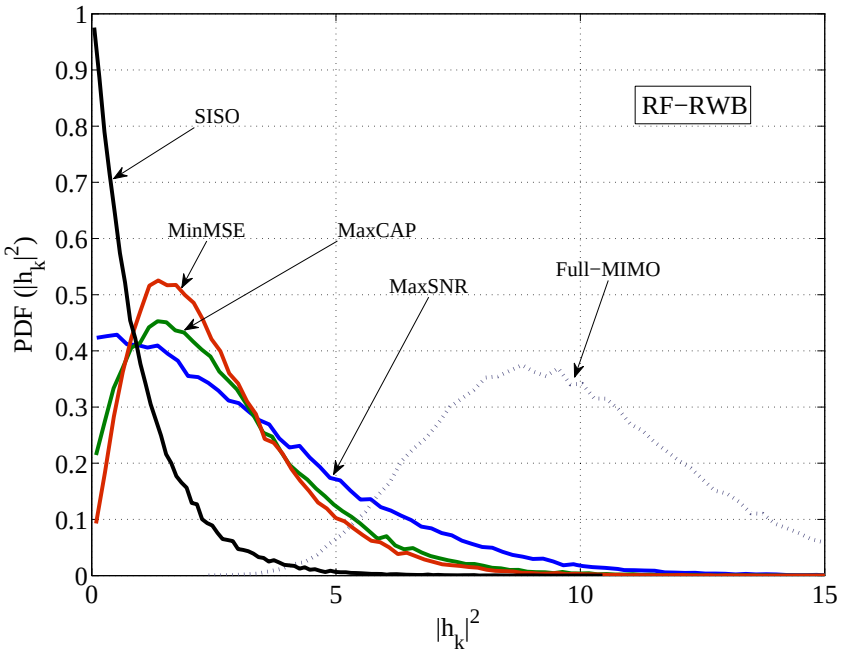

Figure 5.18: Probability density function of the equivalent channel response $|h_k|^2$ for RF-RWB scheme. $\gamma = 10\,\text{dB}$.

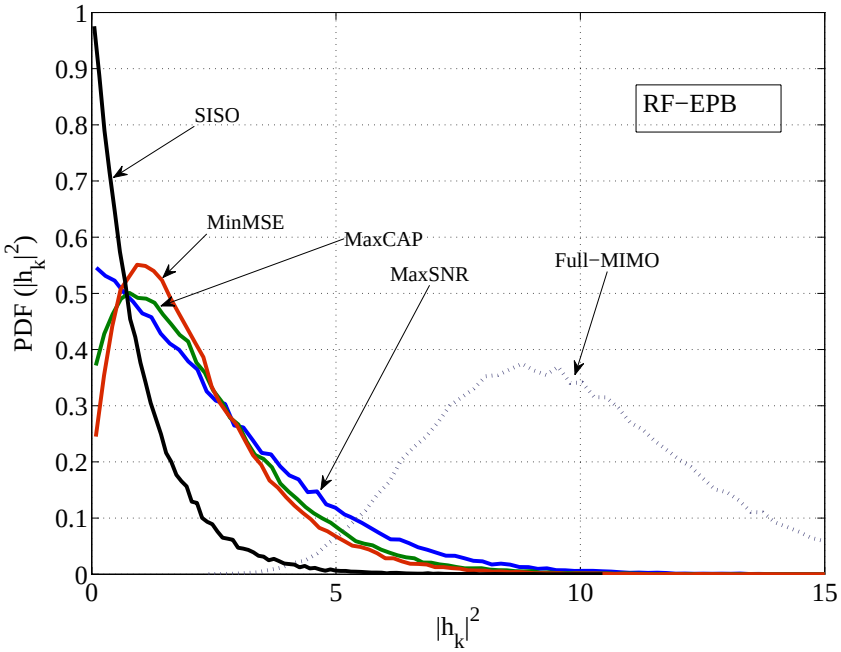

Figure 5.19: Probability density function of the equivalent channel response $|h_k|^2$ for RF-EPB scheme. $\gamma = 10\,\text{dB}$.

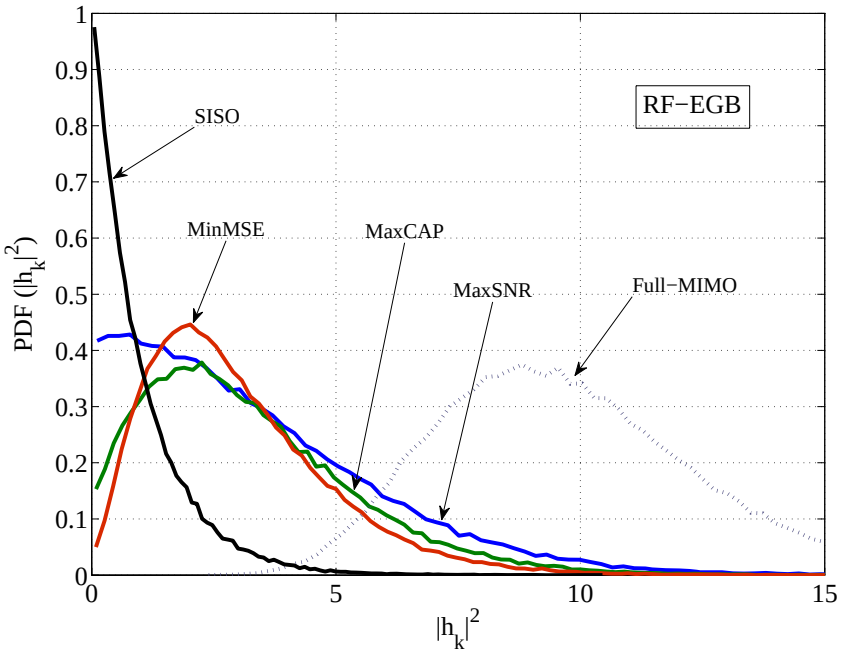

Figure 5.20: Probability density function of the equivalent channel response $|h_k|^2$ for RF-EGB scheme. $\gamma = 10\,\text{dB}$.

5.9 Summary

In this chapter we have proposed a beamforming design of three simplified analog antenna combining architectures (i.e., RF-RWB, RF-EPB and RF-EGB) under multicarrier transmissions. Analogously to Chapter 4, and from the baseband point of view, the three architectures result in new beamforming design problems, in which the Tx-Rx beamformers are constrained to have real weights (RWB), nonnegative real weights (EPB) or constant-modulus complex weights (EGB). With these new combining architectures, the same pair of Tx-Rx beamformers must be applied to all the subcarriers and, due to this coupling, the beamforming design problem poses several new challenges in comparison to conventional MIMO schemes. Considering the case of perfect channel state information (CSI) at the transceiver, we have proposed a beamforming criterion which depends on a single parameter α. This parameter establishes a tradeoff between the energy and spectral flatness of the equivalent channel, and allows us to obtain some interesting design criteria. In particular, the proposed beamforming criterion can be reduced to the maximization of the received SNR (MaxSNR, $\alpha = 0$), the maximization of the system capacity (MaxCAP, $\alpha = 1$), and the minimization of the MSE (MinMSE, $\alpha = 2$) of the optimal linear receiver.

In general, the proposed criterion results in a non-convex optimization problem. For the MaxSNR criterion, this problem is solved in closed-form using a convex relaxation techniques for the SIMO and MISO cases, while for the MIMO case an alternating optimization algorithm was used to find a suboptimal solution. For general case with $\alpha \neq 0$, the closed-form solution for SIMO or MISO cases did not exist, thus, the RF weights were obtained by mean of a simple gradient search algorithm. The proposed algorithms for all criteria provides very good results in practical OFDM-based WLAN standards such as 802.11a, with a proper initialization method. The performance of the proposed architectures has been illustrated by means of several simulation examples, which allows us to conclude that the proposed architectures represent an attractive low-cost alternative to conventional MIMO systems and other (more costly) analog antenna combining architectures. The best results are provided by the MinMSE beamformers, and it was also observed that the performance gap between the MinMSE approach for all schemes and Full-MIMO system increases according to the alternative architectures (in order) RF-MRB, RF-EGB, RF-RWB and RF-EPB. Finally, the best results are provided by the RF-EGB architecture, which reveals the importance of the phase of the RF signals in comparison to their amplitude in beamforming problems.

Chapter 6

Conclusions and Future Work

6.1 Conclusions

In wireless communication, MIMAX architecture (called in this thesis as RF-MRB) was developed based on the 802.11a standard in the context to simplify the hardware complexity and system size. These simplifications have permitted to develop a pervasive, low-power consuming and low-cost MIMO network platform with reliable data-rate in environments with strong multipath and large coverage ranges. The idea of MIMAX scheme was to shift the signal processing from baseband to RF front-end. Specifically, this scheme consisted of applying complex weights (gain factor and phase shift) to the transmitted or the received signals at each branch of RF front-end.

Accordingly, the objective of our thesis was to investigate other alternative analog antenna combining architectures that could further reduce the system complexity without having a high impact on performance. Thus, we have considered three alternative architectures for analog antenna combining, which reduce the complexity of the RF-MRB transceiver. The first architecture was RF-RWB, applies at each branch a sing switch followed by a VGA, which jointly permit to change the amplitude and sign of each incoming RF signal before adding them up. The second architecture was RF-EPB, which uses only a VGA per branch. The third architecture was RF-EGB, which changes only the phase of the RF signals by means of analog phase shifters.

From a baseband point of view, the three RF-MIMO architectures have posed different constrained beamforming problems in which the beamformer weights, instead of being complex number were constrained to be real (RF-RWB), nonnegative real (RF-EPB) or constant-modulus complex numbers (RF-EGB), respectively. The beamforming design problem was consisted in maximizing the signal-to-noise ratio (SNR) at the output of the beamformer, also we have considered other interesting criteria, such as the maximization of the system capacity (MaxCAP) and the minimization of the mean square error (MinMSE) associated to the optimal linear receiver. The design considered perfect channel state information available both at

the transmitter and the receiver.

Our thesis was divided in six chapters. In Chapter 1, we have presented the motivation and the original contributions, jointly with the outline of the work. In Chapter 2, the benefits of multiple antennas systems were summarized along with an overview on the system models of wireless channels used this thesis to design of the alternative RF-MIMO architectures. Additionally, beamforming design of conventional MIMO architecture was considered under orthogonal frequency division multiplexing modulation. Finally, the IEEE 802.11a standard was reviewed and a brief summary concludes the chapter. The RF-MRB architecture developed by MIMAX was presented in Chapter 3 along with their basic concepts (frame format and channel estimation) and benefits (i.e., diversity, multiplexing and array gains). Then, the block diagrams of the alternative analog antenna combining architectures (RF-RWB, RF-EPB and RF-EGB) were proposed with their system models. In Chapter 4, we have addressed to the problem of maximizing the received SNR for flat-fading channels. In those channels, the closed-form solutions in the SIMO case were obtained for different proposed architectures. While for the MIMO case, the optimization problems were non-convex. Therefore, we have proposed an alternative optimization algorithm which converges faster to the desired solution if an adequate initialization approach was tacked into account. In Section 4.4, the performance of the proposed RF-MIMO architecture were evaluated by means of numerical simulations in MATLAB. Specifically, the performance was evaluated in terms of bit error rate (BER). The proposed RF schemes were compared to the conventional SISO system. The comparison among the proposed architectures showed that the best results were obtained by the RF-EGB transceiver for both SIMO and MIMO cases.

In Chapter 5, our proposed RF combining architectures were extended to frequency selective channels and employing of OFDM modulation. With these new combining architectures, the same pair of Tx-Rx beamformers was applied to all the subcarriers and, due to this coupling, the beamforming design problem posed several new challenges. Under Perfect CSI at the transceiver, an beamforming criterion which depends on a single parameter α was proposed. According to this parameter, the proposed beamforming criterion was reduced to the MaxSNR ($\alpha = 0$), the MaxCAP ($\alpha = 1$), and the MinMSE ($\alpha = 2$) criteria. In general, the proposed criterion results in a non-convex optimization problem. For the MaxSNR criterion, this problem is solved in closed-form using convex relaxation techniques for the SIMO and MISO cases, while for the MIMO case an alternating optimization algorithm was used to find a suboptimal solution. For general case with $\alpha \neq 0$, the closed-form solution for SIMO or MISO cases did not exist, thus, the RF weights were obtained by mean of a simple gradient search algorithm. The two proposed algorithms were considered with a proper initialization approach based on MaxSNR closed-form solution. The

simulation results were presented in Section 5.8 to demonstrate the performance of the proposed simplified RF-MIMO architectures by considering of the three different criteria. In this section, we have chosen the standard 802.11a for WLAN, MIMO channel with the frequency selectivity was modeled using an exponential power delay profile. The proposed RF-MIMO schemes have been compared with a SISO and a Full-MIMO schemes in both cases coded and uncoded transmission. Finally, the best results were provided by the MinMSE beamformers, and it was also observed that the performance gap between the MinMSE approach for all schemes and Full-MIMO system increases according to the alternative architectures (in order) RF-MRB, RF-EGB, RF-RWB and RF-EPB. Also, the best results are provided by the RF-EGB architecture, which reveals the importance of the phase of the RF signals in comparison to their amplitude in beamforming problems.

6.2 Future Work

As summarized in the previous section, this thesis has introduced important results in the field of multiple analog antenna combining systems, in the area of reduced-complexity RF-MIMO transceiver design. However, the research presented in this thesis has also opened up numerous research directions that remain the subject of future work. Some of these topics are outlined as follows:

- The simplified RF architectures proposed in this thesis, will be investigated for wireless multiuser scenarios. Taking into account the constrained RF beamformers (i.e., constant-modulus complex weights, real weights or nonnegative real weights), we characterize the capacity region of a broadcast system based on OFDM transmissions. In particular, we consider a downlink channel with one base station (BS), which is equipped with n_T antennas and performs analog combining with the beamformer $\mathbf{u} \in \mathcal{S}^{n_T \times 1}$ to transmit a single OFDM data stream in L subcarriers. At the receiver side, the users have n_R antennas and perform analog combining with beamformers $\mathbf{v} \in \mathcal{S}^{n_R \times 1}$. Therefore, after removing the cyclic prefix and performing FFT, the signal viewed by the k-th user in the l-th subcarrier is given by

  $$y_{k,l} = \mathbf{v}_k^H \mathbf{H}_{k,l} \mathbf{u} s_l + \mathbf{v}_k^H \mathbf{n}_{k,l},$$

  where $\mathbf{H}_{k,l}$ represent the response of the MIMO channel for the k-th user and l-th subcarrier, s_l is the signal transmitted in the l-th subcarrier, and $\mathbf{n}_{k,l}$ is the noise vector (with zero-mean and variance σ^2).

  Assuming a fixed power allocation scheme (i.e., fraction $P_{k,l} \geq 0$ of the total available power P assigned to the l-th subcarrier and user k) and defining a

virtual channels $\tilde{\mathbf{H}}_{k,l} = \mathbf{H}_{k,l}\sqrt{P_{k,l}}$. The problem of designing the Tx and Rx beamformers can be written as

$$\begin{aligned} \underset{\mathbf{u},\mathbf{v}_k}{\text{maximize}} \quad & \sum_{k=1}^{K}\sum_{l=1}^{L} \lambda_k \log\left(1 + \frac{\left|\mathbf{v}_k^H \tilde{\mathbf{H}}_{k,l}\mathbf{u}\right|^2}{\sigma_{k,l}^2}\right) \\ \text{subject to} \quad & \|\mathbf{u}\| \leq 1, \quad \mathbf{u} \in \mathcal{S}^{n_T \times 1}, \\ & \|\mathbf{v}_k\| \leq 1, \quad \mathbf{v}_k \in \mathcal{S}^{n_R \times 1}, \quad k = 1, ..., K, \end{aligned} \tag{6.1}$$

where $\lambda_k \geq 0$ is the user weights (or priorities) and $\sigma_{k,l}^2$ is the noise plus interference seen by the k-th user in the l-th subcarrier.

For all RF-MIMO architectures, the optimization problem in (6.1) is nonconvex, but can be approximately solved following the lines in Chapter 5. Notice that the case of complex weights (i.e., RF-MRB scheme) are proposed in [Santamaría et al., 2010] for $K = 2$.

- The practical implementation of these new architectures will be realized under the 802.11a standard, and will be compared to some practical design of MIMAX architecture. In this case, the MIMO channel estimation will be realized based on the FFT analysis of the $n_T n_R$ training OFDM symbols of the received training frame. Then, the associated RF beamformers (i.e., constant-modulus complex weights, real weights or nonnegative real weights) will be obtained using of MaxSNR criterion (for example), and corrected in order to compensate the effects of the residual frequency offset.

- In this thesis, the transmit and receive beamformers for all RF schemes were selected under three optimization criteria. In contrast to numerical simulation, analytical performance expressions will be defined in order to identify the spatial diversity gain, array gain and better understand their influence on system performance. Therefore, we will provide analytical average and outage performance characterizations in both flat-fading and frequency-selective MIMO channels supported by constant-modulus complex weights, real weights and nonnegative real weights. Specifically, we characterize the average BER and outage probability versus SNR curves in terms of the diversity and array gains.

- Analogously to MIMAX scheme, we will study and evaluate the effects of MIMO channel estimation errors in frequency-selective channels. Therefore, the quadrature error or I-Q unbalancing generated by the phase shifts between the I and Q paths will be investigated.

6.3 List of Publications

List of publications produced during the Ph.D. studies.

6.3.1 International Journals

1. F. Gholam, J. Vía and I. Santamaría, "Beamforming Design for Simplified Analog Antenna Combining Architectures," IEEE Transactions on Vehicular Technology, 2011. (Submitted paper).

2. F. Gholam, J. Vía, I. Santamaría and M. Aghoutane , "Beamforming Design by Maximizing of System Capacity for Simplified RF-MIMO Architectures Under OFDM," (Prepared for Electronic Letters).

6.3.2 International Conferences

1. Á. Gonzalo, I. Santamaría, J. Vía, F. Gholam y R. Eickhoff, "Equal Gain MIMO beamforming in the RF domain for OFDM-WLAN systems," 2nd International ICST Conference on Mobile Lightweight Wireless Systems (Mobilight 2010), Barcelona, Spain, 2010.

2. F. Gholam, J. Vía, A. Nazábal y I. Santamaría, "Equal-Phase beamforming architecture for RF-MIMO antenna systems," 2nd International ICST Conference on Mobile Lightweight Wireless Systems (Mobilight 2010), Barcelona, Spain, 2010.

3. F. Gholam, J. Vía, I. Santamaría, M. Wickert y R. Eickhoff, "Simplified Architectures for Analogue Antenna Combining," ICT-MobileSummit 2009, Santander, Spain, 2009.

Appendix A

Closed-Form Solution of RWB for Flat-fading SIMO Channel

In this appendix, we prove the closed-form solution of RF-RWB scheme in SIMO case. In particular, this solution is derived according to minimum mean square (MMSE) method, where the solution is given by the largest eigenvector of a $n_R \times n_R$ real matrix formed by adding the outer products of the real and imaginary parts of the SIMO channel.

First, let us write the system model in (3.1) for flat-fading SIMO channel as

$$y = \mathbf{w}_R^H \mathbf{h}_{\text{SIMO}} s + \mathbf{w}_R^H \mathbf{n}. \tag{A.1}$$

Now, considering an alternative simplified RF architecture depicted in Figure A.1, which eliminates the adder stage after the vector modulators and IQ mixing of RF-MRB architecture presented in Figure 3.1.

The baseband model corresponding to the operations carried out by this scheme is equivalent to an independent processing of the real and imaginary parts of the received signal, i.e.,

$$\underbrace{\begin{bmatrix} z_R \\ z_I \end{bmatrix}}_{\mathbf{z}\in\mathbb{R}^{2\times 1}} = \underbrace{\begin{bmatrix} \mathbf{w}_R^T & \mathbf{0} \\ \mathbf{0} & \mathbf{w}_I^T \end{bmatrix}}_{\mathbf{W}\in\mathbb{R}^{2\times 2n_R}} \underbrace{\begin{bmatrix} \mathbf{y}_R \\ \mathbf{y}_I \end{bmatrix}}_{\mathbf{y}\in\mathbb{R}^{2n_R\times 1}}. \tag{A.2}$$

where $\mathbf{w}_R$ and $\mathbf{w}_I$ define the real and imaginary parts of the complex beamformer: $\mathbf{w} = \mathbf{w}_R + j\mathbf{w}_I$.

Using now vectors and matrices with real elements, the equivalent baseband signal model can be expressed more compactly as

$$\mathbf{z} = \mathbf{W}\left(\tilde{\mathbf{H}}\mathbf{s} + \mathbf{n}\right), \tag{A.3}$$

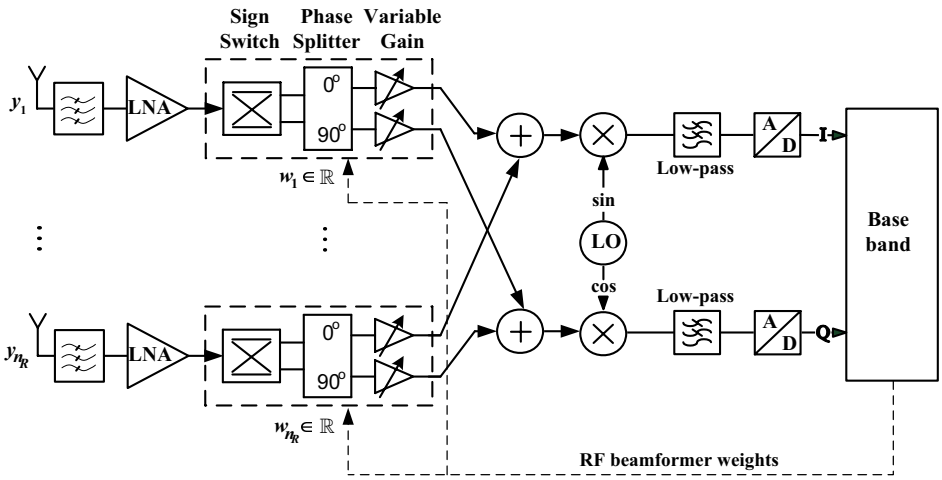

Figure A.1: RF Real-weight beamforming based on VM.

where for instance, the $2n_R \times 2$ real equivalent channel is obtained from the SIMO channel $\mathbf{h}_{\text{SIMO}} = \mathbf{h}_R + j\mathbf{h}_I$ as

$$\tilde{\mathbf{H}} = \begin{bmatrix} \mathbf{h}_R & -\mathbf{h}_I \\ \mathbf{h}_I & \mathbf{h}_R \end{bmatrix}, \tag{A.4}$$

As an optimality criterion we consider the minimum mean-square error (MMSE) between the transmitted signal and its estimate at the output of the beamformer. Thus, the question of what is the optimal (MMSE) beamformer for this new scheme is not as trivial as it might appear at the first glance.

Obviously, according to model (A.3) and under the assumption of unit power transmissions $E\left[|s|^2\right] = 1$, the linear minimum mean square error (LMMSE) estimator of $\mathbf{s}$ given $\tilde{\mathbf{H}}$ and $\mathbf{W}$ is

$$\hat{\mathbf{s}} = \left(\sigma^2\mathbf{I} + \left(\tilde{\mathbf{W}}\tilde{\mathbf{H}}\right)^T\left(\tilde{\mathbf{W}}\tilde{\mathbf{H}}\right)\right)^{-1}\left(\tilde{\mathbf{W}}\tilde{\mathbf{H}}\right)^T\mathbf{y}, \tag{A.5}$$

where

$$\tilde{\mathbf{W}} = \left(\mathbf{W}\mathbf{W}^T\right)^{-1/2}\mathbf{W} = \begin{bmatrix} \tilde{\mathbf{w}}_R & \mathbf{0} \\ \mathbf{0} & \tilde{\mathbf{w}}_I \end{bmatrix}, \tag{A.6}$$

and $\tilde{\mathbf{w}}_R = \mathbf{w}_R/\|\mathbf{w}_R\|$, $\tilde{\mathbf{w}}_I = \mathbf{w}_I/\|\mathbf{w}_I\|$. Thus, the MSE matrix is given by

$$\begin{aligned}\varepsilon\left(\tilde{\mathbf{W}}\right) &= E\left[\left(\mathbf{s}-\hat{\mathbf{s}}\right)\left(\mathbf{s}-\hat{\mathbf{s}}\right)^T\right] \\ &= \left[\mathbf{I}+\frac{1}{\sigma^2}\left(\tilde{\mathbf{W}}\tilde{\mathbf{H}}\right)^T\left(\tilde{\mathbf{W}}\tilde{\mathbf{H}}\right)\right]^{-1}.\end{aligned} \tag{A.7}$$

For any Schur-concave objective function of the vector containing the individual MSEs, the optimal beamformer coefficients are those that diagonalize the MSE the MSE matrix while minimizing its trace [Palomar et al., 2003]. On the other hand, for Schur-convex objective functions the optimal beamformers must give an MSE matrix with equal diagonal elements (i.e., equal MSEs for s_R and s_I) and minimum trace. For our problem, the matrix $\left(\tilde{\mathbf{W}}\tilde{\mathbf{H}}\right)^T\left(\tilde{\mathbf{W}}\tilde{\mathbf{H}}\right)$ in (A.7) is given by

$$\begin{aligned}&\left(\tilde{\mathbf{W}}\tilde{\mathbf{H}}\right)^T\left(\tilde{\mathbf{W}}\tilde{\mathbf{H}}\right) = \\ &= \begin{bmatrix} \tilde{\mathbf{w}}_R^T\mathbf{h}_R\mathbf{h}_R^T\tilde{\mathbf{w}}_R+\tilde{\mathbf{w}}_I^T\mathbf{h}_I\mathbf{h}_I^T\tilde{\mathbf{w}}_I & -\tilde{\mathbf{w}}_R^T\mathbf{h}_I\mathbf{h}_R^T\tilde{\mathbf{w}}_R+\tilde{\mathbf{w}}_I^T\mathbf{h}_R\mathbf{h}_I^T\tilde{\mathbf{w}}_I \\ -\tilde{\mathbf{w}}_R^T\mathbf{h}_R\mathbf{h}_I^T\tilde{\mathbf{w}}_R+\tilde{\mathbf{w}}_I^T\mathbf{h}_I\mathbf{h}_R^T\tilde{\mathbf{w}}_I & \tilde{\mathbf{w}}_R^T\mathbf{h}_I\mathbf{h}_I^T\tilde{\mathbf{w}}_R+\tilde{\mathbf{w}}_I^T\mathbf{h}_R\mathbf{h}_R^T\tilde{\mathbf{w}}_I \end{bmatrix}.\end{aligned} \tag{A.8}$$

Therefore, the MSE matrix is diagonalized as long as the real and imaginary parts of the beamformer are equal, i.e., $\tilde{\mathbf{w}}_R = \tilde{\mathbf{w}}_I$. Interestingly, with this choice of the beamformer, the MSE matrix not only becomes diagonal, but it also has equal diagonal elements

$$\left(\tilde{\mathbf{W}}\tilde{\mathbf{H}}\right)^T\left(\tilde{\mathbf{W}}\tilde{\mathbf{H}}\right) = \begin{bmatrix} \tilde{\mathbf{w}}_R^T\left(\mathbf{h}_R\mathbf{h}_R^T+\mathbf{h}_I\mathbf{h}_I^T\right)\tilde{\mathbf{w}}_R & \mathbf{0} \\ \mathbf{0} & \tilde{\mathbf{w}}_I^T\left(\mathbf{h}_R\mathbf{h}_R^T+\mathbf{h}_I\mathbf{h}_I^T\right)\tilde{\mathbf{w}}_I \end{bmatrix}. \tag{A.9}$$

Finally, to minimize the trace of the MSE matrix, $\tilde{\mathbf{w}}_R$ (and $\tilde{\mathbf{w}}_I$) must be the eigenvector (which obviously will have real entries) corresponding to the largest eigenvalue of the following $n_R \times n_R$ real matrix

$$\mathbf{G}_{\text{SIMO}} = \left(\mathbf{h}_R\mathbf{h}_R^T+\mathbf{h}_I\mathbf{h}_I^T\right). \tag{A.10}$$

Interestingly, the equality between the real and imaginary parts of the optimal beamformer allows a further simplification of the RF-MRB combining architecture, which give rise to the RF-RWB architecture (Figure 3.4) proposed in Chapter 3. Notice that, when the optimal real weight beamformer is used, the architectures shown in Figures 3.4 and A.1 are equivalent in terms of performance.

Appendix B

Analysis of The Cost Function Minima for RF-MRB Architecture

In this appendix, the analysis of the cost function minima for RF-MRB architecture is presented. Although the non-convexity of the optimization problem (5.10) precludes obtaining a closed-form solution. However, we can gain some insights by applying the Lagrange multipliers method and, thus, finding the conditions that must be satisfied by any local minima.

First, let us write the Lagrangian of (5.10) as

$$\mathcal{L}\left(\mathbf{w}_T, \mathbf{w}_R, \lambda_T, \lambda_R\right) = f_\alpha\left(\mathbf{w}_T, \mathbf{w}_R\right) + \lambda_T\left(\left\|\mathbf{w}_T\right\|^2 - 1\right) + \lambda_R\left(\left\|\mathbf{w}_R\right\|^2 - 1\right), \tag{B.1}$$

where λ_T and λ_R are the Lagrange multipliers. Solving with respect to $\mathbf{w}_T$ and $\mathbf{w}_R$, we obtain

$$\nabla_{\mathbf{w}_T^*} f_\alpha\left(\mathbf{w}_T, \mathbf{w}_R\right) = -\lambda_T \mathbf{w}_T, \tag{B.2}$$

$$\nabla_{\mathbf{w}_R^*} f_\alpha\left(\mathbf{w}_T, \mathbf{w}_R\right) = -\lambda_R \mathbf{w}_R, \tag{B.3}$$

where the gradient of the cost function $f_\alpha\left(\mathbf{w}_T, \mathbf{w}_R\right)$ with respect to the transmit and receive beamformers is given by

$$\begin{aligned} \nabla_{\mathbf{w}_T^*} f_\alpha\left(\mathbf{w}_T, \mathbf{w}_R\right) &= -\frac{\gamma}{\sum_{k=1}^{N_c} \mathrm{MSE}_k^{\alpha-1}} \mathbf{R}_{\mathrm{MISO}_\alpha} \mathbf{w}_T, \\ \nabla_{\mathbf{w}_R^*} f_\alpha\left(\mathbf{w}_T, \mathbf{w}_R\right) &= -\frac{\gamma}{\sum_{k=1}^{N_c} \mathrm{MSE}_k^{\alpha-1}} \mathbf{R}_{\mathrm{SIMO}_\alpha} \mathbf{w}_R. \end{aligned} \tag{B.4}$$

Now, left-multiplying (B.2) and (B.3) by $\mathbf{w}_T^H$ and $\mathbf{w}_R^H$, and taking into account the unit-energy constraint on the beamformers, we obtain

$$\lambda_T = \gamma \frac{\mathbf{w}_T^H \mathbf{R}_{\mathrm{MISO}_\alpha} \mathbf{w}_T}{\sum_{k=1}^{N_c} \mathrm{MSE}_k^{\alpha-1}}, \qquad \lambda_R = \gamma \frac{\mathbf{w}_R^H \mathbf{R}_{\mathrm{SIMO}_\alpha} \mathbf{w}_R}{\sum_{k=1}^{N_c} \mathrm{MSE}_k^{\alpha-1}}, \tag{B.5}$$

which combined with (B.2) and (B.3) yields

$$\begin{aligned} \mathbf{R}_{\mathrm{MISO}_\alpha} \mathbf{w}_T &= \left(\mathbf{w}_T^H \mathbf{R}_{\mathrm{MISO}_\alpha} \mathbf{w}_T\right) \mathbf{w}_T, \\ \mathbf{R}_{\mathrm{SIMO}_\alpha} \mathbf{w}_R &= \left(\mathbf{w}_R^H \mathbf{R}_{\mathrm{SIMO}_\alpha} \mathbf{w}_R\right) \mathbf{w}_R. \end{aligned} \tag{B.6}$$

Finally, from (5.13) and (5.14) it is easy to see that

$$\mathbf{w}_T^H \mathbf{R}_{\mathrm{MISO}_\alpha} \mathbf{w}_T = \mathbf{w}_R^H \mathbf{R}_{\mathrm{SIMO}_\alpha} \mathbf{w}_R = \sum_{k=1}^{N_c} \mathrm{MSE}_k^\alpha \left|h_k\right|^2 = \lambda, \tag{B.7}$$

which implies $\lambda_T = \lambda_R$. Thus, we conclude that the local minima of the optimization problem in (5.10) is the solution of the coupled eigenvalue problems in (5.12).

On the other hand, we show that the local minima of our optimization problem are closely related to that of weighted energy maximization problem. Specifically, considering the following weighted energy maximization problem[1]

$$\begin{aligned} \underset{\mathbf{w}_T, \mathbf{w}_R}{\text{minimize}} \quad & -\frac{1}{N_c} \sum_{k=1}^{N_c} c_k \left|h_k\right|^2 \\ \text{subject to} \quad & \|\mathbf{w}_T\| \leq 1, \quad \mathbf{w}_T \in \mathcal{S}^{n_T \times 1}, \\ & \|\mathbf{w}_R\| \leq 1, \quad \mathbf{w}_R \in \mathcal{S}^{n_R \times 1}, \end{aligned} \tag{B.8}$$

with $\mathbf{c} = [c_1, \ldots, c_{N_c}]^T \in \mathbb{R}^{N_c \times 1}$. The local minima of (B.8) are also solution of the coupled eigenvalue problems

$$\mathbf{R}_{\mathrm{MISO}_c} \mathbf{w}_T = \lambda \mathbf{w}_T, \qquad \mathbf{R}_{\mathrm{SIMO}_c} \mathbf{w}_R = \lambda \mathbf{w}_R, \tag{B.9}$$

where $\lambda = \sum_{k=1}^{N_c} c_k \left|h_k\right|^2$ and

$$\mathbf{R}_{\mathrm{SIMO}_c} = \sum_{k=1}^{N_c} c_k \mathbf{h}_{\mathrm{SIMO}_k} \mathbf{h}_{\mathrm{SIMO}_k}^H, \tag{B.10}$$

$$\mathbf{R}_{\mathrm{MISO}_c} = \sum_{k=1}^{N_c} c_k \mathbf{h}_{\mathrm{MISO}_k}^H \mathbf{h}_{\mathrm{MISO}_k}. \tag{B.11}$$

Notice that the proof of local minima of (B.8) can be done by the same methodology followed for our optimization problem (5.10). Thus, the local minima of the proposed

[1]Note that in the case of equal weights ($c_k = c$, $\forall k$) the weighted-energy maximization problem reduces to the MaxSNR criterion.

optimization problem (5.10) are also local minima of (B.8) with weights $c_k = \mathrm{MSE}_k^{\alpha}$. This corroborates our previous finding about the proposed cost function, i.e., for $\alpha > 0$ the higher weights are given to the subcarriers with a worst response (large MSE_k). In other words, for $\alpha > 0$ part of the SNR is sacrificed in order to improve the worst data carriers, and the contrary happens for $\alpha < 0$.

List of Figures

List of Tables

List of Algorithms

Bibliography

[Maxwell, 1865] J. C. Maxwell. *A dynamical theory of the electromagnetic field.* Philosophical Transactions of the Royal Society of London, 1865.

[Story, 1904] A. T. Story. *The story of wireless telegraphy.* New York: D. Appleton and company, 1904.

[Ohrtman and Roeder] Frank Ohrtman and Konrad Roeder. *Wi-Fi Handbook : Building 802.11b Wireless Networks.* McGraw-Hill, New York, 2003.

[Yang et al., 2007] Yaling Yang, Jun Wang, and Robin Kravets. "Distributed Optimal Contention Window Control for Elastic Traffic in Single-Cell Wireless LANs". IEEE/ACM Transactions on Networking, volume 15, no. 6, pages 1373-1386, 2007.

[IEEE 802.11a standard, 1999] IEEE Std. 802.11a, Supplement to Part 11. "Wireless LAN Medium Access Control (MAC) and Physical Layer (PHY) specifications". Highspeed Physical Layer in the 5 GHz Band. IEEE., 1999.

[ISO, 1994] International Organization for Standardization (ISO). "Information Technology Open Systems Interconnections Basic Reference Model: The Basic Model". International Standard, 1994.

[Eickhoff et al., 2008] R. Eickhoff, F. Ellinger, U. Mayer, M. Wickert, I. Santamaría, R. Kraemer, L. González, P. Sperandio, T. Theodosiou. "MIMAX: Exploiting the maximum performance and minimum system costs of wireless MIMO systems". 17th ICT Mobile and Wireless Summit, Stockholm, Sweden, 2008.

[González et al., 2010] Ó. González, J. Gutíerrez, J. Ibáñez, L. Vielva y R. Eickhoff. "Experimental evaluation of an RF-MIMO transceiver for 802.11a WLAN". Future Network and MobileSummit 2010, Florence, Italy, 2010.

[Vía et al., 2010b] J. Vía, I. Santamaría, V. Elvira and R. Eickhoff. "A general Pre-FFT criterion for MIMO-OFDM beamforming". IEEE International Conference on Communications, South Africa, 2010.

[Elvira and Vía, 2009] V. Elvira and J. V´a. "Diversity Techniques for RF-Beamforming in MIMO-OFDM Systems: Design and Performance Evaluation". 17th European Signal Processing Conference, United Kingdom, 2009.

[Sandhu and Ho, 2003] Sumeet Sandhu and Minnie Ho. "Analog combining of multiple receive antennas with OFDM". In IEEE International Conference, volume 5, pages 3428-3432, 2003.

[Eickhoff et al., 2009] R. Eickhoff, R. Kraemer, I. Santamaría, L. González. "Integrated low power RF-MIMO transceiver for enhanced 802.11a short-range communication". IEEE Vehicular Technology Magazine, volume 4 no. 1, pages 34-41, 2009.

[Vía et al, 2010a] J. Vía, I. Santamaría, V. Elvira, R. Eickhoff. "A general criterion for analog Tx-Rx beamforming under OFDM transmission". IEEE Transactions on Signal Processing, volume 58, no. 4, pages 2155-2167, 2010.

[Sidiropoulos et al, 2006] N. Sidiropoulos, T. Davidson, and Z.-Q. Luo. "Transmit beamforming for physical-layer multicasting". IEEE Transactions on Signal Processing, volume 54, no. 6, pages 2239-2251, 2006.

[Phan et al, 2009] K. Phan, S. Vorobyov, N. Sidiropoulos, and C. Tellambura. "Spectrum sharing in wireless networks via QoS-aware secondary multicast beamforming". IEEE Transactions on Signal Processing, volume 57, no. 6, pages 2323-2335, 2009.

[MIMAX Web, 2008] MIMAX Web. "MIMAX: Advanced MIMO systems for maximum reliability and performance". http://www.ict-mimax.eu, 2008.

[Vía et al., 2009a] J. Vía, V. Elvira, I. Santamaría, R. Eickhoff. "Minimum BER beanforming in the RF domain for OFDM transmissions and linear receivers". In IEEE International Conference on Acoustics, Speech and Signal Processing (ICASSP 2009), Taipei, Taiwan, 2009.

[Vía et al., 2009b] J. Vía, V. Elvira, I. Santamaría, and R. Eickhoff. "Analog antenna combining for maximum capacity under OFDM transmission". IEEE International Conference on Communications, Dresden, Germany, 2009.

[Lee et al., 2010] Y. Lee, Y.J. Hsieh, H.-W., Shieh. "Multiobjective optimization for pre-DFT combining in coded SIMO-OFDM systems". IEEE Communication Letters, volume 14, no. 4, pages 303-305, 2010.

[Foschini and Gans, 1998] G. J. Foschini and M. J. Gans. "On limits of wireless communications in a fading environment when using multiple antennas". Wireless Pers. Commun., volume 6, pages 311-335, 1998.

[Telatar, 1999] E. Telatar. "Capacity of multi-antenna Gaussian channels". European Trans. Telecommunications, volume 10, no. 6, pages 585-595, 1999.

[Gesbert et al., 2003] D. Gesbert, M. Shafi, D. Shiu, P. J. Smith, and A. Naguib. "From theory to practice: An overview of MIMO space-time coded wireless systems". IEEE J. Select. Areas Commun., volume 21, no. 3, pages 281-302, 2003.

[Loyka and Levin, 2010] Sergey Loyka, and Georgy Levin. "Finite-SNR Diversity-Multiplexing Tradeoff via Asymptotic Analysis of Large MIMO Systems". IEEE Transactions on Information Theory, volume 56, no. 10, pages 4781-4792, 2010.

[Loyka and Levin, 2007] Sergey Loyka, and George Levin. "Diversity-Multiplexing Tradeoff via Asymptotic Analysis of Large MIMO Systems". Information Theory, ISIT. IEEE International Symposium, 2007.

[Zheng and Tse, 2003] L. Zheng and D. Tse. "Diversity and multiplexing: A fundamental trade-off in multiple-antenna channels". IEEE Transactions on Information Theory, volume 49, no. 5, pages 1073-1096, 2003.

[Wallace and Jensen, 2004] J. W. Wallace and M. A. Jensen. "Mutual coupling in MIMO wireless systems: A rigorous network theory analysis". IEEE Trans. Wireless Commun., volume 3, no. 4, pages 1317-1325, 2004.

[Waldschmidt et al., 2004] C. Waldschmidt, S. Schulteis, and W. Wiesbeck. "Complete RF system model for analysis of compact MIMO arrays". IEEE Trans. Veh. Technol., volume 53, no. 3, pages 579-586, 2004.

[Mishra and Chauhan, 2011] Shailendra Mishra, and D. S. Chauhan. "Low complexity scheduling algorithm for multiuser MIMO system". International Journal of Computer Science and Information Security, volume 9, no. 1, 2011.

[Buehrer et al., 2002] R. M. Buehrer, R. A. Soni and R. D. Benning. "Intelligent antenna system for cdma2000". IEEE Signal Processing Magazine, pages 54-67, 2002.

[Brennan, 2003] D. G. Brennan. "Linear diversity combining techniques". Proc. IRE, volume 47, pages 10751102, 1959, Reprint: Proc. IEEE, volume 91, no. 2, pages 331-356, 2003.

[Balaban and Salz, 1992] P. Balaban and J. Salz. "Optimum diversity combining and equalization in digital data transmission with applications to cellular mobile radio Part I: Theoretical considerations; Part II: Numerical results," IEEE Trans. Commun., volume 40, no. 5, pages 885-894, 895-907, 1992.

[Eng and Milstein, 1996] T. Eng, N. Kong, and L. B. Milstein. "Comparison of diversity combining techniques for Rayleigh-fading channels". IEEE Trans. Commun., volume 44, no. 9, pages 1117-1129, 1996.

[Wittneben, 1991] A. Wittneben. "Basestation modulation diversity for digital simulcast". In Proc. IEEE Veh. Technol. Conf. (VTC), St. Louis, Missouri, USA, pages 848-853, 1991.

[Lo, 1999] T. Y. Lo. "Maximum ratio transmission," IEEE Trans. Communications, volume 47, no. 10, pages 1458-1461, 1999.

[Jakes, 1974] W. C. Jakes, Jr. *Mobile Microwave Communication.* Wiley, New York, 1974.

[Tse and Viswanath, 2005] D. Tse and P. Viswanath. *Fundamentals of Wireless Communications.* Cambridge University Press, 2005.

[Vucetic and Yuan, 2003] Branka Vucetic and Jinhong Yuan. *Space-Time Coding.* John Wiley and Sons Ltd., The Atrium, Southern Gate, Chichester, West Sussex, England, 2003.

[Ergen, 2009] Mustafa Ergen. *Mobile Broadband: Including WiMAX and LTE.* Springer Publishing Company, 1st Edition, 2009.

[Goldsmith, 2005] A. Goldsmith. *Wireless Communications.* Cambridge University Press, 2005.

[Ellinger, 2007] F. Ellinger. *Radio Frequency Integrated Circuits and Technologies.* Springer-Verlag, Berlin, 2007.

[Love et al., 2003] D. J. Love, R. W. Heath Jr, and T. Stohmer. "Grassmannian beamforming for multiple-input multiple-output wireless systems". IEEE Trans. Inform. Theory, volume 49, pages 2735-2747, 2003.

[Choi and Heath, 2005] Jihoon Choi and Robert W. Heath, Jr. "Interpolation Based Transmit Beamforming for MIMO-OFDM With Limited Feedback". IEEE Transactions on Signal Processing, volume 53, no. 11, pages 4125-4135, 2005.

[Sandhu and Ho, 2003] S. Sandhu, M. Ho. "Analog combining of multiple receive antennas with OFDM". In IEEE International Conference on Communications, volume 5, pages 3428-3432, 2003.

[Bingham, 1990] J. A. C. Bingham. "Multicarrier Modulation for Data Transmission: An Idea Whose Time Has Come". IEEE Communicatios Magazine, volume 28, no. 5, pages 5-14, 1990.

[Bhai et al., 2004] Ahmad R. S. Bhai, Burton R. Saltzberg, Mustafa Ergen. *Multi-Carrier Digital Communications Theory and Applications of OFDM.* Springer Science, United States of America, Second Edition, 2004.

[Wang and Giannakis, 2000] Z. Wang, and G. B. Giannakis. "Wireless Multicarrier Communications". IEEE Signal Processing Magazine, volume 17, no. 3, pages 29-48, 2000.

[Matsuoka and Shoki, 2004] H. Matsuoka, H. Shoki. "Comparison of pre-FFT and post-FFT processing adaptive arrays for OFDM systems in the presence of co-channel interference". Personal, Indoor and Mobile Radio Communications, volume 2, pages 1603-1607, 2004.

[Zheng et al., 2007] X. Zheng, Y. Xie, J. Li, P. Stoica. "MIMO transmit beamforming under uniform elemental power constraint". IEEE Transactions on Signal Processing, volume 55, pages 5395-5406, 2007.

[Lee, 2009] Yinman Lee. "Max-Min Fair Pre-DFT Combining for OFDM Systems With Multiple Receive Antennas". IEEE Transactions on Vehecular Technlogy, volume 58, no. 4, pages 1741-1745, 2009.

[Nesterov and Nemirovsky, 1994] Y. Nesterov and A. Nemirovsky. *Interior Point Polynomial Algorithms in Convex Programming.* PA: SIAM, Philadelphia, 1994.

[Gonzalo et al., 2010] Á. Gonzálo, I. Santamaría, J. Vía, F. Gholam y R. Eickhoff. "Equal Gain MIMO beamforming in the RF domain for OFDM-WLAN systems". 2nd International ICST Conference on Mobile Lightweight Wireless Systems (Mobilight 2010), Barcelona, Spain, 2010.

[Love and Heath, 2003] D. J. Love, R. W. Heath. "Equal gain transmission in multiple-input multiple-output wireless systems". IEEE Transactions on Communications, volume 51, pages 1102-1110, 2003.

[Renyi, 1976] A. Renyi. "Some fundamental questions of information theory." in Selected papers of Alfred Renyi, volume 2, pages 526552, 1976.

[Andersen, 2000] J. B. Andersen. "Array gain and capacity for known random channels with multiple element arrays at both ends". IEEE Journal on Selected Areas in Communications, volume 11, pages 2172-2178, 2000.

[Santamaría et al., 2008] I. Santamaría, V. Elvira, J. Vía D. Ramírez, J. Pérez, J. Ibáñez, R. Eickoff and F. Ellinger. "Optimal MIMO Transmission Schemes with Adaptive Antenna Combining in the RF Path". 16th European Signal Processing Conference, Switzerland, 2008.

[Gholam et al., 2009] F. Gholam, J. Vía, I. Santamaría, M. Wickert, R. Eickhoff. "Simplified architectures for analogue antenna combining". 18th ICT Mobile and Wireless Summit, Santander, Spain, 2009.

[Dahl et al., 2004] T. Dahl, N. Christophersen, D. Gesbert. "Blind MIMO eigenmode transmission based on the algebraic power method". IEEE Transactions on Signal Processing, volume 52, no. 9, pages 2424-2431, 2004.

[Palomar et al., 2003] D. P. Palomar, J. M. Cioffi, and M. A. Lagunas. "Joint Tx-Rx beamforming design for multicarrier MIMO channels: A unified framework for convex optimization". IEEE Transactions on Signal Processing, volume 51, pages 2381-2401, 2003.

[Boyd and Vandenberghe, 2004] Stephen Boyd and Lieven Vandenberghe. "Convex Optimization". Cambridge University Press, 2004.

[Rahman et al., 2004] M. Rahman, K. Witrisal, S. Das, F. Fitzek, O. Olsen, and R. Prasad. "Optimum pre-DFT combining with cyclic delay diversity for OFDM based WLAN systems". In IEEE 59th Vehicular Technology Conference (VTC 2004-Spring), volume 4, pages 1844-1848, 2004.

[Lei and Chin, 2004] Z. Lei, F. P.S. Chin. "Post and pre-FFT beamforming in an OFDM system". IEEE Vehicular Technology Conference, volume 1, pages 39-43, 2004.

[Demmel, 1997] J. W. Demmel. *Applied Numerical Linear Algebra.* SIAM, 1st ed., 1997.

[Golub and Loan, 1983] G. H. Golub and C. F. V. Loan. *Matrix Computations.* Johns Hopkins University Press, 3rd ed., 1983.

[Dent et al., 1993] P. Dent, G. E. Bottomley, T. Croft. "Jakes Fading Model Revisited". Electronics Letters, volume 29, no. 13, pages 1162-1163, 1993.

[Okada and Komaki, 2001] M. Okada and S. Komaki. "Pre-DFT combining space diversity assisted COFDM." IEEE Transactions on Vehicular Technology, volume 50, no. 2, pages 487-496, 2001.

[Palomar and Jiang, 2006] D. P. Palomar and Y. Jiang. "MIMO transceiver design via majorization theory." Found. Trends Commun. Inf. Theory, volume 3, no. 4, pages 331-551, 2006.

[Kay, 1993] S. M. Kay. *Fundamentals of Statistical Signal Processing: Estimation Theory.* Englewood Cliffs, NJ: Prentice-Hall, 1993.

[Horn and Johnson, 1990] R. A. Horn and C. R. Johnson. *Matrix Analysis.* Cambridge University Press, 1990.

[Thomas Jr and Finney, 1992] G. B. Thomas Jr. and R. L. Finney. *Calculus and Analytic Geometry.* Addison-Wesley, 8th ed., New York 1992.

[Blake and Zisserman, 1987] A. Blake and A. Zisserman. *Visual reconstruction.* Cambridge, MA, USA: MIT Press, 1987.

[Aalo, 1995] V. A. Aalo. "Performance of maximal-ratio diversity systems in a correlated Nakagami-fading environment," IEEE Trans. Commun., volume 43, pages 2360-2369, 1995.

[Santamaría et al., 2010] I. Santamaría, J. Vía, A. Nazábal and C. Lameiro. "Capacity region of the multiantenna Gaussian broadcast channel with analog TX-RX beamforming". 5th International ICST Conference on Communications and Networking in China (CHINACOM), Beijing, 2010.